

waterloopkundig laboratorium  
delft hydraulics laboratory

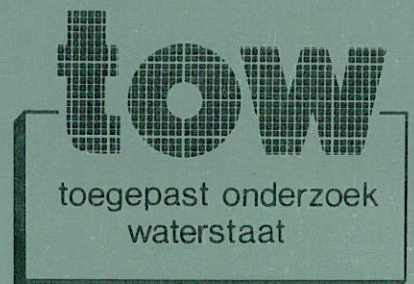
wind effect on the distribution of velocity  
and temperature in stratified enclosed systems

report on literature study

---

R 898 II

October 1978



---

wind effect on the distribution of velocity  
and temperature in stratified enclosed systems

G.A.L. Delvigne

report on literature study

---

R 898 II

October 1978



toegepast onderzoek  
waterstaat

## CONTENTS

### List of symbols

|  | page |
|--|------|
| <u>1</u> <u>General</u> .....  | 1    |
| 1.1    Terms of reference .....  | 1    |
| 1.2    Introduction .....  | 1    |
| 1.3    Scope and outline .....   | 1    |
| <br>   |      |
| <u>2</u> <u>Wind-generated phenomena</u> .....                                   | 3    |
| <br>   |      |
| <u>3</u> <u>Exchange processes</u> .....   | 7    |
| 3.1    Exchange across the air-water interface .....                             | 7    |
| 3.2    Mixing in stratified system .....   | 9    |
| <br>   |      |
| <u>4</u> <u>Influence of wind on water surface</u> .....                         | 14   |
| 4.1    Wind velocity profile $U_w(z)$ over the water surface .....               | 14   |
| 4.2    Roughness height $z_{o,a}$ .....  | 15   |
| 4.3    Shear stress $\tau_o$ at water surface .....                              | 16   |
| 4.4    Wind-driven surface velocity $u_s$ .....                                  | 17   |
| 4.5    Shear stress ( $\tau_o, \tau_s$ ) measurements .....                      | 17   |
| <br>   |      |
| <u>5</u> <u>Wind influence on one-dimensional (1D-vertical) water system</u> ... | 20   |
| 5.1    Vertical water velocity profile .....                                     | 20   |
| 5.2    Wind set-up of water surface and interface .....                          | 22   |
| 5.3    (Internal) seiche .....   | 25   |
| 5.4    Mixing of surface layer by wind (no heat exchange) .....                  | 26   |
| 5.5    Wind influence on thermal stratification .....                            | 31   |
| 5.5.1   Physical phenomena important to thermal stratification .....             | 32   |
| 5.5.2   Heat flux $q$ .....  | 33   |
| 5.5.3   Qualitative description of heat balance .....                            | 33   |
| 5.5.4   Stratification models .....  | 34   |
| <br>   |      |
| <u>6</u> <u>Wind influence on current pattern in 2D- and 3D-water system</u> ... | 38   |
| 6.1    Introduction .....  | 38   |
| 6.2    Hydraulic and mathematic models .....                                     | 39   |
| 6.3    Frequently applied simplifications .....                                  | 40   |
| 6.4    Mathematical description .....  | 41   |

CONTENTS (continued)

|  | page |
|--|------|
| 6.5 Calculation on simplified basins, Homogeneous and two-layer system ..... | 43   |
| 6.6 Bottom and wall influences .....   | 48   |
| 6.7 Influence of horizontal density gradient .....                           | 51   |
| 6.8 Influence of eddy viscosity .....  | 52   |
| 6.9 Special phenomena .....  | 53   |
| <u>7 Summary and conclusions</u> .....                                       | 55   |

LITERATURE

FIGURES

## List of symbols

|              |   |           |
|--------------|---|-----------|
| $C_D$        | drag coefficient (wind shear stress coefficient)                                    | -         |
| $C_T$        | Stanton number  | -         |
| $c_p$        | specific heat of water at constant pressure   | J/kg °C   |
| $D$          | Ekman layer depth (depth of frictional resistance)                                  | m         |
| $E_k$        | kinetic energy  | J         |
| $E_p$        | potential energy  | J         |
| $F$          | Froude number   | -         |
| $f$          | Coriolis parameter, $f = 2\Omega \sin \phi$   | $s^{-1}$  |
| $g$          | acceleration of gravity   | $m/s^2$   |
| $h$          | water depth   | m         |
| $L$          | fetch   | m         |
| $l$          | mixing length   | m         |
| $N$          | buoyancy frequency (Brunt-Väisälä frequency)  | $s^{-1}$  |
| $p$          | pressure  | $N/m^2$   |
| $q$          | heat flux   | $J/m^2 s$ |
| $Q_s$        | sensible heat flux  | $J/m^2 s$ |
| $Re$         | Reynolds number   | -         |
| $Ri$         | Richardson number   | -         |
| $Ri_o$       | overall Richardson number   | -         |
| $Ro$         | Rossby number   | -         |
| $s$          | relative surface slope  | -         |
| $S$          | surface set-up  | m         |
| $t$          | time variable   | s         |
| $T$          | temperature   | °C        |
| $T_a$        | temperature lower layer (hypolimnion)   | °C        |
| $T_s$        | temperature upper layer (epilimnion)  | °C        |
| $u, v, w$    | water flow velocities in directions x, y and z                                      | m/s       |
| $U, V, W$    | air flow velocities in directions x, y and z  | m/s       |
| $u', v', w'$ | turbulent fluctuations of flow velocities   | m/s       |
| $U_{w,z}$    | wind velocity at altitude z over water surface                                      | m/s       |
| $U_{w*}$     | shear velocity of wind ( $U_{w*} \stackrel{\text{def}}{=} \sqrt{\tau_o / \rho_a}$ ) | m/s       |
| $u_*$        | water shear velocity ( $u_{s*} = \sqrt{\tau_s / \rho}$ )                            | m/s       |
| $u_s$        | water flow velocity at the surface  | m/s       |
| $w_e$        | entrainment velocity  | m/s       |
| $x$          | horizontal coordinate in longitudinal direction                                     | m         |
| $y$          | horizontal coordinate in lateral direction  | m         |

List of symbols (continued)

|                    |   |                         |
|--------------------|---|-------------------------|
| $z$                | vertical coordinate   | m                       |
| $z_o$              | roughness height related to water flow profile  | m                       |
| $z_{o,a}$          | roughness height related to air flow profile  | m                       |
| $\alpha$           | thermal expansion coefficient   | $^{\circ}\text{C}^{-1}$ |
| $\delta$           | boundary layer thickness  | m                       |
| $\epsilon_{x,y,z}$ | turbulent mass diffusion coefficient in directions x,<br>y and z  | $\text{m}^2/\text{s}$   |
| $\epsilon_u$       | turbulent momentum diffusion coefficient  | $\text{m}^2/\text{s}$   |
| $\epsilon_o$       | turbulent diffusion coefficient for unstratified system   | $\text{m}^2/\text{s}$   |
| $\kappa$           | Von Kármán constant   | -                       |
| $\nu$              | kinematic water viscosity   | $\text{m}^2/\text{s}$   |
| $\nu_a$            | kinematic air viscosity   | $\text{m}^2/\text{s}$   |
| $\rho$             | density of water  | $\text{kg}/\text{m}^3$  |
| $\rho_a$           | density of air  | $\text{kg}/\text{m}^3$  |
| $\tau, \tau_b$     | shear stress, on bottom   | $\text{kg}/\text{ms}^2$ |
| $\tau_o, \tau_s$   | shear stress on air-water interface, related to air<br>flow profile and water flow profile respectively | $\text{kg}/\text{ms}^2$ |

# WIND EFFECT ON THE DISTRIBUTION OF VELOCITY AND TEMPERATURE IN STRATIFIED ENCLOSED SYSTEMS

## 1 General

### 1.1 Terms of reference

This literature survey was performed within the framework of a basic research program (TOW), executed by Rijkswaterstaat, Directie Waterhuishouding en Waterbeweging (Ministry of Public Works, Directorate of Water Management), the Delft Hydraulics Laboratory, and other institutes.

The survey has been performed by dr. G.A.L. Delvigne (DHL) who also wrote the report.

### 1.2 Introduction

In this literature review the various aspects of wind influence on shallow stratified lakes and seas are presented. An attempt is made at summarizing the present knowledge on each of these aspects, and to indicate their inter-relationship.

Even when restricting the review to shallow basins, the scope is very wide indeed. Since the attempt by Hutchinson [1957] to give a concise presentation of the existing literature, the attention has shifted considerably towards the mathematical solution of the pertaining hydrodynamical equations. For this reason a separate review has been performed by DHL [1976a] on the existing mathematical models, describing horizontal and vertical motions in shallow basins. The general conclusion of DHL [1976a] is that in the majority of cases a validation of the numerical models is lacking, which means that more prototype data will be necessary to evaluate the applicability of these models to engineering problems.

The present report deals rather with the physical description of the phenomena occurring when wind blows over a stratified basin.

### 1.3 Scope and outline

The purpose of this literature study is the indication and description of phenomena important to the temperature and current velocity field of a basin

exposed to wind. The most general situation deals with:

- three-dimensional time-dependent circulations
- wind stress on the water surface
- stratification caused by an inhomogeneous density field (temperature, salinity)
- complicated coastal and bottom configuration.

Mostly attention will be paid to enclosed systems with restricted horizontal and vertical dimensions. Then, generally, the coastal and bottom influences are important.

In Chapter 2 the several phenomena caused by wind on a water system will be treated shortly. A more extended treatment will be given in the Chapters 4, 5 and 6.

Chapter 3 deals with the exchange processes of air and water (exchange of momentum, temperature and humidity) as well as with the exchange processes between several layers of a stratified system (exchange of momentum, temperature and concentration).

## 2 Wind-generated phenomena

As the wind blows over a water surface, the interaction of the wind and water consists of a shear stress at the surface and sometimes a normal pressure component on a wavy surface. Moreover, internal friction exists in the air flow as well as in the water flow, completed by the friction between water and bottom and walls.

These various shear stresses and pressures cause various physical phenomena, generated by the wind-water interaction. Some of these phenomena have already been treated in DHL [1974a] dealing with the influence of wind on the vertical velocity profile in homogeneous water flows. The phenomena are:

### a. Vertical wind velocity profile

Figure 1 shows the wind velocity and the water velocity to be the same at the very water surface. Generally this velocity is much smaller as compared to the velocity at some meters over the surface. The wind velocity profile near the water surface is generally estimated to be of a logarithmic shape. The current velocity at the water surface is of the order of 3 percent of the wind velocity at an altitude of 10 m (see DHL [1974a]).

### b. Vertical water velocity profile

In an originally stagnant water system the wind causes a surface current velocity  $u_s$  by shear stress, indicated in Figure 1 by the shear stress  $\tau_s$ . The internal shear stress in the water gives rise to a vertical velocity profile, mostly supposed to be a logarithmic shape near the water surface (boundary layer).

For an unstratified system in an enclosed, two-dimensional basin the surface flow causes a bottom return flow. The total vertical velocity profile is shown schematically in Figure 1. The exact shape depends among other factors on the bottom shear stress  $\tau_b$ , the surface shear stress  $\tau_s$  and the turbulence of the flow.

For a stratified system consisting of several, more or less homogeneous, layers the whole of flows and counter flows is much more complicated. Moreover, homogeneous flows as well as stratified flows generally are three-dimensional, sometimes resulting in an obvious horizontal shift of flow and counter flow.

### c. Surface waves

In field circumstances a wind velocity  $U_w > 1$  m/s (and  $U_w > 3$  m/s for laboratory tests) causes slowly moving ripples on the water surface, with typical wave lengths of some centimeters and amplitudes of some millimeters. The wind ripples grow and disappear quickly with the rise and fall of the wind. Much slower the gravity waves grow by wind influence. Figure 2 shows a surface with only wind ripples and a surface with gravity waves and superimposed ripples. On a wavy surface the wind-water interaction consists of a shear stress and a normal pressure gradient, but on a smooth surface only the shear stress is important to the energy transfer. In the presence of waves there is much more energy transfer from the wind to the water surface. However, it turns out that the surface velocity  $u_s$  does not change very much with the existence of waves but the effect of surface waves is a deepening of the rapid flowing surface layer.

### d. Wind set-up

In an enclosed (or partly enclosed) basin the wind causes a leveling-down of the water surface by shear stress. For the simple two-dimensional case the effect of the wind is shown schematically in Figure 3a. The wind set-up is the direct mechanism generating the counter flow at the bottom of a homogeneous water system. Whether the exact shape of the water surface is convex, concave, linear, or about linear depends on the wind velocity, and on the length and depth of the water system.

### e. Vertical mixing in stratified system

It has been shown experimentally that an originally continuously stratified system will have a well-mixed upper layer under the influence of wind. The reason is a sharply increasing vertical diffusion by surface currents and surface waves. The position of the interface between well-mixed upper layer and stratified lower layer depends on the wind velocity and on some other effects (see Section 5.3 and 5.4).

In an enclosed system the return flow occurs in the upper layer near the interface. Of course, the shear stress generates a flow in the same direction just below the interface. One can imagine that, this way, the wind changes a (continuously) stratified system into a system of homogeneous layers separated by sharp interfaces. Figure 3b shows a scheme of the flow system.

#### f. Horizontal currents

As already mentioned the wind set-up is dependent on the length and depth of the basin. In case of an inhomogeneous length and depth profile the differences in set-up on one horizontal line perpendicular to the wind direction cause horizontal currents. Also the internal shear stress shifts the system of flow and counter flow, causing horizontal velocity gradients. Figure 4 shows a rectangular basin with parabolic depth profile. Flow and counter flow are shifted horizontally, producing two surface circulations in opposite directions.

An inhomogeneous wind velocity (for instance by partly shielding) may also cause an inhomogeneous horizontal velocity field, of course.

#### g. Heat exchange

Generally the air and water temperatures are different. The heat exchange, either by convection or radiation, is enhanced at increasing wind velocity. Quick mixing of the upper water layer and lower wind layer keeps the air-water temperature difference as large as possible. Moreover, the wind maintains the relative humidity at less than 100 percent near the water surface. Then, by evaporation, a small temperature difference is maintained between the air and water.

#### h. Seiches

In an enclosed system periodic movements of the water surface can occur due to the sudden disappearance of external forces. Such periodic movements of the water surface are called seiches (or internal seiches on the interface). Wind can cause a seiche when it falls down quickly. The non-supported levelling-down of the water surface is the origin of the seiche. Seiches in lakes have been studied very intensively during the last quarter of the nineteenth century and the first few decades of this century (see Hutchinson [1957]).

#### i. Other wind effects

More special wind effects can occur by conjunction of wind force and for instance the Coriolis force, or conjunction of wind drift and waves. Such special effects are Kelvin waves, Poincaré waves, Langmuir circulations, coastal jets, up and down welling, and others. Mostly, these effects have importance only to the local flow field. Sometimes, the influence of the

secondary phenomena on the large scale circulations is taken into account indirectly: for instance, the mixing of the small Langmuir circulations enlarges the horizontal and vertical diffusion coefficients.

### 3 Exchange processes

#### 3.1 Exchange across the air-water interface

In the air-water interaction one distinguishes the exchange of momentum and heat. The humidity exchange is less important to the scope of this report. In all cases wind plays an important role.

The exchange processes cannot always be treated separately. For instance, the formation of the thermocline is the result of the input in the water system of heat and momentum.

The exchange of momentum and heat is described with the parameters  $U_w$  and  $\Delta T$ .  $U_w$  is the mean wind velocity, mostly at the reference height of 10 m above the water surface.  $\Delta T$  is the air-water temperature difference. It holds (see for instance Pond [1973]):

$$\frac{\tau_o}{\rho_a} \stackrel{\text{def}}{=} -\overline{U'W'} = C_D U_w^2 \quad (3.1)$$

$$\frac{Q_s}{\rho c_p} \stackrel{\text{def}}{=} \overline{W'T} = C_T U_w \Delta T \quad (3.2)$$

where

$C_D$  drag coefficient or wind stress coefficient

$C_T$  Stanton number

$\tau_o$  shear stress at the air-water interface

$Q_s$  sensible heat flux

$\rho_a$  air density

$c_p$  specific heat at constant pressure

$T$  temperature

$U', W'$  turbulent velocity fluctuations in directions  $x$  and  $z$  (with wind direction parallel to  $x$ , and  $z$  in vertical direction)

The covariances  $\overline{U'W'}$  and  $\overline{W'T}$  (with  $\overline{W'T'} = \overline{W'T}$ ) are called Reynolds fluxes. One method to determine the values of  $C_D$  and  $C_T$  is to measure the covariances directly (see Pond [1973] for references to several measurements). Moreover,  $C_D$  and  $C_T$  can be determined from profile measurements of  $U_w$  and  $T$ . According to Monin-Obukhov's similarity theory these vertical profiles are similar in a non-stratified boundary layer:

$$\frac{\partial U_w}{\partial z} = \frac{U_{w*}}{\kappa z} \quad (3.3)$$

The friction velocity  $U_{w*}$  depends on the turbulent fluctuations  $U'$  and  $W'$  and the shear stress  $\tau_o$  by definition:

$$U_{w*} \stackrel{\text{def}}{=} \sqrt{-U'W'} \stackrel{\text{def}}{=} \sqrt{\frac{\tau_o}{\rho_a}} \quad (3.4)$$

Integration of Equation (3.3) (and similar equation for  $\frac{\partial T}{\partial z}$ ) results in:

$$U_w = \frac{U_{w*}}{\kappa} \ln \left| \frac{z}{z_{o,a}} \right| \quad (3.5)$$

where  $z = 0$  at the mean water surface. The integration constant  $z_{o,a}$  is called the roughness height and indicates the virtual origin of the logarithmic velocity profile. ( $z_{o,a}$  is of the order of  $10^{-3}$  m.) Equation (3.5) holds for  $z \geq z_{o,a}$ . For non-stratified systems according to Equation (3.1) and (3.5):

$$C_D = \left[ \frac{\kappa}{\ln \frac{z}{z_{o,a}}} \right]^2 \quad (3.6)$$

and  $C_D = C_T$  (similarity).

Recent measurements show:

$$C_D (z = 10 \text{ m}) = 1.5 \times 10^{-3} (\pm 10 \text{ to } 20\%)$$

for wind velocities  $U_w \lesssim 15$  m/s and open sea conditions.

The experiments have been tabulated by Pond [1973].

Five experiments by several authors (see Pond [1973]) induce:

$$C_T \approx 1.5 \times 10^{-3} (\pm 0.5 \times 10^{-3})$$

Some remarks on  $C_D$  and  $C_T$

---

- If  $C_D$  and  $C_T$  are really independent of  $U_w$  then Equations (3.1) and (3.2) show the momentum transport to be proportional to  $U_w^2$  while the heat exchange is only proportional to  $U_w$ . Moreover, in the long run the latter exchange is reduced by decreasing  $\Delta T$ .

- It is not quite certain that  $C_D$  is independent of  $U_w$ . A lot of experiments

have been carried out to find the  $\tau_o - U_w$  relation with the result of  $p$  not always being equal 2 in  $\tau_o \sim U_w^p$ . (See DHL [1974a].)

- Surely  $C_D$  and the surface roughness  $z_o$  are dependent on the fetch. In case of a short fetch the boundary layer (with the logarithmic velocity profile) is not fully developed.

Some remarks on  $\tau_o$  and  $\tau_s$

- The momentum exchange is not always locally. In open sea systems a large portion of the total momentum builds up the wave field (with wind ripples and gravity waves, see Figure 2) with a momentum exchange to the currents later on. Then one can imagine the total momentum flux  $\tau_o$  (with  $\tau_o \stackrel{\text{def}}{=} \rho_a U_{w*}^2$ ) consists of the shear stress momentum  $\tau_s$  (with  $\tau_s \stackrel{\text{def}}{=} \rho u_{s*}^2$ ) and the wave momentum  $\tau_w$ :

$$\tau_o = \tau_s + \tau_w$$

with  $\tau_s \approx 0.2 \tau_o$  for field circumstances (Dobson [1971]). In the laboratory Wu [1975c] suggests  $\tau_s = \alpha \tau_o$  with  $\alpha = 0.2$  to  $0.7$ .

In case of an upper layer well-mixed by turbulence generated in the upper layer this bipartition may be important. As well as breaking waves as shear velocity generate turbulent eddies in the upper layer both with energy dissipation rates. These dissipation rates depend on the velocity scale and on the scale of the generated eddies (see Tucker and Green [1977]).

- The generation of energy depends on the fetch and therefore on the dimensions of the water system.
- At a smooth air-water interface the tangential shear stresses are equal on both sides:

$$\tau_o = \tau_s$$

### 3.2 Mixing in stratified system

This section deals with some characteristics of a stratified system, especially with the view on the stability of a stratified flow. By stability is to be understood the reduced ability of vertical mixing in comparison to an

homogeneous system.

Many lakes and seas are stably stratified, density increasing downwards. In lakes the stratification is caused by temperature differences, and in seas by temperature and salinity differences.

Richardson numbers  $Ri$ ,  $Ri_o$

Some characteristics of the stratification can be expressed by the Richardson number  $Ri$ :

$$Ri = - \frac{g \frac{\partial \rho}{\partial z}}{\rho \left( \frac{\partial u}{\partial z} \right)^2} \quad (3.7)$$

Stratification has a decreasing effect on vertical turbulent diffusion. Munk and Anderson [1948] gave semi-empirical relations for the vertical diffusion coefficients for momentum ( $\epsilon_{u,z}$ ) and mass ( $\epsilon_z$ ) in comparison with a homogeneous system ( $\epsilon_{u,z,N}$  and  $\epsilon_{z,N}$ ):

$$\frac{\epsilon_z}{\epsilon_{z,N}} = \left( 1 + \frac{10}{3} Ri \right)^{-3/2} \quad (3.8)$$

$$\frac{\epsilon_{u,z}}{\epsilon_{u,z,N}} = \left( 1 + 10 Ri \right)^{-1/2} \quad (3.9)$$

Some other relations between the vertical diffusion coefficients and  $Ri$  circulate (see DHL [1974c]). The Munk-Anderson relation seems to agree with measurements (on non-tidal systems) on a large  $Ri$ -range, but the experimental data are widely scattered.

Often, the  $Ri$ -field is inhomogeneous and time-dependent. Lacking knowledge of the local  $Ri$ -value is the reason to introduce the overall Richardson number  $Ri_o$ :

$$Ri_o = \frac{g \Delta \rho}{\rho} \frac{h}{\Delta u^2} \quad (3.10)$$

with  $\Delta \rho$ ,  $\Delta u$  and a depth  $h$  being some characteristic parameters of the stratified flow. In case of a two-layer flow with two homogeneous layers the values

of  $\Delta\rho$  and  $\Delta u$  are evident, and for a two-layer system with only one flowing layer  $h$  is the depth of that flowing layer.

### Turbulent diffusion

The vertical density transport  $T_z$  is given by:

$$T_z = -\epsilon_z \frac{\partial\rho}{\partial z} \quad (3.11)$$

meaning the transport by turbulent diffusion across a unit surface.  $\epsilon_z$  and  $\partial\rho/\partial z$  are the local values at that surface. The density transport velocity is given by:

$$w_t = \frac{T_z}{\Delta\rho} \quad (3.12)$$

and with Equations (3.8) and (3.11):

$$w_t \sim (1 + \frac{10}{3} Ri)^{-3/2} \quad (3.13)$$

### Velocity profile

The suppressing of turbulent eddies in a stratified system influences the vertical velocity profile. Because of the mixing ability of turbulent eddies a weakly stratified area generally has a smaller vertical gradient as compared to a strongly stratified region. Sure enough, measurements below the thermocline in lakes and seas often show the combination of small vertical velocity gradient with a weak stratification, and a large velocity gradient with a large density gradient. (See for instance Kullenberg et al. [1974]).

### Entrainment

Consider a two-layer flow with an interfacial region with a large density gradient and a large velocity gradient. For local Richardson number smaller than 0.25 instabilities occur by breaking internal waves pushing parcels of water from one layer into the other. The interface is sharpened again by the buoyancy effects, as well as by turbulent mixing. The buoyancy effect may push back a parcel of water to the interface. By the mixing ability of adjacent turbulent regions in the layers with weak stratification a parcel of water may be mixed into that layer. By the latter effect mass exchange takes place across the interface while keeping the interface sharp. This process is called

entrainment. It can be easily shown that the most exchange takes place from a weakly turbulent layer to a highly turbulent layer, with decreasing density difference between the layers, and an interface moving upwards or downwards according to the exchange residue. In case of one stagnant layer entrainment takes place only by the flowing layer.

Laboratory experiments on entrainment have been carried out by e.g. Kato and Phillips [1969], Turner [1972], Linden [1975] and Kantha, Phillips and Azad [1977]. The water system always consists of one stagnant layer, the other layer being stirred by a grid (Turner, Linden) or a surface stress was applied by a moving screen at the surface (Kato, Kantha).

A few years ago the relation

$$w_e \sim Ri_o^{-1} \quad (3.14)$$

was considered the most fundamental proportionality of the entrainment velocity  $w_e$  and the stratification parameter  $Ri_o$  (see DHL [1974c]). However, especially the survey of Kantha et al. [1977] concludes to the relation

$$w_e = f(Ri_o) \quad (3.15)$$

with the proportionality (3.14) applies the measurements for small values of  $Ri_o$  ( $90 < Ri_o < 400$  with  $u_{s*}$  instead of  $\Delta u$  in Eq. (3.10)).

#### Diffusion experiments

Kullenberg et al carried out prototype experiments to determine the vertical diffusion coefficient. In the upper 20 m (over the thermocline) of open seas, coastal seas and fjords the empirical expression (Kullenberg [1971]):

$$\epsilon_z N^2 = 8.10^{-8} \overline{U_w^2} \left| \frac{\partial u}{\partial z} \right| \quad (U_w > 4 \text{ to } 5 \text{ m/s})$$

relates the vertical diffusion coefficient  $\epsilon_z$  to the wind velocity  $U_w$  and the stratification parameter  $N$ :

$$N^2 \stackrel{\text{def}}{=} \frac{g}{\rho} \left| \frac{\partial \rho}{\partial z} \right|$$

To relate  $\epsilon_z$  to the fluctuation velocities in the water system, Kullenberg et al [1973, 1974] measured the shear-generated turbulent diffusion in stratified lakes some meters below the water surface. Measurements in Lake Ontario gave

$$\overline{\epsilon_z N^2} = 4.1 \times 10^{-8} (u'^2 + v'^2) \left| \frac{\partial u}{\partial z} \right|$$

(measured on the range  $10^{-7} > \epsilon_z N^2 > 10^{-10} \text{ m}^2/\text{s}^3$ ) with  $u'$  and  $v'$  the turbulent fluctuations of the current velocities in directions  $x$  and  $y$ . In the considered weak wind circumstances the values of  $\epsilon_z$  lie between the values 1 and  $4 \times 10^{-5} \text{ m}^2/\text{s}$ .

Horizontal diffusion coefficients are some orders of magnitude larger than the vertical coefficients, but are still dependent on the dimensions of the diffusing system. Measurements in Lake Ontario indicate horizontal coefficients in the epilimnion (over the thermocline) to be 1 or 2 orders of magnitude larger than in the hypolimnion (below the thermocline).

#### 4 Influence of wind on water surface

Some significant phenomena due to wind force acting on the very water surface are:

- shear stress  $\tau_s$  and  $\tau_o$  at the air-water interface
- wind drift velocity  $U_s$  at the water surface
- surface wind waves and wind ribs.

Moreover, on the whole water system the influence of wind causes:

- vertical wind drift velocity profile
- horizontal and vertical wind drift circulations in enclosed water basins
- wind set-up in water basins
- influence on the stratification: mixing of upper layer, equilibrium position of thermocline, set-up of thermocline
- seiches and internal seiches
- some other effects, due to combined action of wind force and other forces.

#### 4.1 Wind velocity profile $U_w(z)$ over the water surface

The wind-water momentum exchange is dependent on the wind velocity  $U_w$ . Experimentally  $U_w$  is measured above the zone of disturbance due to water waves but within a certain boundary layer. Then, knowledge of the vertical wind velocity profile is necessary for the  $U_w(z) - \tau_s$  relation.

#### Non-stratified air flow

For a non-stratified air flow the boundary layer adjacent to the water surface has a logarithmic vertical velocity profile:

$$U_w = \frac{U_{w*}}{\kappa} \ln \frac{z}{z_{o,a}} \quad (4.1)$$

where  $\kappa = 0.4$  is Von Kármán's constant. In open water systems Equation (4.1) agrees up to a height of the order of 100 m (Bouwmeester [1973]).

The definitions of the wind shear velocity is:

$$U_{w*} \stackrel{\text{def}}{=} \sqrt{\frac{\tau_o}{\rho_a}} \quad (4.2)$$

Another description of  $U_{w*}$  is:

$$U_{w*} = l \left( \frac{\partial U}{\partial z} \right) \quad (4.3)$$

defining a mixing length  $l$ . According to Prandtl mixing length theory  $l$  can be written as  $l = \kappa z$ .

The measuring of the roughness height  $z_{o,a}$  has already been indicated in Section 3.1. From empirical evidence Charnock [1955] and Wu [1967b] related  $z_{o,a}$  and  $U_{w*}$  by

$$\frac{g z_{o,a}}{U_{w*}^2} = \alpha = 0.0156 \quad (4.4)$$

However, other experiments show  $\alpha$  to be not constant (see DHL [1974a]). Recent measurements of Shaw and Lee [1976] indicate a sharply decreasing value of  $\alpha$  (down to  $\alpha \approx 0.001$ ) for small fetches.

#### Stratified air flow

For a stably stratified air flow the wind velocity profile is described by adding a linear term to Equation (4.1):

$$U_w = \frac{U_{w*}}{\kappa} \left\{ \ln \frac{z}{z_{o,a}} + \rho_a \frac{z - z_{o,a}}{L_s} \right\}$$

resulting in the "log linear" velocity profile. The Monin-Obukhov stability length  $L_s$  is related to density and velocity fluctuations. For stably stratified air flows the logarithmic velocity profile agrees with heights of up to a few meters over the water surface (Monin [1972], Marciano and Harbeck [1954]).

#### 4.2 Roughness height $z_{o,a}$

As mentioned before the roughness height  $z_{o,a}$  indicates the virtual origin of the logarithmic profile a small distance over the water surface. The logarithmic profile over a smooth, fixed surface is given by:

$$U_{w,sm} = \frac{U_{w*}}{\kappa} \ln \left( \frac{U_{w*} z}{v_a} \right) + U_{w*} C \quad (4.5)$$

Experimentally  $C$  is fixed on 4.9.  
Measurements on a rough sea surface give

$$\frac{U_w - U_{w,sm}}{U_{w*}} < 0 \quad (4.6)$$

with the exact value dependent on  $U_{w*}$ . In this region Charnock's relation (4.4) holds good.

In case of a smooth water surface and weak winds some investigators found a positive value of the reduced wind velocity difference, mentioned in (4.6). Csanady [1974] explains this effect by a contaminated water surface. Then local differences in surface tension absorb energy from the lower air layer. The consequence is a boundary layer thicker as compared to a smooth fixed surface. Then the water surface is "super smooth".

#### 4.3 Shear stress $\tau_o$ at water surface

The wind-induced shear stress at the water surface is expressed by:

$$\tau_o = \rho_a C_D U_w^p(z) \quad (4.7)$$

where  $U_w(z)$  the wind velocity at reference height  $z$ . Many investigators (see DHL [1974a]) derived empirical values of  $p$  and  $C_D$  with  $p$  equals mostly about 2. The empirical  $C_D$ -values are scattered widely.

Wu [1970] compiled the field (ocean) measurements by:

$$C_D(z = 10 \text{ m}) = 0.5 \times 10^{-3} U_w^{1/2}(10) \text{ for } 1 < U_w(10) < 15 \text{ m/s}$$

$$C_D(z = 10 \text{ m}) = 2.6 \times 10^{-3} \text{ for } U_w(10) > 15 \text{ m/s} \quad (4.8)$$

(The discontinuity at  $U_w(10) = 15 \text{ m/s}$  ( $C_D = 1.9 \rightarrow 2.6 \times 10^{-3}$ ) is equal to the (accidental?) discontinuity of the averaged measurements.)

Wu [1970] argued the scatter of  $C_D$ -values and especially the discrepancy between field- and laboratory measurements to be caused by the reference height of wind measurements, generally being fixed on  $z = 10 \text{ m}$  for field experiments and  $z = 0.1 \text{ m}$  for laboratory experiments. Scaling up the reference height with the wind velocity according to a constant value of the Froude number:

$$F = \frac{U_w(z)}{\sqrt{gz}} \quad (4.9)$$

the discrepancy disappears.

#### 4.4 Wind-driven surface velocity $u_s$

The wind drift velocity  $u_s$  is dependent on the fetch. Wu [1973b,c] scaled the reference height of  $U_w$ -measurement in such a way that the fetch is taken into account. Then the wind drag coefficient  $C_D$  can be derived from (Wu [1969a]):

$$\frac{1}{\sqrt{C_D}} = \frac{1}{K} \ln \left( \frac{91}{C_D F^2} \right) \quad (4.10)$$

with the value of  $z$  in the Froude number  $F$  (Eq. (4.9)) proposed by Wu [1971]:

$$\begin{aligned} z &= 7.35 \times 10^{-7} \text{ Re}_s^{2/3} \text{ m} && \text{for } \text{Re}_s < 5 \times 10^{10} \\ z &= 10 \text{ m} && \text{for } \text{Re}_s > 5 \times 10^{10} \end{aligned} \quad (4.11)$$

and the fetch Reynolds number  $\text{Re}_s$  defined by:

$$\text{Re}_s = \frac{U_w(z)L}{\nu_a} \quad (4.12)$$

On a wavy surface the total surface drift  $u_s$  can be split up into two contributions: the directly wind-induced surface drift  $u_{s,dw}$  and the wave-induced Stokes current  $u_{s,wave}$  (Wu [1975c]). Both contributions are dependent on fetch. In laboratory tanks generally  $u_{s,wave}$  is about 10% or less of the total surface drift  $u_s$ , but  $u_{s,wave}$  is a large contribution to  $u_s$  in field conditions. (See also the difference of  $\tau_o$ ,  $\tau_s$  and  $\tau_w$  as mentioned on page 9.) Experimentally is found (Wu [1973b]):

$$u_{s,dw} \approx 0.53 U_{w*} \quad (4.13)$$

for the surface drift without Stokes transport.

From Equations (4.13), (4.10) and (4.11) the surface drift can be calculated in dependence of the fetch. The results are shown in Figure 5 (Wu [1975b]). Then, by scaling the reference height  $z$  of the wind velocity measurement on the fetch, the total surface drift is almost independent of the fetch and is about 3.5% of the wind velocity at large fetch.

#### 4.5 Shear stress ( $\tau_o$ , $\tau_s$ ) measurements

Several quite different methods exist to derive, experimentally, the shear

stress  $\tau_o$  or  $\tau_s$  (see also DHL [1974a]).

- velocity profile method

With this method the vertical velocity profile of the air flow adjacent to the water surface is measured. Then, from Equation (4.1) the shear stress velocity  $U_{w*}$  is known and from the definition (4.3) the shear stress  $\tau_o$  is derived. In exactly the same way the measurement on the water flow profile leads to the shear stress  $\tau_s$ .

- wind set-up method

The phenomenon of inclination of the water surface of an enclosed system under influence of wind is treated extensively in Section 5.2.

In case of a rectangular closed channel the wind set-up satisfies:

$$\frac{\partial h}{\partial x} = \frac{\tau_s}{g\rho h} \quad (4.14)$$

where  $h$  the local water depth. For more difficult bathymetry the set-up shear stress relation is difficult to derive. Moreover, the reliability of surface inclination measurements is rather low because of the small value of the inclination proper and because of necessary correction terms in case of surface waves.

- eddy correlation method

With this method the covariance  $\overline{u'w'}$  is measured directly with  $u'$  and  $w'$  the turbulent velocity fluctuations of two perpendicular velocity components.

By definition

$$\tau_o = \rho_a \overline{U'W'} \quad (4.15)$$

and

$$\tau_s = \rho \overline{u'w'} \quad (4.16)$$

assuming constant values of  $\tau$  in the region of the logarithmic velocity profile.

- other methods

Some other methods to derive the shear stress at the water surface are described by Pond [1973]:

According to the Monin-Obukhov similarity (Eq. (3.6)) the wind velocity profile measurement can be replaced by the measurement of the temperature profile and the humidity profile.

Energy balance methods describe the balance of mechanic production  $-\overline{U'W'}$   $\frac{\partial U_w}{\partial z}$  and the molecular dissipation  $E_{diss}$ .  $E_{diss}$  can be measured. Another energy balance method takes into account the radiation and conduction of heat to and from the atmosphere.

With the geostrophic wind method the Coriolis force plays an important role.

Wieringa [1973] applied the wind profile method, the wind set-up method and the eddy correlation method on the same lake. The results are:

eddy correlation method:

$$C_D(z = 10 \text{ m}) = 0.0007 U_w^{0.3} (10) \quad \text{for } 5 < U_w < 15 \text{ m/s} \quad (4.17)$$

wind set-up:

$$C_D \approx 0.0024 \quad \text{for } 6 < U_w < 12 \text{ m/s} \quad (4.18)$$

wind profile: for  $U_w$  up to 10 m/s good agreement with the eddy correlation method. Deviations above  $U_w \approx 10$  m/s.

The results are shown in Figure 6. The discrepancy of the eddy correlation results and the wind set-up results may indicate the false assumption of  $\tau_{\text{air layer}} = \tau_0$ .

Hsu [1974] compiled 1000 log-linear wind profile measurements over the sea. The results for (nearly) neutral stratification conditions are:

$$C_D(z = 10 \text{ m}) = 0.00122$$

and

$$z_0 = 0.01 \text{ m}$$

## 5 Wind influence on one-dimensional (1D-vertical) water system

In this chapter the influence of wind in an open or closed water system is treated irrespective of the shape of walls and bottom. Then, the water system is supposed to be one-dimensional (in vertical direction) with only a restriction in the longitudinal direction (parallel to the wind direction) in case of a closed system.

### 5.1 Vertical water velocity profile

#### Surface layer in open systems

The wind-induced shear stress  $\tau_s$  on the water surface causes a drift velocity at the very water surface of about 3.5% of the wind velocity at an altitude of 10 m:

$$u_s \approx 0.035 U_w \quad (10) \quad (5.1)$$

The internal shear stress  $\tau(z)$  causes a decreasing drift velocity to greater depths in the surface layer. Near the water surface (boundary layer) the drift velocity satisfies (see also Eqs. 4.2 and 4.3):

$$\frac{\partial u(z)}{\partial z} = - \frac{u_*}{\kappa z} \quad (5.2)$$

with

$$u_* = \sqrt{\frac{\tau_s}{\rho}} \quad (5.3)$$

In these equations  $\tau(z)$  is supposed to be equal to  $\tau_s$  in the surface layer. Similar to the treatment of the wind velocity profile (see Section 4.1) integration of Equation (5.2) leads to

$$u(z) - u_s = - \frac{u_*}{\kappa} \ln \frac{z}{z_0} \quad (5.4)$$

In the above mentioned equations the water surface is supposed to be smooth without waves.

Measurements of Wu [1975c] in a flume (depth 1.5 m) show logarithmic velocity profiles near (but not immediately below) the water surface down to the lowest measurements of 0.8 m below surface. However, immediately below the water

surface the current varies linearly with depth. Figure 8a shows the linear profile just below the water surface for various wind velocities, and Figure 8b shows the surface current  $u_s$  as obtained by extrapolating the curves of Figure 8a. Figures 8c, d show the velocity profile (in terms of  $(u(z) - u_s)$ ) more below the surface in the logarithmic velocity profile range.

### Closed basins

In a closed basin the drift flow generates a counter flow because of continuity. Generally the system of drift flow and counter flow is a three-dimensional circulation because of the three-dimensional geometry of the basin. Moreover, the Coriolis force has opposite directions (side-wards) for drift flow and counter flow. In the following the water circulation is supposed to be two-dimensional (vertical) as an approximation of the flow in a not too large closed channel.

For the stationary case in a two-dimensional basin the vertical integral of the velocity profile is zero. Figure 7a shows some experimental and theoretical two-dimensional velocity profiles. For a laminar flow the velocity  $u(z)$  satisfies (see DHL [1974a]):

$$\frac{u(z)}{u_s} = 3\left(\frac{z}{h} + 1\right)^2 - 2\left(\frac{z}{h} + 1\right) \quad (5.6)$$

The same profile is applicable for a turbulent flow with  $\epsilon_z$  is constant over the whole depth. Some characteristic points of the Equation (5.6) profile are:

$$\begin{aligned} u &= 0 && \text{at } z = 1/3 h \\ u_{\max} &= \frac{1}{3} u_s && \text{at } z = 2/3 h \end{aligned}$$

with  $z = 0$  at the water surface.

However, generally the flow is neither laminar nor has a constant vertical diffusion coefficient  $\epsilon_z$ . Obviously the measured velocity profile of Baines and Knapp [1965] differ very much from the profile of Equation (5.6). Baines and Knapp's profile are in good agreement with a theoretical calculation of Reid [1957]. Reid makes use of mixing lengths derived from a  $\epsilon_z$ -profile as shown in Figure 7b.  $\epsilon_z$  has the largest value in the centre part of the flow, diminishes to a small value at the surface and to zero at the bottom. Then,

the momentum exchange in the central part is large, and smaller near the surface and near the bottom, resulting in a jet at the surface and a jet at the bottom. Reid's solution is independent of the Reynolds number  $Re$  (also Baines and Knapp's measurements seem to be independent on  $Re$ ), but one of the parameters is the shear stress ratio  $\tau_s/\tau_b$ . This ratio is essentially 2 in laminar flows but is often taken to be

$$\tau_s/\tau_b \approx 10$$

for turbulent flows.

In small basins the circulation often shows an even more obvious surface and bottom flow with a slow homogeneous velocity in the centre part. This is caused by too small a fetch so that the surface and bottom boundary layers do not overlap.

## 5.2 Wind set-up of water surface and interface

### Water surface

Ekman [1923] treated the inclination of the water surface of a deep-closed sea under influence of wind. However, it turns out that Ekman's theory is doubtful for deep oceans, but reliable with small, shallow seas (Welander [1957]), with a depth  $H$  of the same order of magnitude as the depth of frictional resistance  $D$ :

$$D = \pi \sqrt{\frac{2\varepsilon_{u,z}}{f}} \quad (5.7)$$

$f$  is the Coriolis parameter. Ekman took account of the Coriolis force. However, in this section the Coriolis force will be neglected, which is permitted in basins of small lateral dimensions.

The wind influence on the water surface of a small basin with rectangular cross-section has been studied by Hellstrom [1941]. The inclination of the water surface satisfies:

$$\frac{\partial h}{\partial x} = \frac{\tau_s + \tau_b}{g\rho h} \quad (5.8)$$

(A correction term  $-\frac{1}{\rho g} \frac{\partial p}{\partial x}$  can be added in Equation (5.8) to take into account

the static air pressure  $p$ . Another correction term is described by Ursell [1956] and Shemdin [1973] to correct laboratory measurements in shallow models, but negligible in field circumstances.)

To apply Equation (5.8) to a basin with variable depth and width  $\frac{\partial h}{\partial x}$  can be approximated by substitution of a depth  $\bar{h}$  equal to the averaged value of  $h$  over the cross-section (at  $x$ ) perpendicular to the wind direction.

Keulegan's [1951] flume measurements gave, for a smooth water surface:

$$\frac{S}{a} = 3.3 \times 10^{-6} \frac{U_w^2}{gh} \quad (5.9)$$

where  $S$  = the set-up between two points of separation  $a$  (in the wind direction). The proportional constant in Equation (5.9) depends on the measuring height of  $U_w$ . For a wavy water surface another term must be added (see Keulegan's paper or DHL [1974a]).

#### Interface of two-layer system

In a closed two-layer basin the water surface as well as the interface are inclined by influence of wind. A scheme of such a system has been given in Figure 9.

Chatou [1961] derived the governing expressions for a closed two-dimensional two-layer circulation, subjected to the following assumptions.

- $U_w$  is uniform, then  $\tau$  is constant and homogeneous and the circulation is two-dimensional
- hydrostatic pressure exists
- density difference  $\rho_i - \rho_s$  is small (index  $s$  refers to surface and surface layer, index  $i$  to interface and lower layer)
- static equilibrium is considered.

The derived expressions for the inclination of surface and interface are (notation as in Figure 9):

$$\frac{d\Delta h_s}{dx} = \frac{\tau_s - \tau_i}{\rho_s g h_s} \frac{l}{l + \frac{\Delta h_s - \Delta h_i}{h_s}} \quad (5.10)$$

$$\frac{d\Delta h_i}{dx} = - \frac{\rho_s}{\rho_i - \rho_s} \left[ \frac{d\Delta h_s}{dx} + \frac{\tau_b - \tau_i}{\rho_s g h_i} - \frac{l}{l + \frac{\Delta h_i}{h_i}} \right] \quad (5.11)$$

where  $\tau_s$  and  $\tau_b$  are positive and  $\tau_i$  is negative.  
Consequences of Equations (5.10) and (5.11) are:

$$\frac{d\Delta h_s}{dx} > 0 \quad \text{as long as} \quad \frac{\Delta h_s - \Delta h_i}{h_s} > -1 \quad (5.12)$$

$$\frac{d\Delta h_i}{dx} < 0 \quad \text{as long as} \quad \frac{\Delta h_i}{h_i} > -1 \quad (5.13)$$

The right-hand side inequalities of (5.12) and (5.13) mean that the lower layer does not reach the water surface and the upper layer does not reach the bottom respectively. Moreover:

$$\left| \frac{d\Delta h_i}{dx} \right| \geq \frac{\rho_s}{\rho_i - \rho_s} \left| \frac{d\Delta h_s}{dx} \right| \quad (5.14)$$

From Equation (5.10) and (5.11) can be derived that

$$\frac{d\Delta h_s}{dx}(H_s - H_b) + \frac{\rho_i - \rho_s}{\rho_s}(H_i - H_b) = \frac{\tau_s - \tau_b}{\rho_s g} \quad (5.15)$$

The total set-ups  $\Delta h_{s,tot}$  of the free surface and  $\Delta h_{i,tot}$  of the interface, on the whole length of the basin can be determined by integration of Equation (5.15) and application of Equation (5.10) and Equation (5.11):

$$\frac{\Delta h_{s,tot}}{a} = \frac{\tau_s - \tau_i}{\rho_s g h_s} \quad (5.16)$$

$$\frac{\Delta h_{i,tot}}{a} = - \frac{\rho_s}{\rho_i - \rho_s} \left[ \frac{\tau_s}{\rho_s g h_s} - \frac{\tau_i}{\rho_s g h_s} \cdot \frac{h_s + \bar{h}_i}{\bar{h}_i} + \frac{\tau_b}{\rho_s g \bar{h}_i} \right] \quad (5.17)$$

with

$$\frac{1}{h_i} = \frac{1}{a} \int_{x_0}^{x_0+a} \frac{dx}{h_i} \quad (5.18)$$

Note 1. Neglecting  $\tau_i$  and  $\tau_b$  with respect to  $\tau_s$  the wind drag coefficient  $C_D$  can be determined from Equation (5.16).

Note 2. Atmospheric pressure differences can be taken into account by

$$H'_s = H_s + \frac{p_a}{\rho_s g} \quad \text{and} \quad \Delta h'_s = \Delta h_s + \frac{p_a}{\rho_s g}$$

where  $p_a$  = the pressure difference with a reference pressure.

### Experiments on interfacial set-up

Hellström [1953] concluded to the empirical relation:

$$s = \frac{0.037 a U_w^{1.8}}{g h_s \Delta \rho} \quad (5.19)$$

where  $s$  = the slope of the interface.  $a$  is a constant between 1 and 1.5, and  $\Delta \rho$  is the density difference between the homogeneous upper layer and the lower layer just below the interface.

Wu [1975a] studied in a laboratory flume, the wind set-up on a system of a mixed upper layer, interface and stratified lower layer. The slope of the interface satisfies:

$$s = 5.4 \times 10^{-4} Ri^{-1} \quad (5.20)$$

with  $Ri$  defined to be

$$Ri = \frac{g \Delta \rho h_s}{\rho u_*^2}$$

$u_*$  is determined by fitting the velocity profile just below the water surface to the logarithmic profile.

Wu [1977] shows the Equations (5.19) and (5.20) to be almost identical.

### 5.3 (Internal) Seiche

Wind set-up in a closed basin and a time-varying wind cause oscillations on the free surface and on interfaces. A special type of oscillation is a standing surface wave or standing internal wave with the largest wave length in the considered basin. Those waves are called seiches and internal seiches, with only one node in the middle of the basin.

Simple seiches occur in a rectangular basin with a suddenly decreasing wind.

The period of the surface seiche is

$$t_s = \frac{2L}{\sqrt{gh}} \quad (5.21)$$

and the internal seiche on the interface of a two-layer system:

$$t_i = \frac{2L}{\sqrt{g \frac{\Delta\rho}{\rho} \left( \frac{1}{h_s} + \frac{1}{h_i} \right)}} \quad (5.22)$$

where  $L$  and  $h$  are the length and depth of the basin,  $h_s$  and  $h_i$  are the layer depths and  $\Delta\rho =$  the density difference of the layers. Length and depths satisfy  $L \gg h_s + h_i$ .

In complex systems the oscillations are more complicated by standing waves of higher order, lateral seiches, internal waves, friction forces, Coriolis forces and so on.

Seiches in a three-layer system in a rectangular basin have been described by Longuet-Higgins [1952].

The most extensive field measurements in stratified lakes have been made by Mortimer [1952a, b, 1953]. In large lakes the Coriolis effect is important. Then, the maximum period of an (internal) seiche is half a pendulum day (pendulum day =  $\frac{\pi}{\phi}$  day with  $\phi =$  the latitude).

Linear theory describes a sine-shaped seiche. Non-linear theory concludes to a seiche with a steep front, in agreement with observations (Thorpe [1974]).

#### 5.4 Mixing of surface layer by wind (no heat exchange)

##### Kinetic and potential energy; dissipation of kinetic energy

Wind induces kinetic energy in the water surface by the shear stress  $\tau_o$ .

A large part of the energy is used to generate waves, the other part to generate drift currents. In turn, waves and drift currents induce turbulent eddies. In a stratified system the turbulent eddies cause mixing of the upper layer. The depth  $h_s$  of the mixed upper layer increases, while the increase of the potential energy is given by:

$$\frac{\Delta E_p}{\Delta t} = \frac{1}{\Delta t} \left[ \left( \frac{\Delta h_s \Delta \rho}{h_s} \right) g (h_s + \Delta h_s) \left( \frac{h_s + \Delta h_s}{2} \right) \right] \approx \frac{1}{2} h_s \Delta \rho g \frac{\Delta h_s}{\Delta t} \quad (5.23)$$

where  $\Delta\rho =$  the density difference between the upper layer and the part of the lower layer mixed up in the upper layer in the time interval  $\Delta t$ .

The kinetic energy induced by wind on a smooth surface is

$$\frac{\Delta E_k}{\Delta t} = \tau_s u_s \quad (5.24)$$

per unit surface and per unit time.

The deepening of the surface layer is not only a balance of the kinetic energy  $E_k$  and the potential energy  $E_p$ . Most of the kinetic energy is converted into heat by viscous dissipation, in experiments the ratio  $\Delta E_p / \Delta E_k$  can be of the order of  $10^{-2}$  or  $10^{-3}$  (Wu [1973a]). Generally, with increasing  $h_s$  more kinetic energy is dissipated before reaching the interface.

### Entrainment, laboratory experiments

The wind-induced kinetic energy (in the form of turbulent eddies) partly reaches the interface and deepens the mixed surface layer. The deepening process is called entrainment with the entrainment velocity  $w_e$  (see also Section 3.2). Many laboratory investigations have been done to study the phenomena of turbulent mixing and entrainment in stratified systems. Reviews have been given by Turner [1973] and DHL [1974c], while more recent experiments have been carried out by Linden [1975] and Kantha et al [1977]. The overall shear Richardson number  $Ri_*$ , defined by

$$Ri_* = \frac{g \frac{\Delta \rho}{\rho} h_s}{u_*^2} \quad (5.25)$$

seems to be an important parameter to the entrainment in a layered system ( $u_* = \sqrt{\tau_s / \rho}$  by definition). In a theoretical model Tennekes [1973] makes acceptable the dependence of  $w_e$  on a Richardson number.

However, several experimental investigations show different results on the  $w_e$ - $Ri_*$  relation.

Kato and Phillips [1969] investigate the entrainment in a layered system in a cylindrical tank with a mechanically entrained water surface. They found

$$w_e = 2.5 \frac{u_*}{Ri_*} \quad (5.26)$$

Experiment of Wu [1973] and DHL [1974d] in rectangular tanks with wind resulted in:

$$w_e = 0.234 \frac{u_*}{Ri_*} \quad (5.27)$$

Ottesen-Hansen [1974] suggested the discrepancy of Equation (5.32) and (5.33) by a factor of 10 to be caused by an incompletely developed turbulence in the latter experiments.

The experiments mentioned show the proportionality (see the definition of  $Ri_*$ , Equation (5.31)):

$$w_e \sim u_*^3 \quad (5.28)$$

However, Phillips' [1966] similarity considerations, as well as the early stage of the Kato and Phillips experiment result in:

$$w_e \sim u_* \quad (5.29)$$

Moreover, Ottesen-Hansen [1975] derived a theoretical expression for the entrainment velocity immediately after the loading of the wind shear stress on a two-layer system

$$w_e = 0.2 u_* \quad (5.30)$$

The problem of the right  $w_e$ - $u_*$  proportionality seems to be a question of which of the forces actually are balanced in the specific stratified system. The various relevant phenomena are: surface shear stress, wall stress, acceleration of the surface layer, pressure forces, Coriolis forces, buoyancy and viscous dissipation.

Kato and Phillips [1969] and Turner [1973] gave a physical explanation of the  $w_e \sim u_*^3$  proportionality by suggesting a balance between the increase of potential energy (buoyancy), viscous dissipation and input of kinetic energy (surface shear stress).

Nihoul [1972] gave several notes to these estimates as the result of the investigation of the global energy budget of the turbulent region. One of his remarks is that the balance of  $(E_k - E_{diss})$  and  $E_p$  is only possible if the Brunt-Väisälä frequency  $N$  is large (meaning  $N^2$  ranging from 1 to 10 as is generally the case in laboratory experiments. However, in oceans  $N^2 \approx 10^{-6}$ ). Nihoul shows that in the early stage of a laboratory experiment as well as in the normal situation in the ocean  $E_k$  and  $E_{diss}$  are balanced. Buoyancy and Coriolis force influence the process after  $h_s$  has reached some critical value. This critical value is reached soon in laboratory experiments. So in the initial stage Equation (5.29) applies, after some time the entrainment satisfies the relation (5.28). Equation (5.30),  $w_e = 0.2 u_*$  has

been derived theoretically by Ottesen-Hansen for the entrainment velocity in the early stage of a two-layer experiment.

Ottesen-Hansen approximated (also theoretically) an expression for the deepening of the surface flow of an homogeneous system immediately after the loading of the wind:

$$w_e = 0.267 u_* \quad (5.31)$$

Ottesen-Hansen's Equations (5.30) and (5.31) indicate a somewhat slower deepening (in the early stage) for the stratified system. However, a weak point of these equations is the non-continuous transition from (5.30) to (5.31) in case of  $Ri \rightarrow 0$ .

The two Equations (5.30) and (5.31) apply to the period immediately after starting the wind force. Then, the Coriolis force and the pressure force due to wind set-up are negligible. After some time, the initial rate of deepening may be neglected and, in a not too large two-layered lake, there may be a balance of pressure force (wind set-up) and shear stress  $\tau_s$ :

$$-\frac{\tau_s}{\rho} = g \frac{\Delta\rho}{\rho} h_s \frac{dh_s}{dx} \quad (5.32)$$

With some approximations (e.g. uniform density in the upper layer, certain  $\epsilon_u$ -profile) and making use of an experimental value of an energy dissipation length scale Ottesen-Hansen derived:

$$w_e = 2.36 \frac{u_*}{Ri_*} \quad (5.33)$$

in agreement with the experiments of Kato and Phillips (Eq. (5.26)). Ottesen-Hansen suggests as general formula for the entrainment rate:

$$w_e = \frac{0.2 u_*}{\sqrt{1 + 0.0064 Ri_*^2}} \quad (5.34)$$

obtained by data-fitting with the experimental results of Kato and Phillips, Lofquist [1960] and Mortimer [1952]. Moreover the Equation (5.34) is chosen because for  $Ri$  with large values, the Equations (5.26) and (5.33) are found. Equation (5.34) and the experimental results are given in Figure 10.

The most recent laboratory experiments of Kantha, Phillips and Azad [1977] lead to the conclusion that  $w_e/u_*$  has no simple power-law dependence on  $Ri_*$  over the range studied. The formula  $w_e/u_* = f(Ri_*)$  equals  $w_e/u_* \sim Ri_*^{-1}$  on the range  $90 < Ri_* < 400$ .

Summing up the theoretical and experimental results on entrainment rate due to wind in a layered system there an initial stage exists (balance of  $\tau_s$  and  $E_{diss}$ ) with  $w_e \sim u_*$ , and after some time (influence of buoyancy, wind set-up Coriolis effect) with  $w_e \sim u_*^3$ . In laboratory experiments the initial stage is very short. In ocean circumstances with weak stratification Nihoul's energy consideration suggests an initial stage up to a depth of the upper layer  $h_s$  comparable to the Ekman depth  $u_*/\Omega$ .

#### Final remarks on $E_k$ , $E_p$ , $E_{diss}$

Generally, a "global" energy model is used in the energy balance of the entrainment process. That means that the energy equation of the upper layer has been integrated over the depth of the upper layer.

Nihoul [1972] has solved the energy equations for the initial stage of an initially linearly stratified system by taking into account the exact density distribution in the upper layer. The results of this "local" model, Figure 11b, show the mean density profile in the "mixed" turbulent layer. Figure 11a is the approximation of the density profile in the global model.

#### Influence of shear velocity on entrainment

In most entrainment experiments the wind-induced kinetic energy has been divided into turbulent motions, shear flow and surface waves. For instance, in Kato and Phillips' experiments a shear flow near the surface as well as turbulent eddies have been induced. Then, the following question arises: does it make any difference to the deepening process whether the turbulence at the interface is originated directly at the surface, or is originated by shear stress in the upper layer?

Linden [1974] consciously separated the sources of turbulent eddies. In his experiments he generated turbulent eddies in the upper layer by an oscillating grid, and measured the proportionality:

$$h_s \sim t^{0.18(+0.02)} \quad (5.35)$$

in agreement with Thorpe's corresponding experiments. The close agreement give some evidence to the assumption that in systems with no mean shear flow the turbulence decays with distance from the grid. The rate of decay appoints the exponent of  $t$  in Equation (5.35).

The relation between turbulent energy at the surface and turbulent energy at the interface as measured by Thompson and Turner [1975] to be a power law

(dependent on  $h_s$ ) for all grid experiments, relates

$$h_s \sim t^{2/15} \tag{5.36}$$

so not too much different from Equation (5.35).

The assumption of Niiler (in his description of the deepening of the upper layer of the ocean) the turbulent energy at the interface to be a constant fraction of the kinetic energy generated at the surface, independent of the  $h_s$ , concludes to

$$h_s \sim t^{1/2}$$

The experiments of Kato and Phillips (as mentioned before in Equation 5.26), with shear flow in the upper layer, lead to

$$h_s \sim t^{1/3} \tag{5.37}$$

Then the conclusion is that the way of generation of the turbulent eddies at the interface (with or without shear) is important to the deepening process of the upper layer. It is not quite clear how exactly the transport of turbulence from the surface to the interface takes place.

The influence of shear on the interfacial mixing has also been discussed by Long [1975]. Long concludes that  $w_e \sim Ri^{-1}$  where  $Ri$  is expressed in terms of the velocity and length characteristic of the turbulence near the interface. But the intensity of the turbulence near the interface decreases with  $Ri_*$  (expressed in terms of stirring rate and upper layer depth) when shear is absent.

### 5.5 Wind influence on thermal stratification

Many deep lakes are thermally stratified in the summer season, while shallow lakes can be stratified in special periods in summer, dependent on meteorological circumstances.

The annual stratification cycle of a deep lake may be described shortly in the following way:

In spring increasing sun radiation causes a warm surface layer, while this surface layer may be mixed quite homogeneously by turbulence. In lakes turbulence is mainly caused by wind. (The mixed upper layer is called the epilimnion, and it is separated from the hypolimnion by a shallow layer with large density gradient, called the thermocline, see Figure 13.) The depth of epilimnion as well as the density jump at the thermocline increase during

summer. In autumn the density jump decreases due to less sun radiation, while the epilimnion depth  $h_s$  still increases by enhanced wind influence. Reaching the bottom, the stratification is neutralized.

#### 5.5.1 Physical phenomena important to thermal stratification

Several phenomena are important to the occurrence of thermal stratification and to the specific temperature profile:

##### a. Heat flux $q$

The net heat transport across the air-water interface, per square meter and per second, is called the heat flux  $q$ . Contributants to  $q$  are the radiation and conduction from air to water, radiation and conduction from the water to the air, and evaporation (loss of evaporation heat).

##### b. Turbulent diffusion

Turbulent eddies are caused by surface waves and shear flows. In lakes both are generated mainly by wind. Then, the turbulence is generated mainly near the water surface and extends to deeper parts of the water system. The turbulent mixing decreases temperature differences in the water, however, the turbulent diffusion coefficient itself is strongly dependent on density differences (see Section 3.2, Equations (3.8) and (3.9)).

(Note: Some authors (e.g. Myer [1969]) state the vertical heat exchange in the epilimnion to be caused mainly by Langmuir oscillations. However to the description of the thermal stratification on not too small a scale the mixing effect of the Langmuir oscillations can be incorporated in turbulent diffusion.)

##### c. Entrainment

Water from the (stagnant) hypolimnion is entrained by the flowing (wind-induced flow) turbulent epilimnion. The high degree of turbulence mixes the entrained water over the whole upper layer.

##### d. Vertical advection

Vertical transport of heat may occur by inlets or outlets of water (e.g. rivers, cooling-water outlets and inlets).

The various phenomena b, c, d have a different order of importance to the description of thermal stratification in different water basins. Turbulent diffusion, entrainment and vertical advection all are small in case of a sheltered lake, while turbulent diffusion is important to a lake with some flows. Entrainment has the priority in a basin exposed to wind, while vertical advection is important to a sheltered storage lake.

For Dutch circumstances, especially turbulent diffusion and entrainment seem to be important in addition to the heat flux.

### 5.5.2 Heat flux $q$

There are quite different methods to describe the heat flux  $q$ . Dake and Harleman [1969] stated  $q$  (heat absorption) to be a function of depth. For Dutch circumstances (troubled water) the assumption of heat exchange at the water surface is expected to be reasonable. In all cases several empirical relations are necessary to transform the meteorological parameters (temperature, humidity, wind velocity, degree of cloudiness) to the heat flux  $q$ , averaged over a time interval.

In case of a negative net heat flux an unstable stratification is found because the density of the cool surface layer is larger than the density of the adjacent layer. Then, mixing takes place by vertical circulations. In stratification models this effect can be introduced by taking an infinite vertical diffusion coefficient ( $\epsilon_z = \infty$ ) in case of  $\partial\rho/\partial z < 0$ .

### 5.5.3 Qualitative description of heat balance

The influence of heat flux, turbulent diffusion, entrainment and vertical advection on thermal stratification will be described in this section in a short and qualitative manner:

The surface layer of the water system is heated by a positive net heat flux  $q$ , giving rise to a stable stratification. This stable stratification may be (partly) broken down by turbulence. Then, a fraction of the turbulent kinetic energy is used to increase the potential energy, the other part is converted into heat by viscous dissipation.

Setting up the energy balance equations (kinetic energy  $E_k$ , potential energy  $E_p$  and dissipated energy  $E_{diss}$ ) it may turn out that mixing can occur only in an upper layer of restricted depth. Then, the warm homogeneous epilimnion is separated from the cold hypolimnion by a layer with large temperature gradient.

Once a thermocline exists, increasing influence of wind may deliver enough kinetic energy to reach the thermocline and to decrease the hypolimnion by entrainment. Assuming a net heat flux to the water system and a decreasing wind influence the mixing capacity diminishes, raising the thermocline to a higher level. Then, the stratification structure of the hypolimnion (consisting of old thermocline) is preserved, except for some erosion by molecular diffusion and slight turbulence.

By vertical advection (e.g. selective withdrawal or discharge) the thermocline may be moved upwards or downwards.

All stratification models are energy balance models. Wind shear stress, radiation and mixing deliver kinetic energy, heat and potential energy, respectively. In a stationary process the kinetic energy is transformed to potential energy (mixing of the upper layer and the entrained fluid of the lower layer) and heat (viscous dissipation); in non-stationary processes the generation of flows also takes up part of the wind energy.

One of the problems of stratification models is how to describe the mixing process at the interface (the erosion of the hypolimnion). A criterion for erosion may be to suppose an unstable state at the interface, meaning the whole range of local Richardson numbers with  $Ri \leq 1$ . The Richardson number has a more definite value with the approximation that erosion takes place in such a way that the state at the interface is just stable (or just instable), then  $Ri$  is of the order of 1.

#### 5.5.4 Stratification models

Several investigators have developed models to describe thermal stratification in different circumstances. Not all models include descriptions of heat flux, turbulent diffusion, entrainment as well as vertical advection, and the descriptions originate from different approximations:

- Sundaram and Rehm [1973] take into account heat flux and turbulent diffusion. The turbulent diffusion coefficient in vertical direction  $\epsilon_z$  as a function of location ( $z$ ) and time ( $t$ ) is deduced from the Rossby-Montgomery relation:

$$\epsilon_z = \epsilon_{z,0} (1 + \sigma Ri)^{-1} \quad (5.38)$$

where  $\sigma$  = a semi-empirical constant.  $Ri(z,t)$  must be determined. However, the stratification with Equation (5.38) can be described only in case

of weak, stable stratification. To describe a stratified system with a pronounced thermocline specific assumptions are made concerning the value of  $\epsilon_z$ .

- Spalding and Svensson [1976] also treated the one-dimensional stratification process with heat flux and turbulent diffusion. They set up four differential equations to describe the turbulence model. Including two equations of motion and a heat energy equation seven differential equations must then be solved.
  
- The stratification models of Kraus and Turner (Turner and Kraus [1967], Kraus and Turner [1971]), Harleman et al (Dake and Harleman [1969], Ryan and Harleman [1971], Harleman and Hurley Octavio [1977]) and Verhagen and Kok (Verhagen [1974], Kok [1976], Kok [1977]) describe the wind influence on stratification by the entrainment process. In these models the production of potential energy by heat flux is compared to the production of kinetic energy by wind stress. The thermocline is maintained at the position of balance of both energy productions. With increasing production of kinetic energy the depth of the epilimnion  $h_s$  increases by entrainment while decreasing kinetic energy restricts the homogeneous mixing to the upper part of the epilimnion. In the latter case the lower part becomes a part of the hypolimnion.
  
- Darbyshire and Edwards [1972] derived an empirical expression  $h_s$  as a function of wind velocity, sun radiation and temperature difference of air and water. The formula satisfies the case of rising as well as falling thermocline.

For Dutch circumstances with important influence of wind, the stratification models including entrainment are the most suitable. Hereinafter a description will be given of the stratification as a function of time, as given by one of the models including entrainment:

#### Stratification model of Verhagen and Kok

The thermal profile of an epilimnion-thermocline-hypolimnion system includes:

- The depth of the epilimnion  $h_s$
- the temperature of the homogeneous epilimnion  $T_s$

- the temperature jump at the thermocline ( $T_s - T_a(z = h_s)$ )
- the temperature profile of the hypolimnion.

The former three parameters are described in the model of Verhagen and Kok by Equations (5.39), (5.40) and (5.41).

$$h_s(t) = \frac{\tau_o u_*}{\frac{g\alpha}{c_p} q + \frac{1}{2} c_e g\Delta\rho \left( \frac{\partial h_s}{\partial t} + \left| \frac{\partial h_s}{\partial t} \right| \right)} \quad (5.39)$$

where:

$$\tau_o = C_{D_a} \rho_a U_w^2$$

$$u_* = \sqrt{\tau_o / \rho}$$

$\alpha$  = thermal expansion coefficient

$c_p$  = specific heat of water

$c_e$  = a constant

In Equation (5.39) the term  $\tau_o u_*$  is the kinetic energy delivered by the wind on the water surface.  $g\alpha q h_s / c_p$  is the work to be done by the kinetic energy to mix the heat flux over the whole upper layer. At last  $\frac{1}{2} g\Delta\rho h_s \left( \frac{\partial h_s}{\partial t} + \left| \frac{\partial h_s}{\partial t} \right| \right)$  is the increase of potential energy by mixing a part of the hypolimnion in the epilimnion.

(Note:  $c_e$  is the ratio of total kinetic energy delivered by the wind at the interface and the part of the kinetic energy that supports the entrainment process at the interface. Assuming the criterion  $Ri \approx 1$  then  $c_e = 1$  (in other models the dissipation of kinetic energy  $E_{diss}$  is sometimes written explicitly). In Equation (5.39)  $c_e$  is a constant independent of  $h_s$ , supposing a constant fraction of the wind-induced kinetic energy to contribute to the mixing process. As stated already in Section 5.4 this supposition does not agree with the measurements of Linden [1974] showing a  $h_s$ -dependent fraction.)

Equation (5.39) describes the position and the movement of the thermocline, influenced by heat flux  $q$  and wind stress  $\tau$ . The temperature of the epilimnion  $T_s$  is expressed by

$$q = \rho c_p \frac{\partial h_s T_s}{\partial t} - \frac{1}{2} \rho c_p T_s \left( \frac{\partial h_s}{\partial t} - \left| \frac{\partial h_s}{\partial t} \right| \right) - \frac{1}{2} \rho c_p T_a \left( \frac{\partial h_s}{\partial t} + \left| \frac{\partial h_s}{\partial t} \right| \right) \quad (5.40)$$

where  $T_a$  = the temperature of the hypolimnion just below the thermocline. The influence of vertical diffusion on the temperature profile  $T_a(z)$  of the hypolimnion is given by:

$$\frac{\partial T_a(z)}{\partial t} = \epsilon_z \frac{\partial^2 T_a(z)}{\partial z^2} \quad (5.41)$$

The solution of the differential equations needs the boundary conditions:

$$\frac{\partial T_a(z = h_s)}{\partial z} = 0$$

and

$$T_a(z = h_s) = T_s$$

The latter boundary conditions are replaced by:

$$\rho c_p \epsilon_z \frac{\partial T_a(z = 0)}{\partial z} = q$$

in case of a stagnant situation with  $h_s = 0$  and  $u_* = 0$ .

The stratification model of Verhagen and Kok has been applied successfully to the Oostvoornse Meer (Lake Oostvoorn, DHL [1976c]). The meteorological conditions have been transformed to daily averaged values in the calculations.

### Notes

- According to Equation (5.39) and the definitions of  $\tau_0$  and  $u_*$  the depth of the epilimnion satisfies

$$h_s \sim U_w^3$$

Averaging the weather conditions on a certain time interval the proportionality is expected to be  $h_s \sim \bar{U}_w^3$  and not  $h_s \sim U_w^3$  because there is no direct coupling of  $h_s$  and  $U_w$ . The  $h_s - U_w$  relation exists through the wind-induced flow currents, while those currents satisfy  $u_s \sim U_w$ .

- From Equation (5.39) it can be derived (see Verhagen [1978]) that  $\frac{\partial h_s}{\partial t} \sim t^{1/2}$  in case of an increasing wind or decreasing heat flux (compared to the equilibrium state before).
- $h_s$  cannot exceed the depth of frictional resistance (Ekman layer). This is important to ocean currents where the Coriolis force cannot be ignored.

## 6 Wind influence on current pattern in 2D and 3D water system

### 6.1 Introduction

The air-water momentum exchange influences the current pattern in the water system. In an initially stagnant system wind drift currents are generated. Those currents at least have components in the wind direction. In enclosed system the principle of continuity provides a system of wind drift flows and counter flows, called wind drift circulation.

The wind drift circulation in a basin is subjected to several influences, e.g.:

- wind velocity and wind direction
- geometry of coasts and bottom
- horizontal density differences
- vertical density differences (stratification)
- Coriolis effect
- atmospherical pressure differences
- inlets and outlets.

The wind drift circulations may be considered to be two-dimensional in simplified models. In case of a closed channel the circulation is two-dimensional in a vertical sense, while in a shallow basin the circulation is about horizontal.

Horizontal wind drift circulations can be generated by several sources:

- Inhomogeneous wind field. The drift current is in the direction of the wind in strong wind regions, while the counter flow is in the regions with weaker wind.
- Coriolis effect. The Coriolis forces have opposite directions for drift flow and counter flow, introducing a horizontal shift.
- Inhomogeneous depth. The drift current occurs in the shallow regions, the return flow in the deep regions. The shift is caused by the inclination of the water surface (wind set-up) that must balance on each location with the shear stresses over the whole depth. The inclination itself has a value belonging to the averaged depth. Then the inclination is too large in shallow regions (and balances only with the shear stress in case of a too strong drift current) and too small in deep regions (balance in case of too strong return flow).

In this explanation the shear stress profile is supposed to be linear from surface to bottom.

- Inhomogeneous  $\tau_o - U_w$  relation. The  $\tau_o - U_w$  relation is dependent on the temperature of the water surface. Then an inhomogeneous temperature field causes an inhomogeneous shear stress field (see also Section

### Coriolis effect and the Ekman spiral

The earth rotation causes a (seeming) force to the right-hand side on a current on the Northern hemisphere. The Coriolis force causes an angle  $\alpha_s$  (typical order of magnitude  $30^\circ$ ) between the wind direction  $\vec{U}_w$  and the wind-generated surface current  $\vec{u}_s$ . Due to viscosity the current velocity extends to lower layers while decreasing in magnitude. In the first instance viscosity generates a current in the lower layer in the same direction, but the Coriolis force increases  $\alpha$  (angle between  $\vec{U}_w$  and the local current  $\vec{u}$ ). The decreasing  $u$  and increasing  $\alpha$  (going from the water surface to deeper layers) is called the Ekman spiral.

### 6.2 Hydraulic and mathematical models

In principle drift circulations may be studied with mathematical models as well as with hydraulic models. However, the study of complicated circulations in an hydraulic model with a real bathymetry is rather unattractive because of the great expenses to build in the model in a wind flume. Moreover, in large or stratified basins the Coriolis effect cannot be neglected forcing a rotating model (measurements on a rotating model of Lake Superior have been carried out in a wind flume by Lien and Hoopes [1977]).

For those reasons hydraulic models are restricted to study successfully the principles of wind drift circulations in simplified basins (rectangular or cylindrical basin). Considerations on the modelling of wind drift circulations have been given by Hecker and Yale [1973] and Shemdin [1973]).

Generally the prediction of wind drift circulations in basins is based on mathematical models. In turn the mathematical models are composed of several phenomena, based on simple model experiments. In very simple open systems (e.g. rectangular infinite channel) a one-dimensional model can be applied. To other circulations two-dimensional (either in horizontal or in vertical sense) or three-dimensional mathematical models are necessary.

### 6.3 Frequently applied simplifications

As mentioned in Section 6.1 many phenomena influence the circulation pattern. However, it shall be necessary to make some simplifications in the calculations or in the experimental model. The following list sums up the simplifications that are often or sometimes applied in literature:

#### Geometrical simplifications

- Atmospheric pressure differences can be neglected in systems with not too large horizontal dimensions. In Dutch circumstances, the dimensions of lakes and basins do not exceed the order of 10 kilometers. Then, neglection is surely possible.
- The wind field over the lake is often supposed to be homogeneous.
- Horizontal density differences are often neglected. Sometimes the vertical stratification is simplified by considering a two-layer system with homogeneous layers and density difference  $\Delta\rho$ .
- Coastal and bottom shape is often simplified by a rectangular or cylindrical basin with either a homogeneous depth or a very simplified depth profile.
- In lakes currents due to inlets or outlets often are small compared to the influence of wind. Then, these current may be considered to occur only around the inlet and outlet.

#### Mathematical simplifications

- Wind and wind drift currents are mostly assumed to be stationary. Generally the assumption of the stationary state is not very realistic because in a lake the stationary state appears after some days (see Liggett and Lee [1971]).
- A hydrostatical pressure is supposed generally because the vertical velocities are small compared to the horizontal flow velocities. Then  $\frac{\partial p}{\partial x}$  and  $\frac{\partial p}{\partial y}$  are independent of depth.
- The Coriolis effect is negligible in shallow lakes with depth  $h$  small as compared to the depth of frictional resistance  $D$ , given by:

$$D = 7.6 U_w (\sin \phi)^{-1/2}$$

where  $\phi$  = the latitude.  $D$  is dependent on  $U_w$ , so the Coriolis effect has the most (relatively speaking) influence with weak wind. Moreover the effect of the

Coriolis force depends on the width of the basin. Because of the Coriolis force the flow follows a trajectory with radius of curvature

$$r = \frac{u}{f}$$

The Coriolis parameter  $f$  is of the order of  $10^{-4} \text{ s}^{-1}$  (at not too small latitude). Mortimer [1952] states the rotation effects of the Coriolis force to be significant to basins with width larger than  $5r$ , while the rotation is dominant in basins with widths larger than  $20r$ .

- Usual simplifications in the calculation of circulations are the neglect of non-linear terms in the equations of motion. The neglect is very reasonable in case of a small Rossby number  $Ro = u/fL$  (meaning a small ratio of inertial and rotational forces;  $L =$  length scale) (Liggett and Lee [1971]).
- The horizontal eddy viscosity (with coefficients  $\epsilon_{u,x}$  and  $\epsilon_{u,y}$ ) is often neglected. Generally the eddy viscosity is only important to the circulation pattern in the coastal zone where the horizontal velocity gradient perpendicular to the wall is large. Then a large diffusion coefficient tries to make the currents more homogeneous.

The vertical diffusion is important to the surface and bottom shear layers but in some cases (in deep lakes) the vertical diffusion is neglected at the bottom (or at the interface). Then, the friction constant  $k$  equals 0.

#### 6.4 Mathematical description

The principal equations are (averaged over the turbulent fluctuations) (see also DHL [1976a]):

$$\frac{\partial u}{\partial x} + \frac{\partial v}{\partial y} + \frac{\partial w}{\partial z} = 0 \quad (\text{incompressibility}) \quad (6.1)$$

$$\begin{aligned} \frac{\partial u}{\partial t} + \frac{\partial}{\partial x} (uu) + \frac{\partial}{\partial y} (uv) + \frac{\partial}{\partial z} (uw) - fv + \frac{1}{\rho_0} \frac{\partial p}{\partial x} - \frac{\partial}{\partial x} \left\{ \epsilon_{u,x} \frac{\partial u}{\partial x} \right\} - \\ - \frac{\partial}{\partial y} \left\{ \epsilon_{u,y} \frac{\partial u}{\partial y} \right\} - \frac{\partial}{\partial z} \left\{ \epsilon_{u,z} \frac{\partial u}{\partial z} \right\} = 0 \end{aligned} \quad (6.2)$$

$$\begin{aligned} \frac{\partial v}{\partial t} + \frac{\partial}{\partial x} (vu) + \frac{\partial}{\partial y} (vv) + \frac{\partial}{\partial z} (vw) + fu + \frac{1}{\rho_0} \frac{\partial p}{\partial y} - \frac{\partial}{\partial x} \left\{ \epsilon_{u,x} \frac{\partial v}{\partial x} \right\} - \\ - \frac{\partial}{\partial y} \left\{ \epsilon_{u,y} \frac{\partial v}{\partial y} \right\} - \frac{\partial}{\partial z} \left\{ \epsilon_{u,z} \frac{\partial v}{\partial z} \right\} = 0 \end{aligned} \quad (6.3)$$

$$\begin{aligned} \frac{\partial w}{\partial t} + \frac{\partial}{\partial x} (wu) + \frac{\partial}{\partial y} (wv) + \frac{\partial}{\partial z} (ww) + \frac{\rho}{\rho_0} g + \frac{1}{\rho_0} \frac{\partial p}{\partial z} - \frac{\partial}{\partial x} \left\{ \epsilon_{u,x} \frac{\partial w}{\partial x} \right\} - \\ - \frac{\partial}{\partial y} \left\{ \epsilon_{u,y} \frac{\partial w}{\partial y} \right\} - \frac{\partial}{\partial z} \left\{ \epsilon_{u,z} \frac{\partial w}{\partial z} \right\} = 0 \end{aligned} \quad (6.4)$$

$$\begin{aligned} \frac{\partial T}{\partial t} + \frac{\partial}{\partial x} (uT) + \frac{\partial}{\partial y} (vT) + \frac{\partial}{\partial z} (wT) - \frac{\partial}{\partial x} \left\{ \epsilon_{T,x} \frac{\partial T}{\partial x} \right\} - \frac{\partial}{\partial y} \left\{ \epsilon_{T,y} \frac{\partial T}{\partial y} \right\} - \\ - \frac{\partial}{\partial z} \left\{ \epsilon_{T,z} \frac{\partial T}{\partial z} \right\} = 0 \end{aligned} \quad (6.5)$$

$$\begin{aligned} \frac{\partial c}{\partial t} + \frac{\partial}{\partial x} (uc) + \frac{\partial}{\partial y} (vc) + \frac{\partial}{\partial z} (wc) - \frac{\partial}{\partial x} \left\{ \epsilon_x \frac{\partial c}{\partial x} \right\} - \frac{\partial}{\partial y} \left\{ \epsilon_y \frac{\partial c}{\partial y} \right\} - \\ - \frac{\partial}{\partial z} \left\{ \epsilon_z \frac{\partial c}{\partial z} \right\} = 0 \end{aligned} \quad (6.6)$$

$$\rho = \rho_0 + \Delta\rho(T, c) \quad (6.7)$$

Equation (6.2) reduces to:

$$-fv + \frac{1}{\rho_0} \frac{\partial p}{\partial x} - \epsilon_{u,z} \frac{\partial^2 u}{\partial z^2} = 0 \quad (6.8)$$

in case of neglect of non-linear terms  $\left(\frac{\partial}{\partial x} (uu), \frac{\partial}{\partial y} (uv) \text{ and } \frac{\partial}{\partial z} (uw)\right)$ , neglect of horizontal diffusion ( $\epsilon_{u,x} = \epsilon_{u,y} = 0$ ), and when considering a stationary state ( $\frac{\partial u}{\partial t} = 0$ ). Equation (6.8) is called an Ekman equation, with the characteristic property of neglected lateral shear ( $\epsilon_{u,y} = 0$ ). Ekman equations are frequently applied to ocean and great lakes.

For the determinations of boundary conditions for the solution of the differential equations one is referred to DHL [1976a]. Usual boundary conditions are the statement of no heat and concentration flux across solid walls as well as the no-slip condition ( $u = v = w = 0$ ) at walls and bottom. The boundary condition concerning the wind shear stress may often be simplified to

$$\frac{\tau_0}{\rho} = \epsilon_{u,z} \frac{\partial u}{\partial z}$$

where  $U_w$  and wind drift velocity are parallel to the x-direction. Moreover special approximations may be made to the boundary conditions concerning bottom and interfacial shear stress, and the density at the bottom, surface and interface.

The equations for mass transport in the horizontal directions x and y come

about by integration of the momentum Equations (6.2) and (6.3) in vertical direction over the whole depth. The boundary condition is a zero component of mass transport perpendicular to the wall. Then the equations can be drafted to describe the wind drift circulation in a two-dimensional (horizontal) framework. Neglecting the non-linear terms:

$$\begin{aligned} \frac{\partial M_x}{\partial t} + gh \frac{\partial \xi}{\partial x} - fM_y - \frac{\tau_{o,x}}{\rho} + \frac{\tau_{b,x}}{\rho} + \epsilon_{u,x} \frac{\partial^2 M_x}{\partial x^2} + \epsilon_{u,y} \frac{\partial^2 M_x}{\partial y^2} &= 0 \\ \frac{\partial M_y}{\partial t} + gh \frac{\partial \xi}{\partial y} + fM_x - \frac{\tau_{o,y}}{\rho} + \frac{\tau_{b,y}}{\rho} + \epsilon_{u,x} \frac{\partial^2 M_y}{\partial x^2} + \epsilon_{u,y} \frac{\partial^2 M_y}{\partial y^2} &= 0 \\ \frac{\partial \xi}{\partial t} + \frac{\partial M_x}{\partial x} + \frac{\partial M_y}{\partial y} &= 0 \end{aligned}$$

$\xi$  is the deviation of the water surface compared to the mean position. The components of mass transport in directions x and y, viz.  $M_x$  and  $M_y$  are defined by:

$$M_x \stackrel{\text{def}}{=} \int_0^{-h} u dz \quad M_y \stackrel{\text{def}}{=} \int_0^{-h} v dz$$

The bottom shear stress  $\tau_{b,x}$  and  $\tau_{b,y}$  is sometimes written by

$$\tau_{b,x} = k\rho M_x$$

where  $k$  = a friction constant (dimensionless).

In literature the stream function  $\psi$  defined by

$$\begin{aligned} M_x &\stackrel{\text{def}}{=} \frac{\partial \psi}{\partial y} \\ M_y &\stackrel{\text{def}}{=} - \frac{\partial \psi}{\partial x} \end{aligned}$$

is frequently used.

The stream function  $\psi$  is very illustrative by drawing stream lines with  $\psi$  is constant.

### 6.5 Calculation on simplified basins. Homogeneous and two-layer system

In this section the effect of several phenomena and parameters on the wind drift circulation in a homogeneous as well as a stratified basin shall be shown adstructed by some calculations and experiments given in the literature.

The calculations of Hamblin [1969] and Liggett and Lee [1971] are very schematically by the choice of the basin (round basin and an infinite water system, respectively) and by the choice of stratification (homogeneous two-layer system). Moreover, the circulations are supposed to be stationary.

Calculations of Hamblin [1969]  
-----

Hamblin carried out calculations for a circular basin, with homogeneous depth as well as with a depth varying parabolically from a low value at the coast up to 70 m in the middle. The model represents a schematized Lake Erie. The calculations are very illustrative because the influences of variable depth, stationary wind, hydraulic forcing (in the model a combination of oppositely located inlet and outlet) and diffusion coefficients have been surveyed on an homogeneous system and a two-layer system. The result is shown in Figures 14, 15 and 16.

To describe the homogeneous situation, Hamblin uses the Equations (6.1), (6.2) and (6.3). The calculation model is two-dimensional (in horizontal sense) indicating depth-integrated Equations (6.2) and (6.3). Non-linear terms and time-dependent terms are omitted. The boundary conditions are:

at solid walls:  $u = v = w = 0$

at the surface:  $\frac{\tau_{0,x}}{\rho} = \epsilon_{u,z} \frac{\partial u}{\partial z}$ ,  $\frac{\tau_{0,y}}{\rho} = \epsilon_{v,z} \frac{\partial v}{\partial z}$

The shear stress at the bottom  $\tau_b$  must be known because of the vertical integration of the two differential equations.  $\tau_b$  can be derived from the Ekman solution (see Hamblin's original publication).

Figures 14, 15 and 16 show the calculation results with the aid of stream functions (see Section 6.4) integrated vertically.

Figure 14a. Homogeneous h;  $\tau_0 = 0$ ; hydraulic forcing (inlet + outlet system);

$$\epsilon_{u,x} = \epsilon_{u,y} = 10^3 \text{ m}^2/\text{s}; \epsilon_{u,z} = 10^{-2} \text{ m}^2/\text{s}.$$

The result is a rather homogeneous flow field.

Figure 14b. As 14a, except parabolic h (0 → 70 m).

Strong coastal currents occur on both sides, with gyres on the right-hand side of the inlet and on the left of the outlet. The asymmetrical situation is caused by a somewhat stronger flow along the right coast by the Coriolis effect. In case of a deeper basin (h = 0 → 200 m) these gyres disappear.

Figure 14c, d. As 14b, except  $\epsilon_{u,xy} = 10^4$  and  $\epsilon_{u,xy} = 10^5$  m<sup>2</sup>/s respectively. The horizontal diffusion coefficients now have unrealistically large values, but it is remarkable to note a crossing lateral flow instead of two gyres. Actually, changing  $\epsilon_{u,xy}$  from  $10^3$  to  $10^4$  m<sup>2</sup>/s, a change of balance occurs between the geostrophic forces (inclination of water surface) and friction forces. At increasing  $\epsilon_{u,xy}$  up to  $10^5$  m<sup>2</sup>/s (see Figure 14d) the flow is very homogeneous with much correspondence to Figure 14a.

Figure 14e. Parabolic h;  $\tau_{u,x} = 10^{-4}$  m<sup>2</sup>/s;  $\tau_{u,y} = 0$ ; no hydraulic forcing;  $\epsilon_{u,xy} = 10^3$  m<sup>2</sup>/s,  $\epsilon_{u,z} = 10^{-2}$  m<sup>2</sup>/s. A depth-integrated transport in the middle of the basin in a direction of 80° to the right of the wind stress is indicated (Coriolis effect), with a shore-ward return flow. In case of h = 0 → 200 m (see Hamblin) the transport direction has been shifted to 100° with wind stress, while the transports proper become smaller.

Figure 14f. As 14e, except for hydraulic forcing. The wind effect dominates the hydraulic circulation. Increasing  $\epsilon_{u,z} = 10^{-2} \rightarrow 3 \cdot 10^{-2}$  keeps the hydraulic circulation rather unchanged, but now the wind drift currents form an angle of only 40° with the wind direction, while the intensity has been decreased to 65 percent

Figure 15a, b. As 14b and 14f respectively. The vertical velocity components of hydraulic circulation and wind drift current are very small (the units used in the figure are 10<sup>-4</sup> m/s). The vertical velocities cause the phenomena of up-welling and down-welling.

The two-layer system consists of two homogeneous layers with shear stress at the interface. To solve the differential equations of both layers the boundary conditions of the homogeneous system are completed by the boundary conditions of continuous velocities and shear stress across the interface.

Some assumptions are  $h_s \ll h_b$  (depth of upper layer much smaller than depth of lower layer), the upper layer reaches the bottom nowhere, no mass exchange across the interface, and the local value of  $h_s$  can be calculated assuming the lower layer to be at rest. Concerning the other assumptions the reader is referred to Hamblin [1969].

The phenomena to be calculated are:

- $h_s(xy)$ , local depth of upper layer
- upper layer circulation
- lower layer circulation.

With the initial quantities to be

$$h_s = 15 \text{ m} \quad , \quad \epsilon_{u,z} = 10^{-2} \text{ m}^2/\text{s} \text{ (in both layers)}$$
$$\Delta\rho = 2 \text{ kg/m}^3 \text{ and } \tau_o = 0.14 \times 10^{-4} \text{ m}^2/\text{s}$$

the results are:

Figure 15c, d, e. The figures show the local depths (in m) of the upper layer in case of

- hydraulic flow (Figure 15c)
- wind flow (Figure 15d)
- combined effect (with  $\tau_o = 0.19 \times 10^{-4} \text{ m}^2/\text{s}$ ) (Figure 15e).

Figure 16a, b, c. The lower layer circulations have been given in the cases of hydraulic force, wind force and combined effect.

Figure 16d, e, f. The figures show the upper layer circulations (with  $\tau_o = 0.14 \times 10^{-4} \text{ m}^2/\text{s}$ ) for the cases of hydraulic flow, wind drift circulation and combined effect.

The preceding calculations have been carried out in the order:

- $h_s(xy)$  has been calculated with a supposed stagnant lower layer.  
The driving forces are the hydraulic force and wind force.
- With known position of the interface the shear stress at the interface can be calculated, leading to the determination of the lower layer circulation.
- With known lower layer circulation the pressure forces in the lower layer can be derived, leading to the determination of the upper layer circulation.

Gedney et al. [1972] have carried out calculations very similar to the survey of Hamblin. However, Gedney's simplified model consists of a rectangular basin of homogeneous depth.

#### Calculations of Liggett and Lee [1971]

The calculations of Liggett and Lee are very illustrative as well. The model consists of a two-layer system with two homogeneous layers. Bottom and wall influences and horizontal diffusion have been neglected. A stationary state has been considered, and the non-linear terms of the momentum equations have been omitted (small Rossby number, see Section 6.3).

For both layers the following equations are given:

$$-fv_k = -\frac{1}{\rho_k} \frac{\partial p_k}{\partial x} + \epsilon_{u,k} \frac{\partial^2 u_k}{\partial z^2}$$

$$fu_k = -\frac{1}{\rho_k} \frac{\partial p_k}{\partial y} + \epsilon_{u,k} \frac{\partial^2 v_k}{\partial z^2}$$

$$g = -\frac{1}{\rho_k} \frac{\partial p_k}{\partial z}$$

$$\frac{\partial u_k}{\partial x} + \frac{\partial v_k}{\partial y} + \frac{\partial w_k}{\partial z} = 0$$

where  $k = 1$  and  $2$  for upper and lower layer respectively. Liggett and Lee solve the equations to determine the horizontal current velocities and the inclinations of the free surface and the interface. A sensitivity survey has been carried out to know the influence of several parameters. The standard values of the surveyed system are

|                                  |   |
|----------------------------------|---|
| $f = 10^{-4} \text{ s}^{-1}$     | $\rho_2 = 999.97 \text{ kg/m}^3$              |
| $g = 9.8 \text{ m/s}^2$          | $\epsilon_{u,1} = 0.004 \text{ m}^2/\text{s}$ |
| $\tau_x = 0$                     | $\epsilon_{u,2} = 0.004 \text{ m}^2/\text{s}$ |
| $\tau_y = 0.1 \text{ N/m}^2$     | $h = 80 \text{ m}$ (total water depth)        |
| $\rho_1 = 997.77 \text{ kg/m}^3$ | $h_s = 18 \text{ m}$ (upper layer depth)      |

Figure 17a shows the inclinations of free surface and thermocline (interface) as a function of  $h_s$ . The inclinations are indicated with  $\frac{\partial h}{\partial x}$  and  $\frac{\partial h_i}{\partial x}$  as the deviations of the mean position. Obviously the set-up of the interface is much larger.

The inclinations as a function of  $\Delta\rho$  have been given in Figure 17b. There is nearly no  $\Delta\rho$ -dependence on  $\Delta h_s$ , but a large influence on  $\Delta h_i$ .

Figure 17c shows the inclination as functions of the eddy viscosity. Along the horizontal axis, the viscosity parameter  $K$  has been given defined by:

$$K = \sqrt{\frac{1}{2} f \epsilon_{u,1} \epsilon_{u,2}} \left( \frac{\rho_1 \rho_2}{\rho_1 \epsilon_{u,1}^{1/2} + \rho_2 \epsilon_{u,2}^{1/2}} \right)$$

Figure 18a gives the vector velocities in the epilimnion (upper layer) as a function of  $h_s$ . The flow velocities have been given on  $z = 0$  (free surface),  $z = -\frac{1}{7} h_s, \dots, z = -\frac{6}{7} h_s, z = -h_s$  (thermocline). The velocity increases with increasing  $h_s$  (assuming equal wind stress) while the Ekman spiral (see Section 6.1) is more complete.

Figure 18b shows the vector velocities in the epilimnion as a function of  $\epsilon_u$ . Decreasing  $\epsilon_u$  increases the velocities with more complete spirals.

Figure 19a and 19b give again the (scalar) velocities in the epilimnion (and adjacent part of the hypolimnion) as functions of  $h_s$  and  $\epsilon_u$  respectively. Current speed as determined by Verber [1975] is shown in Figure 19c.

Liggett and Lee doubt the quantitative accuracy of the preceding results because of the numerical approximations and the assumption of the stationary state. In real lakes the stationary case occurs only after a few days.

## 6.6 Bottom and wall influences

### Current patterns near the coast

Two direct influences of the coast on wind drift currents exist:

- an onshore wind directed perpendicular to the coast causes the wind set-up of the water surface, with a surface current directed to the coast and a return bottom current
- in addition a wind not exactly perpendicular to the coast causes a current along the coast.

The former phenomenon (wind set-up) has been treated in Section 5.2.

The current direction and current velocity of the latter phenomenon (coastal current) have been surveyed experimentally and theoretically by Murray [1975]. Figure 20 shows the results of the calculations (numerical solutions of the differential equations, including Coriolis terms and an onshore-offshore surface slope) to determine the vertical velocity profile of an unstratified system in the vicinity of a coast. The current velocity as well as the current direction have been given, assuming the wind reaches the coast with the angle of incidence of  $60^\circ$ .

Murray derived some relations for the parallel and perpendicular component of the near-shore current as a function of wind velocity, wind direction (as compared to coastal direction), eddy viscosity, water depth (assuming flat bottom), latitude (in relation to Coriolis effect) and surface and bottom friction.

The conclusion of the calculations is that the current direction is less dependent on wind direction and wind force, the direction is almost along the

coast. The current velocity is more dependent on the wind direction than on wind velocity. The drift current velocity perpendicular to the coast is directed to the coast near the water surface, and direction from the coast near the bottom, all in case of onshore wind.

#### Current patterns in coastal-bounded system

The coast influences the wind drift currents giving rise to a long-shore current as well as a system of onshore and offshore currents. Then in a basin the wind-induced currents cause a complex three-dimensional circulation with horizontal (gyres) as well as vertical velocity gradients.

Some consequences of the presence of walls on the wind-induced circulation can be obtained from the experiments of Bembaron [1975]. The wind is flowing over a cylindrical basin (flat bottom) with variable depth. Often a 120° circle sector has been blocked in varying positions to the wind direction. The combined system of gyres and flows and back-flows form a complex three-dimensional circulation. Figure 21a, b show two examples of the experiments, indicating the influence of wind velocity on the circulation pattern.

Birchfield [1971] surveyed mathematically the portioning of the horizontal mass transport between the Ekman layer transport (drift because of wind stress on the water surface) and geostrophic transport (gradient current because of the surface inclination caused by wind set-up in a closed system). Another question is how the surface drift transport normal to a coast is returned to the interior of the basin. Birchfield's mathematical model is a rectangular basin with homogeneous depth. The stationary state has been considered, and the turbulence was treated in a simple way ( $\epsilon_{u,xy}$  and  $\epsilon_{u,z}$  being constant).

It turns out that down-welling occurs on the coast to the right of the wind stress and up-welling on the left coast while the return flow occurs as a geostrophic interior flow across the basin to the up-welling coast.

According to Birchfield the rectangular shape of the basin can be quite simple changed, mathematically, to a smooth, continuous coast. Also the stationary state can be easily changed to the non-stationary case. However, the uniform depth cannot be removed as easily.

#### Current patterns with bottom- and wall influence

Bennett [1974] theoretically calculated the large-scale circulations in a lake

induced by a storm, with special interest to the relative importance of topography, earth rotation, friction and stratification. The state is non-stationary. Bennett's model is two-dimensional (in vertical sense) with no variations parallel to the coast. A cross-section of the model is given in Figure 22a, modelled after Lake Ontario. Some simplifications are a two-layer system of two homogeneous layers, no friction on bottom and interface, neglect of all non-linear terms, and a uniform wind field.

Figure 22b shows the long-shore current velocities (averaged over the upper and lower layer) and the position of the thermocline. In this example the wind has blown during 1.1 day with  $\tau_0 = 0.1 \text{ N/m}^2$ . In the calculation  $\Delta\rho = 0$  has been substituted. The result is an only narrow zone of coastal current and up-welling. (The result of a set-up of the thermocline up to 40 m in case of a depth at the coast of only 20 m show the invalidity of the linearization.) Figure 22c gives the situation with  $\Delta\rho/\rho = 1.25 \times 10^{-3}$  and a uniform depth up to the coast (in contrast to Figure 22a).

Figure 22d shows the combined result of the topography of Figure 22a with the  $\Delta\rho$  of Figure 22c. Finally Figure 22e shows the situation of 22d with halved  $\Delta\rho$  and Figure 22f the situation of 22b with doubled bottom slope.

(In Figure 22 the wind is always parallel to the coast, so perpendicular to the cross section of Figure 22a.)

Bennett calculated, analytically, the preceding results. Using a numerical model he critically surveyed the linearization and the friction neglected before. Starting with the cross section of Figure 23a and a temperature stratification of Figure 23b the drift current generated by a wind has been calculated (with  $\tau_0 = 0.1 \text{ N/m}^2$ ) blowing during 1.1 day and then suddenly falling back to zero. The vertical eddy viscosity is assumed to be  $\epsilon_{u,z}(z) = 0.01 \text{ m}^2/\text{s}$  with the water surface decreasing exponentially to  $0.001 \text{ m}^2/\text{s}$  at a depth of 100 m, while the latter value is valid over the whole depth in the absence of wind. The horizontal eddy viscosity is  $1 \text{ m}^2/\text{s}$ .

The deepening of the upper layer has been calculated according to the empirical relation of Kato and Phillips [1969]:

$$h_s(t) = u_* \left( \frac{15t}{N^2} \right)^{1/3}$$

where  $t$  = the time variable in the period of blowing wind,  $u_* = \sqrt{\tau_0/\rho}$  ( $\approx 0.01 \text{ m/s}$ ) and  $N$  = the buoyancy frequency;

Figures 23c, d, show the transports parallel to the coast according to the linearized numerical model of a two-layer system, with wind parallel to the

coast and blowing during 1.1 day ( $10^5$  s).

Also the long-shore component of bottom stress dependent on time has been calculated, as compared to the shear stress  $\tau_0$  at the water surface. The results for the homogeneous system and the two-layer system are given in Figure 23e and 23 f.

Figure 24 represents the complete picture of coastal currents and vertical flow velocities for homogeneous as well as stratified systems, all with a long-shore wind during  $10^5$  s.

Bennett's expectation of his two-dimensional model is that generally (at least applied to the American Great Lakes) it can explain not only the magnitude of wind-driven flows but many of the qualitative features of it as well.

Some other calculations of wind-driven flows influenced by the coastal and bottom contours have been carried out by Simons [1971a, 1971b, 1972] for Lake Ontario, and by Shkudova and Kovalev [1969] for the Aral Sea. The latter survey considers only the stationary case.

The results of Lake Ontario have been published as vertically integrated flow velocities. Obvious horizontal circulations are shown.

The results of the Aral Sea have been published as flow velocities on several depths. The circulations are clearly three-dimensional with flows and back-flows.

In the former survey the Coriolis effect has been taken into account; in the calculations on the shallow Aral Sea it was not.

### 6.7 Influence of horizontal density gradient

Horizontal density gradients are caused generally by temperature or salinity differences.

Collecting the large-scale circulation pattern of 40 lakes and bays on the Northern hemisphere Emery and Csanady [1973] give an explanation of the fact that all circulations (except one) are counter-clockwise. The wind-driven warm upper layer of the lake is moved to the right coast by the Coriolis force, while at the left-hand up-welling may occur. Then, generally, the water at the right-hand side is warmer than on the left side. Considering the effect described by Roll [1965] that  $\tau_0$  strongly depends on the air-water temperature difference (with a stable stratification of the lower air layer in case of an air temperature some degrees higher than the water, suppressing the turbulence in the layer), a temperature gradient causes a  $\tau_0$ -gradient. Especially in the

summer season the temperature stratification will cause a horizontal temperature gradient by the combined effect of wind force and Coriolis force.

Emery and Csanady give an example of a horizontal temperature difference of  $1^{\circ}\text{C}$  generating differences in  $\tau_o$  of a factor 3. Applied to the Great Lakes the generated circulation has a tangential velocity of 3.6 cm/s after a period of 8 hours (see also Csanady [1972]).

Generally the temperature dependence of  $\tau_o$  is not taken into account in the literature. This is justified in shallow lakes where the Coriolis effect can be ignored.

Brongersma and Groen [1969] and Groen [1971] calculated (two-dimensional, vertical) flow generated by the combined effect of an horizontal density gradient and a counter-acting wind force. It turns out that wind-driven current dominates in shallow regions, density circulations dominating in deep regions. A critical depth  $h_{\text{crit}}$  can be derived from:

$$\frac{4\tau_o}{D^2} \ln \frac{h_{\text{crit}}}{z_o} = -g \frac{\partial \rho}{\partial x}$$

A scheme has been given in Figure 25, including the definition of D.

Density currents due to horizontal temperature gradient are very important near cooling-water outlets. However, Uzzell and Özişik [1977] mathematically demonstrated the horizontal gradient may be important to the three-dimensional circulation velocities in the whole cooling-pond.

### 6.8 Influence of eddy viscosity

It may be expected that the value of the eddy viscosity in several directions is important to the wind-driven circulations.

Csanady [1963, 1964] measured some values of the eddy viscosity in the Great Lakes to be of the order of

$$\epsilon_{u,x} = 0.2 \text{ m}^2/\text{s} \text{ (x parallel to wind direction)}$$

$$\epsilon_{u,y} = 0.04 \text{ m}^2/\text{s}$$

$$\epsilon_{u,z} = 0.0003 \text{ to } 0.003 \text{ m}^2/\text{s}$$

Bengtsson [1973] measured in Swedish lakes (5 to 25 km<sup>2</sup>):

$$\epsilon_{u,x} \approx 0.03 \text{ m}^2/\text{s}$$

$$\epsilon_{u,y} \approx 0.005 \text{ m}^2/\text{s}$$

$$\epsilon_{u,z} \approx 2 \times 10^{-5} h \frac{U}{s_w}$$

where  $h_s$  = the depth of the epilimnion.

The values of  $\epsilon_{u,z}$  may be considered to be averaged over the depth; generally the  $\epsilon_{u,z}$ -profile is very inhomogeneous.

In case of small values of  $\epsilon_{u,z}$  the wind-driven flows are concentrated in the surface layer and are strongly influenced by the Coriolis effect.

The partitioning of the flow over the epilimnion and hypolimnion depends on the choice of the eddy viscosities in both layers and on the interface.

Figure 26 (Bengtsson [1973]) shows the velocity profiles for the following situations:

- the eddy viscosity of the epilimnion and the hypolimnion both are proportional to the depth of the relevant layer (curve a)
- the eddy viscosity of the epilimnion is 4 times the value of the hypolimnion (curve b)
- thermocline acts as the bottom (curve c)
- stress of the thermocline is small (curve d + e)
- stress of the thermocline is zero (curve d + f).

## 6.9 Special phenomena

### Fluctuating wind field

Generally the wind field is expected to be stationary during one or two intervals. Then in case of two intervals the wind either starts at  $t = 0$  or falls to zero. Pedlosky [1967] surveyed the effect of a fluctuating wind (sine wave) with a period corresponding to one of the resonance frequencies of the water basin. (The model is a schematized ocean model with Rossby resonance frequencies of the order of a few days.) The generated flow field consists of a fluctuating response and a stationary circulation. The current velocities of the stationary circulation are two orders of magnitude larger than the current velocities of the circulation due to a stationary wind field with the same amplitude. For special cases some attention to this may be desirable.

### Inhomogeneous wind field

Belyaev [1969] investigated the effect of an inhomogeneous wind field and a non-stationary wind field on the wind drift circulation. It is very remarkable that the time scale of the inhomogeneity is important to the wind drift velocities in a deep basin while the space scale is rather unimportant. The

contrary situation occurs in case of a shallow basin.

### Interfacial oscillations

Oscillations on the thermocline have not been treated in this report except for the simple case of the one-dimensional internal seiche (Section 5.3). Csanady [1972b, 1975] pointed out that several remarkable phenomena in the American Great Lakes are due to oscillations on the thermocline; the oscillations proper are caused by temporal wind influence. The phenomena are among others Kelvin waves, Poincaré waves, coastal jets, more complex internal seiches.

## 7 Summary and conclusions

This report reviews the physical phenomena concerning the influence of wind on the velocity field and temperature field of water basins. The basins treated are either homogeneous or stratified.

### Velocity field in homogeneous basins

Because the wind force acts only directly on the water surface the wind-induced flow field is inhomogeneous in vertical direction. In special cases the horizontal flow field may be considered homogeneous.

Many experiments exist on the vertical velocity profile. Well-defined theoretical velocity profiles are possible only in case of laminar currents. In turbulent flow the turbulence model considered influences the calculated profile. Empirically the vertical velocity profile has a logarithmic shape near the surface and near the bottom. In the central part of the flow the shape strongly depends on the turbulence in the (stratified) flow.

Surface waves are less important to the actual value of the wind-generated surface drift velocity. However, the surface waves are important to the total shear stress at the water surface; the increased turbulence level in case of waves leads to a slower decrease of flow velocity down from the surface.

The wind drift velocity at the surface  $u_s$  can be stated:

$$u_s \sim 0.035 U_w$$

however, with  $U_w$  to be measured at an altitude dependent on the wind velocity and fetch (L). Calculating  $u_s$  in this way, the proportionality constant 0.035 is practically independent on wind velocity and fetch.

The wind-induced shear stress at the water surface is the direct source of the vertical flow velocity profile, the inclination of the water surface in an enclosed system (wind set-up), and the turbulence near the surface. By means of the direct relations (in the case of very simplified systems like a rectangular tank) between  $\tau_s$  and the phenomena mentioned,  $\tau_s$  can be determined from measurements on the velocity profile, wind set-up and eddy correlation.

### Velocity field in stratified basins

The wind-induced currents generate turbulence and entrainment that influence

the position (depth) of the interface.

The turbulent mass exchange is reduced by a vertical density gradient. Often, the reduction is described by the empirical Munk-Anderson relation (for non-tidal systems), however, the spread of the experimental results is large. Also direction measurements have been made on  $\epsilon_{u,z}$  as a function of wind velocity and stratification.

Many experiments have been done to derive the relation between stratification and entrainment velocity  $w_e$ . (The stratification has been quantified by the "local" or "overall" Richardson number.) A unique  $w_e - Ri$  relation has not been found but the relation seems to depend on the way turbulence is generated in the turbulent layer (e.g. by a stirring grid, or by applying a shear stress at the water surface).

The shear stress  $\tau_s$  causes the inclination of the surface, and the interface as well. The inclination of the interface can be calculated for the simple case of a rectangular basin.

#### Thermal stratified basins

In a thermal stratified basin the wind causes a well-mixed upper layer. At increasing wind a deepening of the upper layer takes place by entrainment. However, in case of sufficient (solar) radiation from the atmosphere to the water, stratification may appear again in the mixed upper layer.

In case of no heat exchange with the atmosphere the deepening of the mixed upper layer is a matter of balance between the kinetic energy  $E_k$  (generated at the surface), the increase of the potential energy  $\Delta E_p$  by entrainment, and the viscous dissipation of the kinetic energy  $E_d$  on the way from the surface down to the interface. Experimentally the ratio  $(E_k - E_d)/E_k$  is of the order of  $10^{-2}$  to  $10^{-3}$ , with  $E_d$  dependent on several parameters (e.g. depth of the upper layer, way of generating kinetic energy).

In field situations the water-atmosphere heat flux  $q$  must be taken into consideration. Several empirical constants (not described in this report) are necessary to determine the heat flux as a function of the atmospheric conditions and the conditions of the water basin. The depth and the temperature of the mixed upper layer depends on the balance of  $E_k$ ,  $E_d$ ,  $\Delta E_p$  and  $q$ , and relation between these quantities may be derived, however, containing some constants that must be derived experimentally (especially the constant for the energy dissipation).

### Field conditions

In field conditions a lot of factors influence the wind drift circulations e.g. the wind velocity and wind direction, geometry and bathymetry, stratification and Coriolis effect in case of extended, deep basins. Because the survey on scale models is difficult and expensive, mathematical models are often used. Then several simplifications are necessary. For instance, the geometry and bathymetry of the basin, and the spatial and temporal wind field must be schematized. Moreover, simplification in the momentum equations may be the consideration of a stationary system, neglect of Coriolis effect (for shallow systems), neglect of non-linear term (in case of smooth variation of bottom- and wall configuration).

The various phenomena induced by wind, are generally surveyed in highly simplified laboratory models. Then, one has the opportunity to survey only one or a few phenomena together. Some feeling to the combined action of a few phenomena can be obtained from calculations known from the literature. Then, the wind-induced flows have been calculated depending on several relevant parameters, for simplified basins (Section 6.5).

## LITERATURE

- [1965] BAINES, W.D. and KNAPP, D.J., "Wind-driven water currents".  
Proc. ASCE 91, HY2, 205.
- [1967] BELYAEV, V.S., "The dependence of the spectra of the velocity components of a wind-driven current on the spectrum of the tangential wind force".  
Izv., atm. & Ocean. Phys. 3.
- [1975] BEMBARON, A.M.C., "Driedimensionaal stromingsbeeld in modellen van meren onder invloed van wind, in het bijzonder van de Petrusplaat in de Biesbosch".  
Kandidaatsverslag, TH Delft, Lab. Fys. Techn.
- [1973] BENGTTSSON, L., "Conclusions about turbulent exchange coefficient from model studies".  
Bull. Ser. A23, 306, Univ. Lund, Div. Hydr.
- [1973b] BENGTTSSON, L., "Mathematical models of wind-induced circulation in a lake".  
Bull. Ser. A23, 313, Univ. Lund, Div. Hydr.
- [1974] BENNETT, J.R., "On the dynamics of wind-driven lake currents".  
J. Phys. Ocean. 4, 400.
- [1971] BIRCHFIELD, G.E., "Wind-driven currents in a large lake or sea".  
ANL/ES-6, Argonne Nat. Lab., Argonne, Illinois.
- [1973] BOUWMEESTER, R.J.B., "Windsnelheidsprofiel boven zee".  
Afd. Weg- en Waterbouw, Vakgroep Kustwaterbouw, TH Delft.
- [1969] BRONGERSMA-SANDERS, M. and GROEN, P., "Wind and water depth and their bearing on the circulation in evaporite basins".  
Proc. 3<sup>rd</sup> Symp. On Silt, Cleveland, Ohio.
- [1955] CHARNOCK, H., "Wind stresses on a water surface".  
Quart. J. Roy. Met. Soc. 81, 639.

LITERATURE (continued)

- [1961] Chatou, "Effet du vent sur deux nappes de liquides superposées et de densités différentes".  
Note DR.D 04, Lab. Nat. d'Hydr., Electricité de France.
- [1963] CSANADY, G.T., "Turbulent diffusion in Lake Huron".  
J. Fluid Mech. 17, 360.
- [1964] CSANADY, G.T., "Turbulence and diffusion in the great lakes".  
Great Lakes Res. Div. Publ., No. 11, p. 326.
- [1972] CSANADY, G.T., "Geostrophic Drag, Heat and Mass Transfer Coefficients for the diabatic Ekman Layer".  
J. Atmos. Sci. 29, 97.
- [1972b] CSANADY, G.T., "Response of large stratified lakes to wind".  
J. Phys. Ocean. 2, 3.
- [1974] CSANADY, G.T., "The "roughness" of the sea surface in light winds".  
J. Geophysical Res. 79, 2747.
- [1975] CSANADY, G.T., "Hydrodynamics of large lakes".  
Woods Hole Ocean. Inst., Contr. nr. 3340.
- [1969] DAKE, J.M.K. and HARLEMAN, D.R.F., "Thermal stratification in lakes, analytical and laboratory studies".  
Water Resources Res. 5, 484.
- [1972] DARBYSHIRE, J. and EDWARDS, A., "Seasonal formation and movement of the thermocline in lakes".  
Pure and Applied Geophysics 93, 141.
- [1974a] Delft Hydraulics Laboratory, "Influence of wind on the vertical velocity profile in homogeneous flows" (in Dutch).  
Report W 152, Delft.

LITERATURE (continued)

- [1974c] Delft Hydraulics Laboratory, "Momentum and mass transfer in stratified flows".  
Report R 880, Delft.
- [1974d] Delft Hydraulics Laboratory, "Mixing of a two-layered system by wind".  
Report M 1235 (in Dutch), Delft.
- [1976a] Delft Hydraulics Laboratory, "Three-dimensional circulation models for shallow lakes and seas".  
Report R 900-I, Delft.
- [1976c] Delft Hydraulics Laboratory, "Calculation of thermal stratification at variable meteorological conditions, Lake Oostvoorn 1972, 1974".  
Report R 870-LH 2214 (in Dutch), Delft.
- [1971] DOBSON, F.W., "Measurements of atmospheric pressure on wind-generated sea waves".  
J. Fluid Mech. 48, 91.
- [1923] EKMAN, V.W., "Über Horizontalcirkulation bei winderzeugten Meeresströmungen".  
Arkiv Mat. Astr. Fysik 17.
- [1973] EMERY, K.O. and CSANADY, G.T., "Surface circulation of lakes and nearly land-locked seas".  
Proc. Nat. Acad. Sci. 70, 93.
- [1972] GEDNEY, R.T., LICK, W. and MOLLS, F.B., "Effect of eddy diffusivity on wind-driven currents in a two-layer stratified lake".  
Lewis Research Center, Rep. No. NASA TN D-6841, Cleveland, Ohio.
- [1971] GROEN, P., "A simplified theory of the combined effect of an anti-estuarine circulation and a superimposed counter-acting wind drift".  
Proc. B74, 358, Kon. Nederl. Acad. Wetenschappen, Amsterdam.

LITERATURE (continued)

- [1969] HAMBLIN, P.F., "Hydraulic and wind-induced circulation in a model of a great lake".  
Proc. 12<sup>th</sup> Conf. Great Lakes Res., Vol. 2, 567.
- [1977] HARLEMAN, D.R.F. and HURLEY OCTAVIO, K., "Heat transport mechanisms in lakes and reservoirs".  
Proc. IAHR Conf., Baden-Baden.
- [1973] HECKER, G.E. and YALE, G.A., "On modelling wind-induced water currents".  
Proc. 21<sup>st</sup> Ann. Hydr. Div. Specialty Conf., Montana State University, Montana.
- [1941] HELLSTRÖM, B., "Wind effect on lakes and rivers".  
Ingeniörsvetenskapsakademien, Bull. 158.
- [1953] HELLSTRÖM, B., "Wind effect on Ringköbing Fjord".  
Trans. American Geophys. Union 34, 194.
- [1974] HSU, S.A., "On the log-linear wind profile and the relationship between shear stress and stability characteristics over the sea".  
Boundary layer Met. 6, 509.
- [1957] HUTCHINSON, G.E., "A treatise on limnology", Vol. I.  
New York, John Wiley.
- [1977] KANTHA, L.H., PHILLIPS, O.M. and AZAD, R.S., "On turbulent entrainment at a stable density interface".  
J. Fluid Mech. 79, 753.
- [1969] KATO, H. and PHILLIPS, O.M., "On the penetration of a turbulent layer into a stratified fluid".  
J. Fluid Mech. 37, 643.
- [1951] KEULEGAN, G.H., "Wind tides in small closed channels".  
J. Res. Nat. Bur. Stand. 46, 358.

LITERATURE (continued)

- [1976] KOK, G.J.G., "Interim rapport: Berekening van thermische stratifikatie; het rechte-bakmodel".  
Landbouwhogeschool Wageningen, Lab. Hydr. & Afvoerhydr., Nota 37.
- [1977] KOK, G.J.G., "Thermal stratification during variable weather conditions".  
Proc. IAHR Conf. A85, Baden-Baden.
- [1967] KRAUS, E.B. and TURNER, J.S., "A one-dimensional model of the seasonal thermocline"  
Tellus 19, 98.
- [1971] KULLENBERG, G., "Vertical diffusion in shallow waters".  
Tellus 23, 129.
- [1973] KULLENBERG, G., MURTHY, C.R. and WESTERBERG, H., "An experimental study of diffusion characteristics in the thermocline and hypolimnion regions of Lake Ontario".  
Proc. 16<sup>th</sup> Conf. Great Lakes, 774.
- [1974] KULLENBERG, G., MURTHY, C.R. and WESTERBERG, H., "Vertical mixing characteristics in the thermocline and hypolimnion regions of Lake Ontario".  
Report of the Canadian Centre for Inland Waters.
- [1977] LIEN, S.L. and HOOPES, G.A., "Wind-induced, steady-state circulation patterns in Lake Superior".  
Symp. Modelling Transport Mechanisms in Ocean and Lakes, Ottawa.
- [1971] LIGGETT, J.A. and LEE, K.K., "Properties of circulation in stratified lakes".  
Proc. Asce 97, HY1, 15.
- [1974] LINDEN, P.F., "The deepening of a mixed layer in a stratified fluid".  
Euromech. Colloquium, Cambridge.

LITERATURE (continued)

- [1960] LÖFQUIST, K., "Flow and stress near an interface between stratified liquids".  
Phys. of Fluids 3.
- [1975] LONG, R.R., "The influence of shear on mixing across density interfaces".  
J. Fluid Mech. 70, 305.
- [1952] LONGUET-HIGGINS, M.S., "Oscillations in a three-layered stratified basin".  
Appendix to Mortimer [1952a].
- [1954] MARCIANO, J.J. and HARBECK, G.E., "Mass transfer studies, water loss investigations: Lake Hefner studies technical report".  
Geol. Survey Prof. Paper, U.S. Dept. Interior, No. 269.
- [1972] MONIN, A.S., "The atmospheric boundary layer".  
Ann. Rev. Fluid Mech. 2, 225.
- [1952a] MORTIMER, C.H., "Water movements in lakes during summer stratification evidence from the distribution of temperature in Windermere".  
Phil. Trans. Roy. Ser. London 236B, 355.
- [1952b] MORTIMER, C.H., "Water movements in stratified lakes, deduced from observations in Windermere and model experiments".  
Assoc. Intern. Hydr. Sci, C.R. rapp. 3, 335.
- [1948] MUNK, W.H. and ANDERSON, E.R., "Notes on the theory of the thermocline".  
J. Marine Res. 1, 276.
- [1975] MURRAY, S.P., "Trajectories and speeds of wind-driven currents near the coast".  
J. Phys. Ocean. 5, 347.
- [1969] MYER, G.E., "A field study of Langmuir circulations".  
Proc. 12<sup>th</sup> Conf. Great Lakes Res., 652.

LITERATURE (continued)

- [1972] NIHOUL, J.C.J., "The effect of wind blowing on turbulent mixing and entrainment in the upper layer of the ocean".  
Mem. Soc. Roy. Sciences Liège 6, 115.
- [1975] NIILER, P.P., "Deepening of the wind-mixed layer".  
J. Mar. Res. 33, 405.
- [1974] OTTESEN-HANSEN, N.E., "The effect of wind stress on a stratified deep lake".  
Progress Rep. 32, 17, Inst. Hydrodyn. and Hydr. Engng., Tech. Univ. Denmark.
- [1975] OTTESEN-HANSEN, N.E., "Effect of wind stress on stratified deep lake".  
Proc. ASCE 101, HY8, 1037.
- [1967] PEDLOSKY, J., "Fluctuating winds and the ocean circulation".  
Tellus 19, 250.
- [1966] PHILLIPS, O.M., "The dynamics of the upper ocean".  
Cambridge University Press.
- [1973] POND, J.S., "The exchanges of momentum, heat and moisture at the ocean-atmosphere interface".  
From: "Numerical models of ocean circulation", Nat. Acad. of Sciences.
- [1957] REID, R.O., "Modification of the quadratic bottom-stress law for turbulent channel flow in the presence of surface wind stress".  
Tech. Memo 93, Beach Erosion Board, U.S. Dept. Army, Wash. D.C.
- [1965] ROLL, H.U., "Physics of the marine atmosphere".  
Acad. Press, New York.
- [1971] RYAN, P.J. and HARLEMAN, D.R.F., "Prediction of the annual cycle of temperature changes in a stratified lake or reservoir: mathematical model and user's manual".  
R.M. Parsons Lab., M.I.T., Rep. No. 137.

LITERATURE (continued)

- [1976] SHAW, C.Y. and LEE, Y., "Wind-induced turbulent heat and mass transfer over large bodies of water".  
J. Fluid Mech. 77, 645.
- [1973] SHEMDIN, O.H., "Modelling of wind-induced current".  
J. Hydr. Res. 11, 281.
- [1969] SHKUDOVA, G.Ya. and KOVALEV, N.P. "An experiment in applying a stationary hydrodynamic model in calculating currents in a shallow sea".  
Meteorologiya i Gidrologiya 10, 76.
- [1971b] SIMONS, T.J. and JORDAN, D.E., "Computed water circulation of Lake Ontario for observed winds".  
Canada Centre for Inland Waters, CCIW Paper No. 9.
- [1971] SIMONS, T.J., "Development of numerical models of Lake Ontario".  
Proc. 14<sup>th</sup> Conf. Great Lake Res., 654.
- [1972] SIMONS, T.J., "Development of numerical models of Lake Ontario, II".  
Proc. 15<sup>th</sup> Conf. Great Lake Res.
- [1976] SPALDING, D.B. and SVENSSON, U., "The development and erosion of the thermocline".  
Proc. Int. Center Heat and Mass Transfer, Dubrovnik.
- [1973] SUNDARAM, T.R. and REHM, R.G., "The seasonal thermal structure of deep temperate lakes".  
Tellus 25, 157.
- [1973] TENNEKES, H., "Turbulent entrainment in stratified fluids".  
Mém. Soc. Roy. Sc. de Liège 6, 131.
- [1975] THOMPSON, S.M. and TURNER, J.S., "Mixing across an interface due to turbulence generated by an oscillating grid".  
J. Fluid Mech. 67, 349.

LITERATURE (continued)

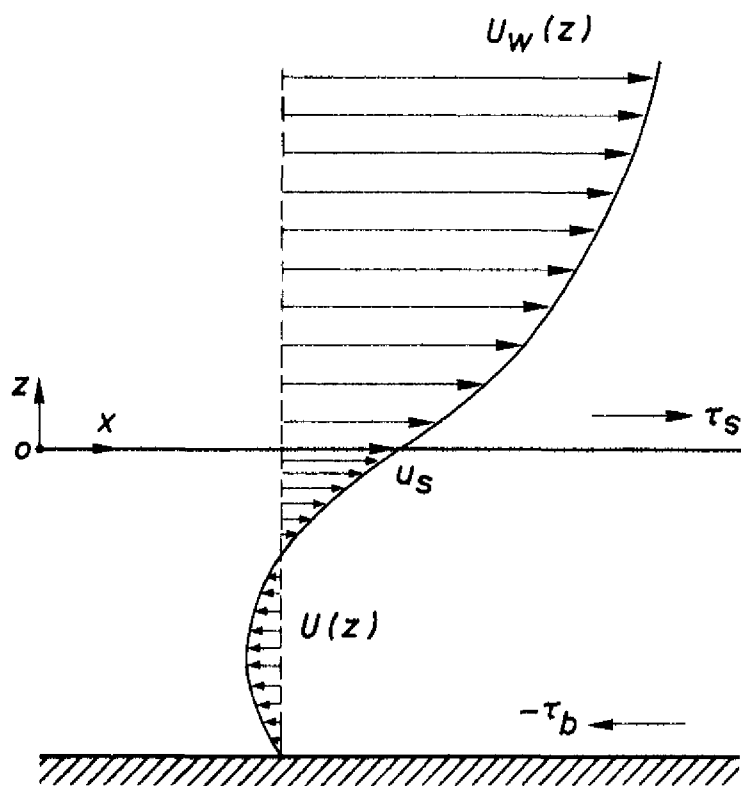
- [1974] THORPE, S.A., "Near resonant forcing in a shallow two-layer fluid: a model for the internal surge in Loch Ness?".  
J. Fluid Mech. 63, 509.
- [1977] TUCKER, W.A. and GREEN, A.W., "Thermocline formation in large and small lakes".  
Symp. Mod. Transport Mechanisms in Ocean and Lakes, Ottawa.
- [1973] TURNER, J.S., "Geophysical examples of layering and microstructure: interpretation and relation to laboratory experiments".  
4<sup>th</sup> Coll. Ocean. Hydrodyn., Liège [1972].
- [1974] TURNER, J.S., "Buoyancy effects in fluids".  
University Press, Cambridge.
- [1956] URSELL, F., "Wave generation by wind".  
Symp. on Surveys in Mech., New York.
- [1977] UZZELL, J.C. and ÖZİŞİK, M.N., "Far field circulation velocities in shallow lakes".  
Proc. ASCE 103, HY4, 395.
- [1974] VERHAGEN, J.H.G., "A calculation method of thermal stratification at variable wind and radiation".  
Report R 898-I (in Dutch), Delft Hydr. Inst., Delft.
- [1978] VERHAGEN, J.H.G., "Thermal stratification for several meteorological conditions" (in Dutch).  
H<sub>2</sub>O 11, 207.
- [1957] WELANDER, P., "Wind action on a shallow sea: some generalizations of Ekman's theory".  
Tellus 9, 45.

LITERATURE (continued)

- [1973] WIERINGA, J., "Comparison of three methods for determining strong wind stress over lake Flevo".  
Boundary layer Meteorology 7, 3.
- [1969a] WU, J., "Froude number scaling of wind stress coefficients".  
J. Atm. Sci. 26, 408.
- [1969b] WU, J., "Wind stress and surface roughness at air-sea interface".  
J. Geophys. Res. 74, 444.
- [1970] WU, J., "Laboratory studies of wind boundary layers; wind stress coefficients and scalings".  
Von Kármán Institute for fluid dynamics.
- [1971] WU, J., "Anemometer height in Froude scaling of wind stress".  
Proc. ASCE 97, WW1, 131.
- [1973a] WU, J., "Wind-induced turbulent entrainment across a stable density interface".  
J. Fluid Mech. 61, 275.
- [1973b] WU, J., "Prediction of near-surface drift currents from wind velocity".  
Proc. ASCE 99, HY9, 1291.
- [1973c] WU, J., "Wind-induced drift current".  
Hydronautics, Tech. Rep. 7303-3.
- [1975a] WU, J., "Slope of a stable density interface under wind".  
16<sup>th</sup> IAHR Congress, Sao Paulo.
- [1975b] WU, J., "Sea surface drift currents".  
7<sup>th</sup> Ann. Offshore Tech. Conf., Houston, Paper OTC 2294.

LITERATURE (continued)

- [1975c] WU, J., "Wind-induced drift currents".  
J. Fluid Mech. 68, 49.
- [1977] WU, J., "A note on the slope of a density interface between two stably stratified fluids under wind".  
J. Fluid Mech. 81, 335.



QUALITATIVE VERTICAL PROFILE OF WIND AND FLOW  
CURRENT FOR A TWO-DIMENSIONAL ENCLOSED SYSTEM

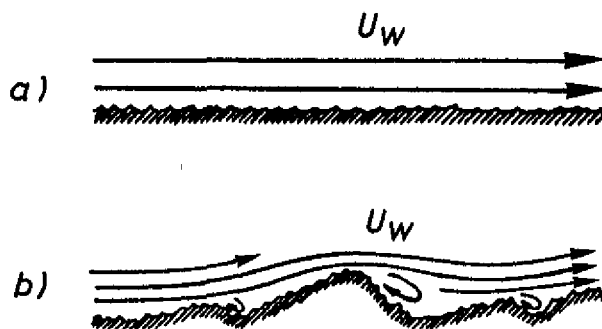
JM

A4

DELFT HYDRAULICS LABORATORY

R898-II-1004

FIG. 1

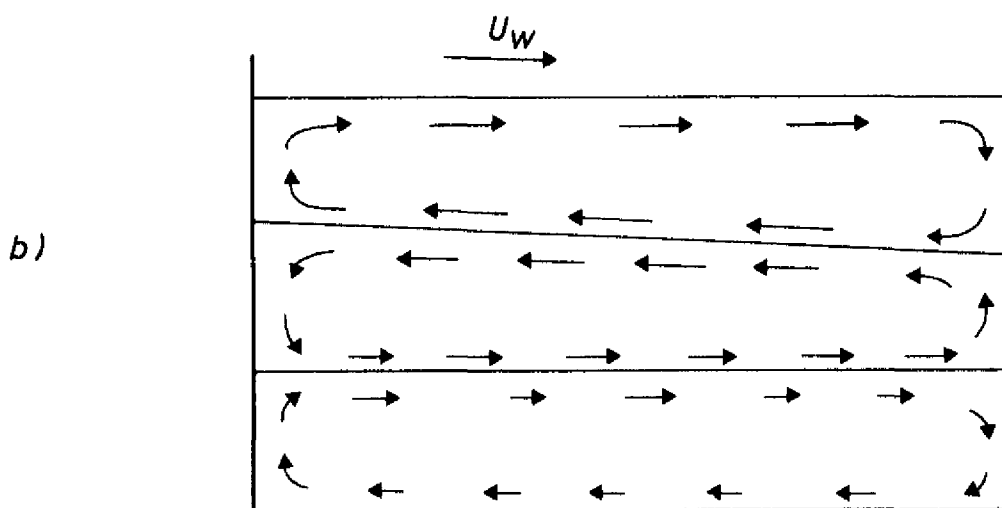
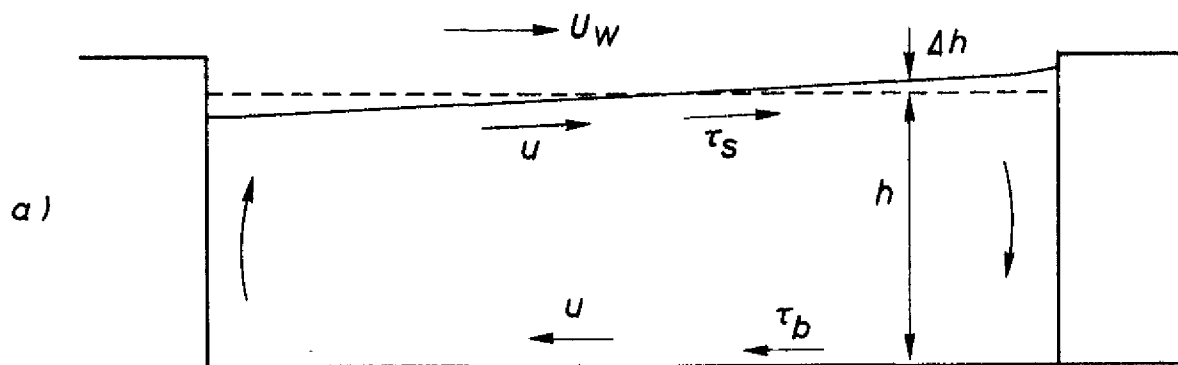


a) CAPILLARY WAVES (WIND RIBS) ON A WATER SURFACE

JM

b) CAPILLARY WAVES SUPERIMPOSED ON GRAVITY (WIND) WAVES

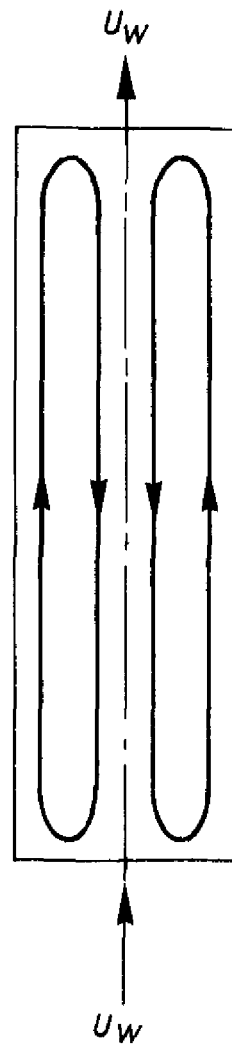
A4



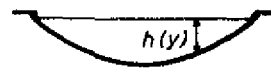
SCHEME OF WIND SET-UP AND INDUCED VERTICAL CIRCULATION IN AN TWO-DIMENSIONAL ENCLOSED SYSTEM  
 a) UNSTRATIFIED                      b) LAYERED SYSTEM

JM

A4



a)

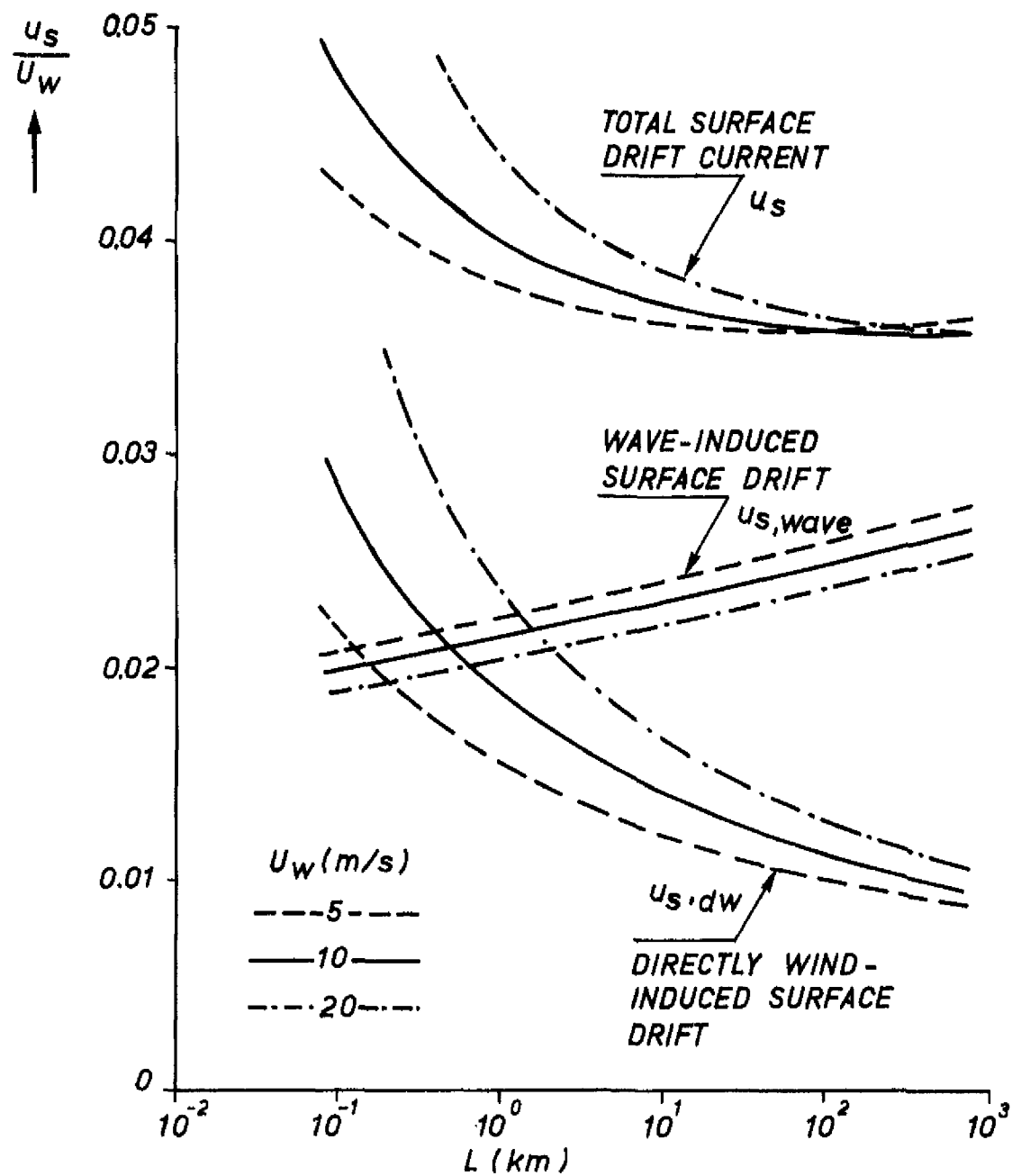


b)

a) WIND-INDUCED CURRENT PATTERN IN A BASIN  
WITH INHOMOGENEOUS DEPTH PROFILE  
b) DEPTH PROFILE

JM

A4



SURFACE DRIFT  $u_s$  INDUCED BY WIND AND WAVES  
 VERSUS FETCH  $L$  ( $z$  DEPENDENT ON  $L$ )

JM

WU (1975 b)

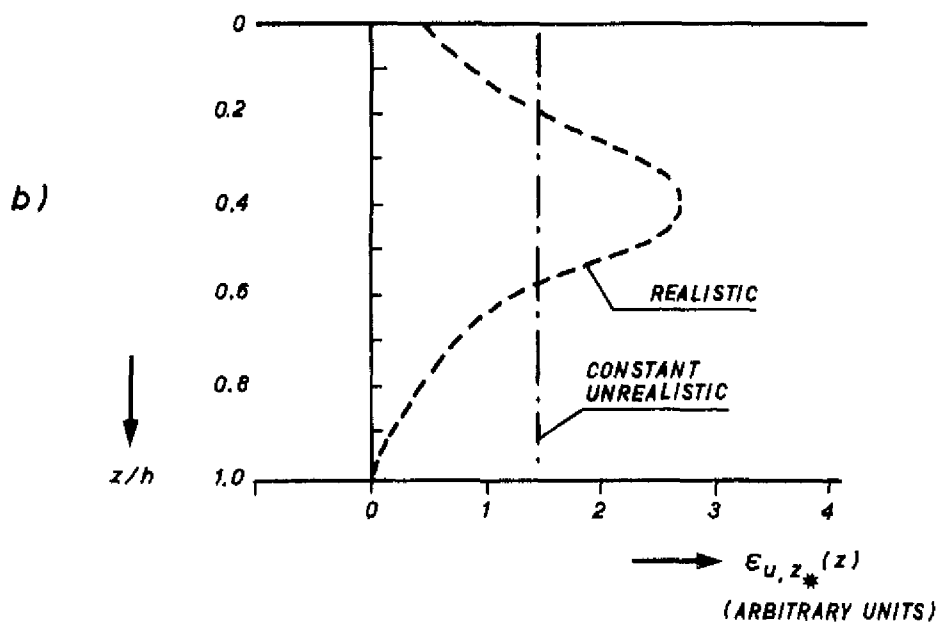
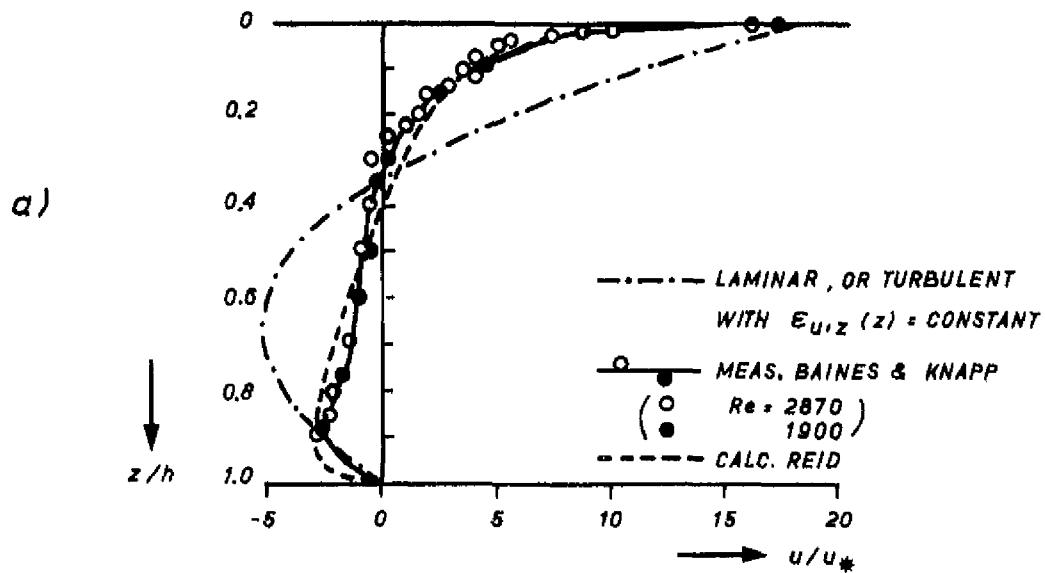
A4

DELFT HYDRAULICS LABORATORY

R898-II-1008

FIG. 5



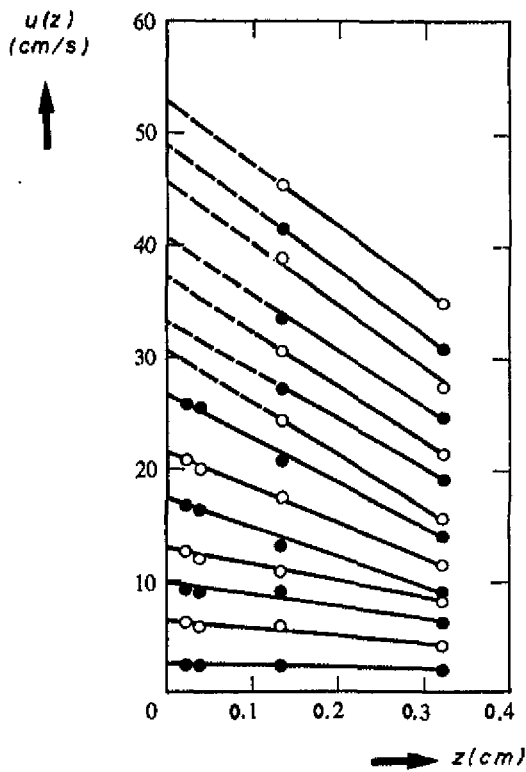


a) VERTICAL VELOCITY PROFILES FOR 2D CLOSED BASIN

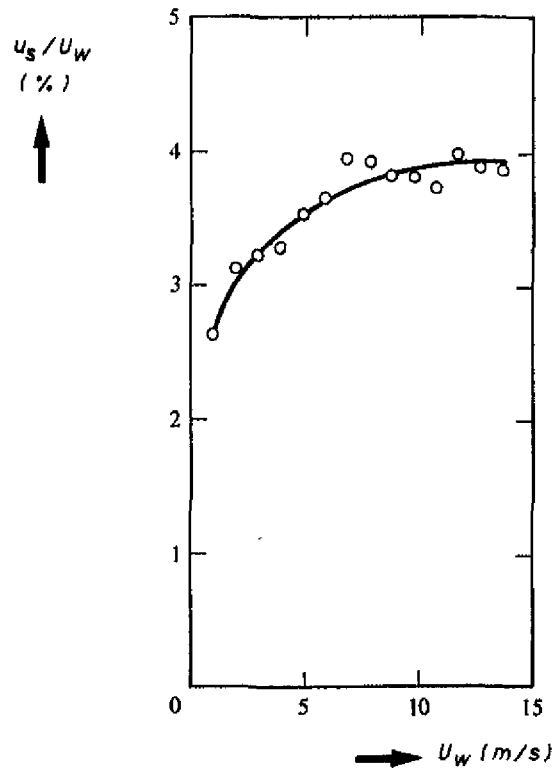
b) VERTICAL EDDY VISCOSITY DISTRIBUTION

JM

A4



a)



b)

a) WIND-DRIFT VELOCITY  $u(z)$  VERSUS  $z$  ( $z=0$ , WATER SURFACE)  
 b) RATIO  $u_s/U_w$  VERSUS  $U_w$

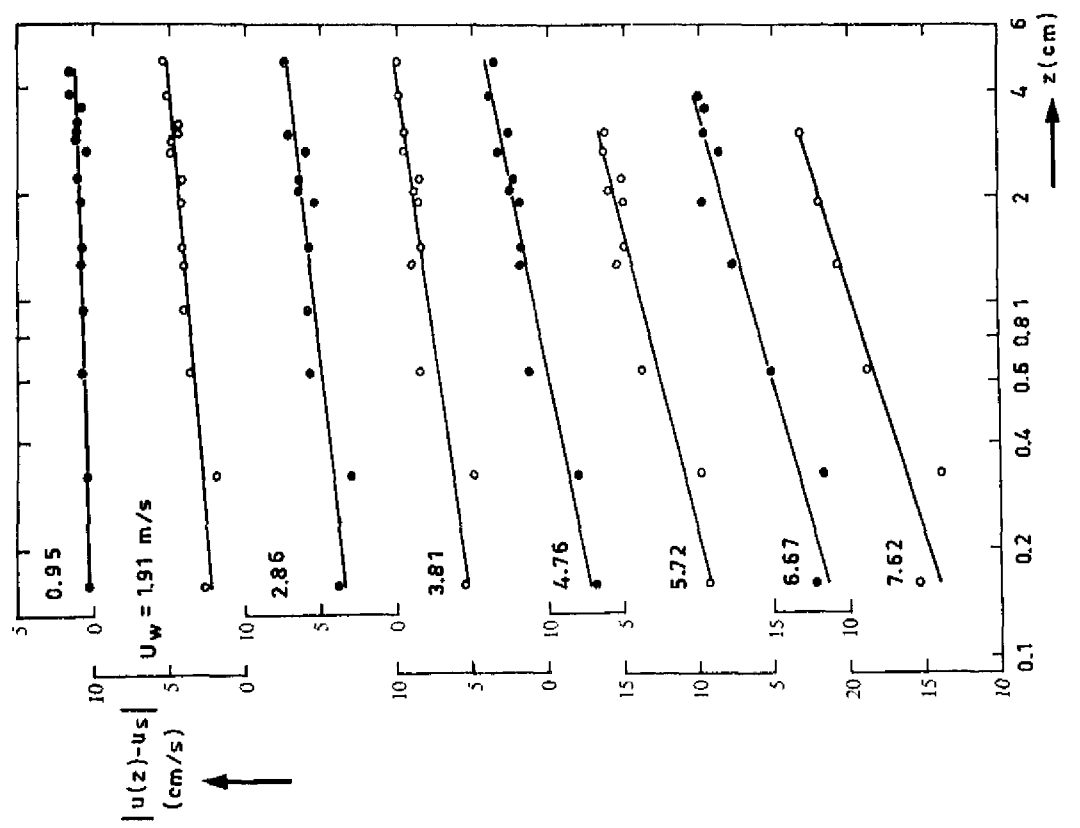
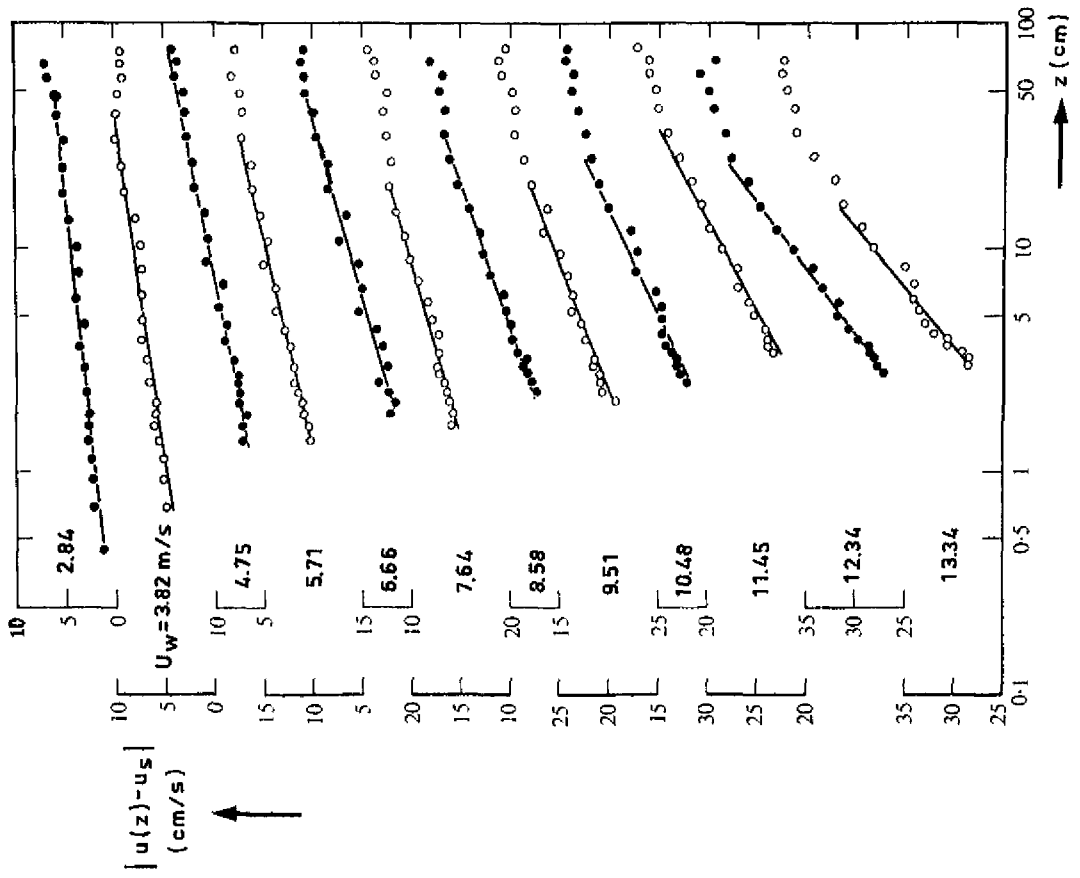
JM

WU (1975 c)

A4

DELFT HYDRAULICS LABORATORY

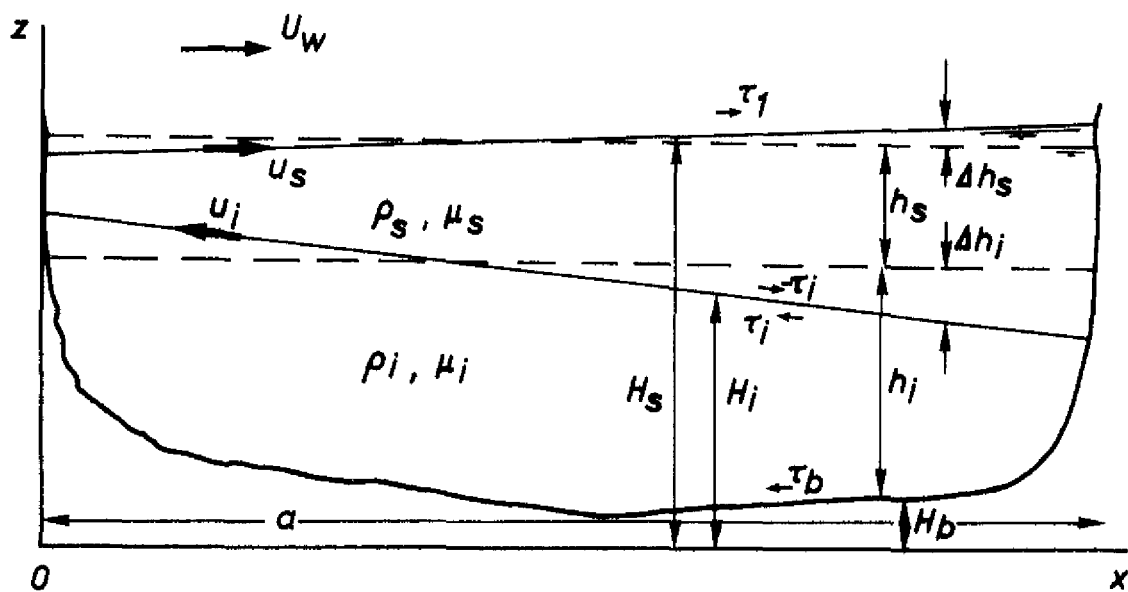
R 898-II-1023 FIG. 8a,b



VERTICAL WIND DRIFT VELOCITY PROFILE  $u(z)$   
 FLUME DEPTH 1.5 m  $z = 0$  IS MEAN WATERSURFACE

DELFT HYDRAULICS LABORATORY

|                |          |
|----------------|----------|
|                | JM       |
| $W_u$ (1975 c) | A4       |
| R898-II-1024   | FIG.8c,d |



DEFINITION SCHEME OF WIND SET-UP IN TWO-LAYER SYSTEM

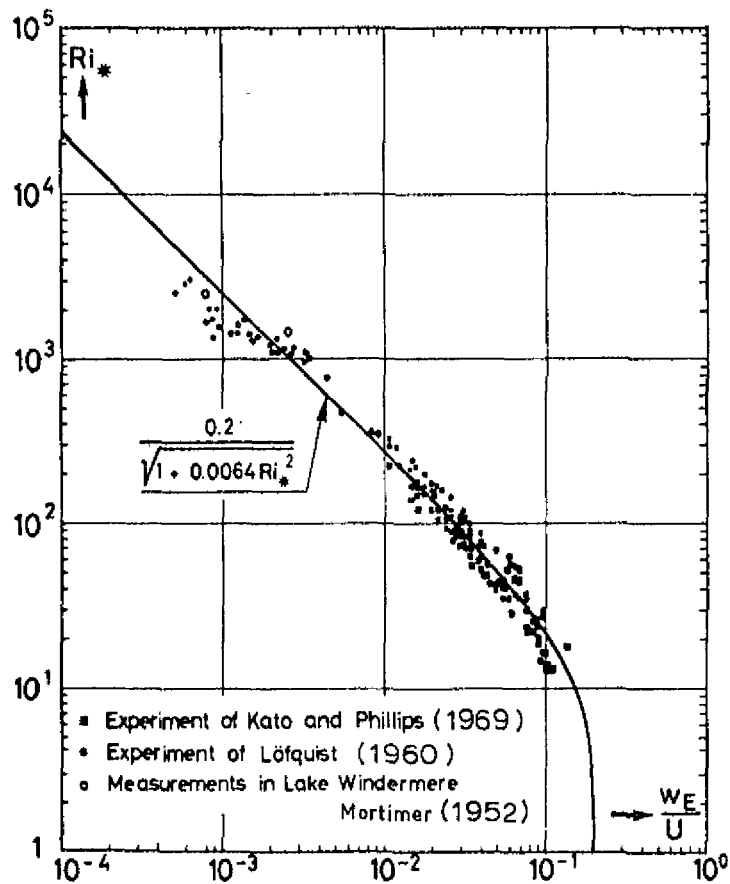
JM

CHATOU (1961)

A4

DELFT HYDRAULICS LABORATORY

R898-II-1011 FIG. 9



ENTRAINMENT VELOCITY  $W_e$  VERSUS  $Ri_*$

OTTESEN  
HANSEN (1975)

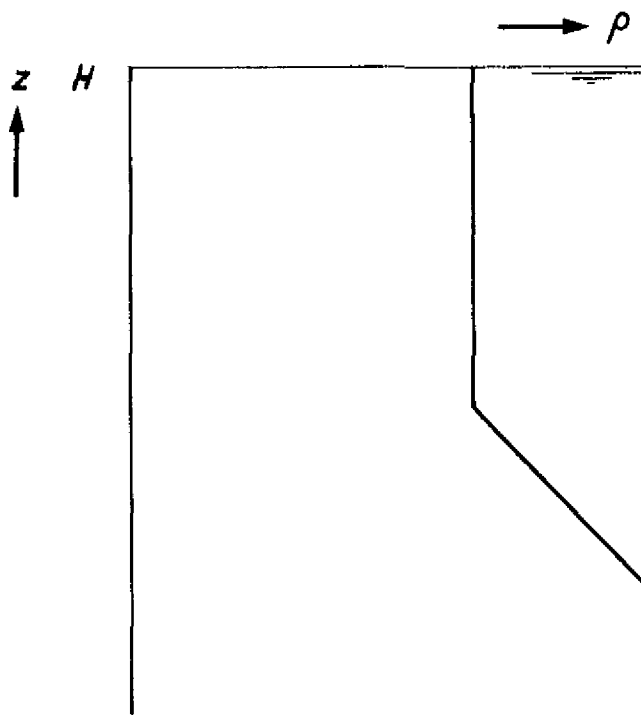
JM

A4

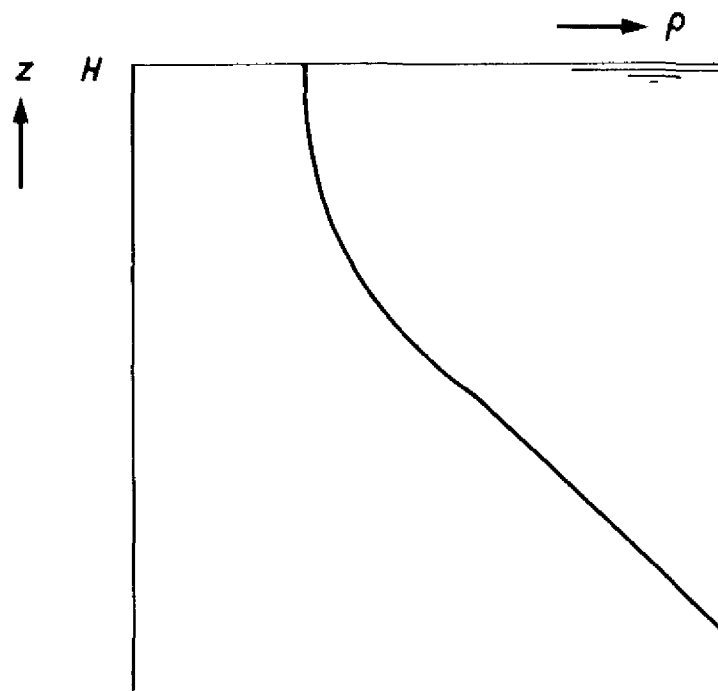
DELFT HYDRAULICS LABORATORY

R898-II-1025

FIG.10



a)



b)

CALCULATED TEMPERATURE STRATIFICATION  
 a) GLOBAL MODEL  
 b) LOCAL MODEL

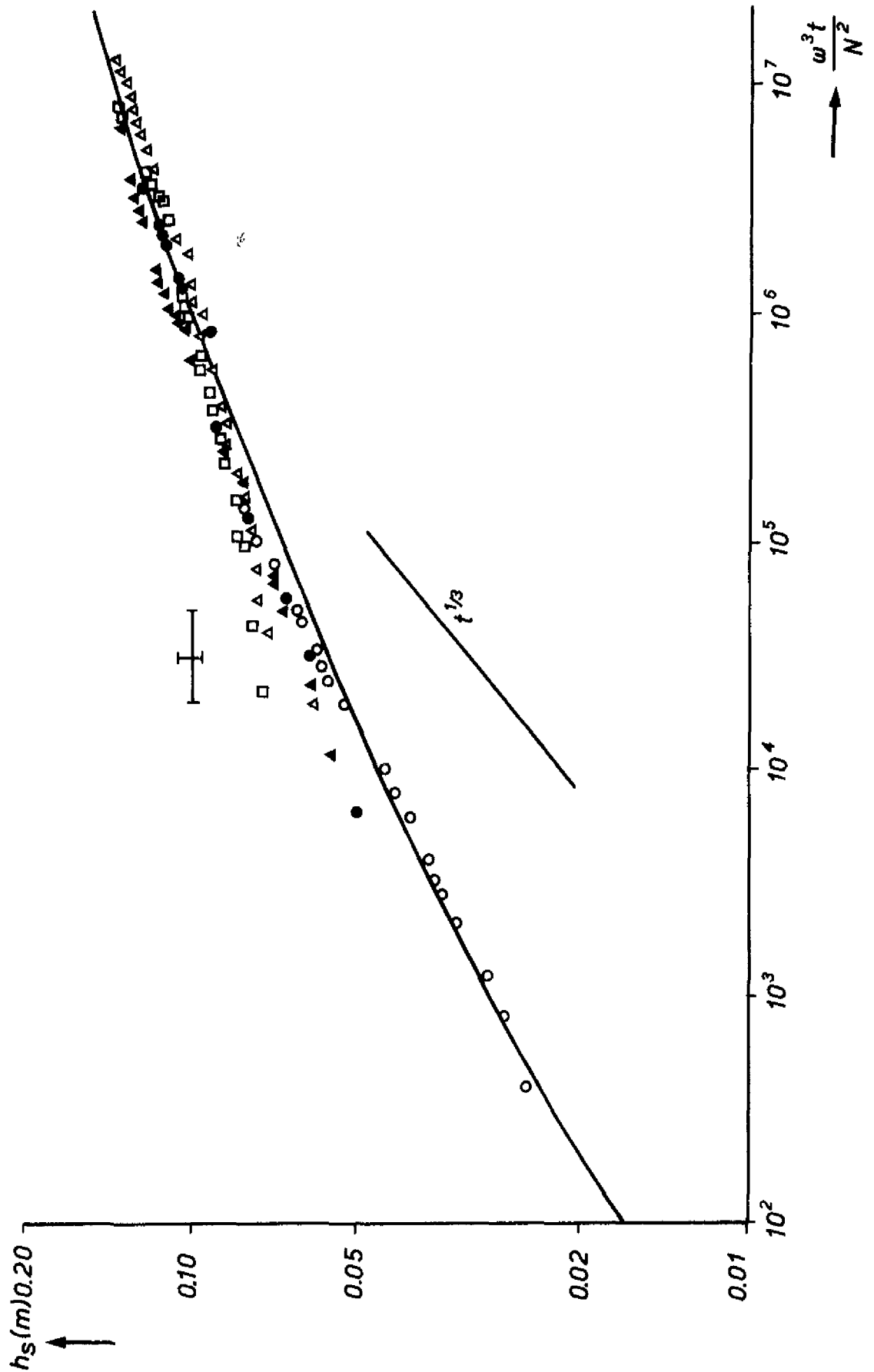
JM

NIHOUL (1972)

A4

DELFT HYDRAULICS LABORATORY

R 898-II-1012 FIG. 11



TIME-DEPENDENT EPILIMNION DEPTH  $h_s(t)$  VERSUS  
 STABILITY PARAMETER  $\omega^3 t/N^2$

JM

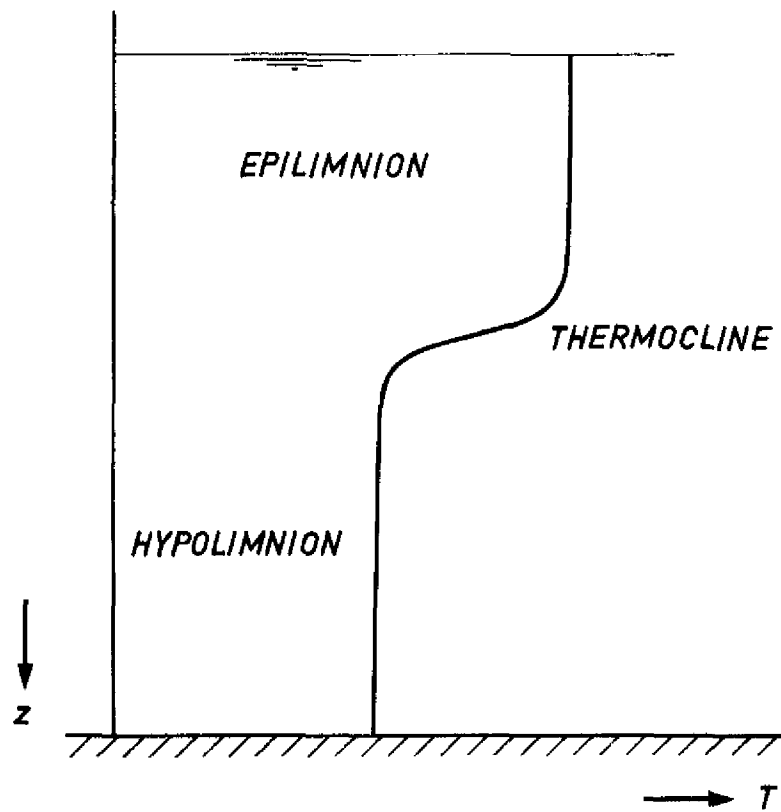
LINDEN (1974)

A4

DELFT HYDRAULICS LABORATORY

R898-II-1013

FIG.12



CHARACTERISTIC TEMPERATURE PROFILE FOR  
DEEP BASINS IN SUMMER

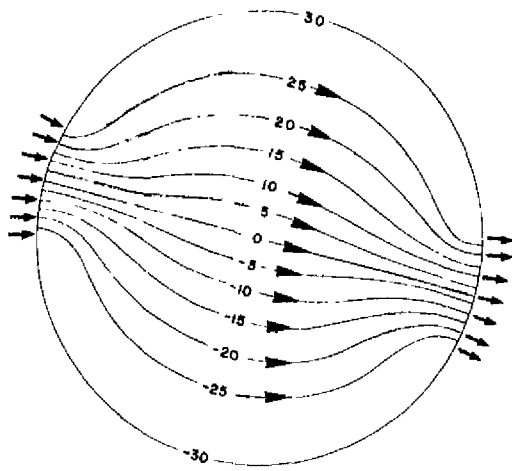
JM

A4

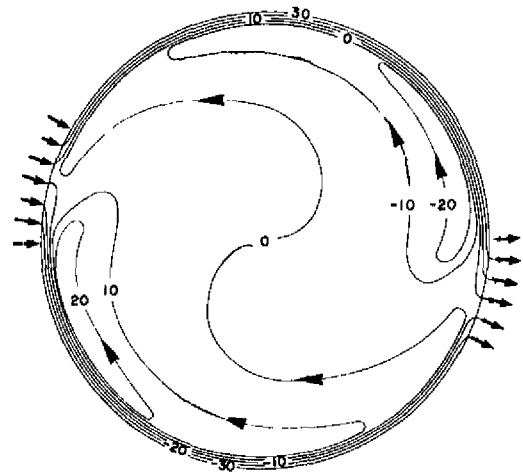
DELFT HYDRAULICS LABORATORY

R898-II-1014

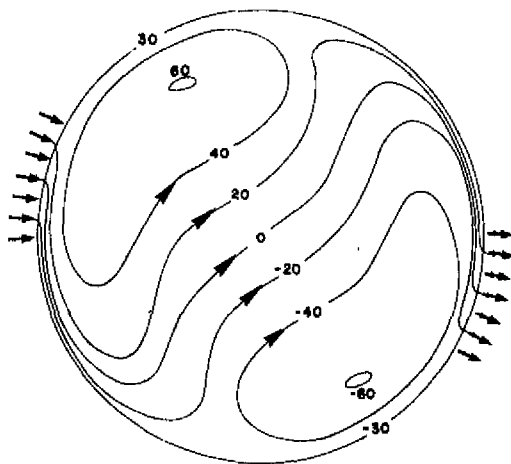
FIG.13



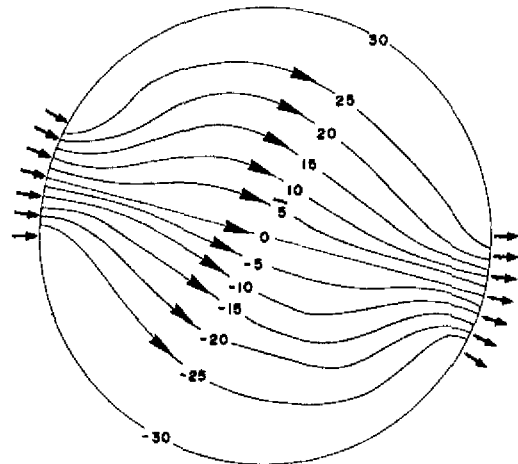
a) HYDR. FLOW, HOMOGENEOUS H



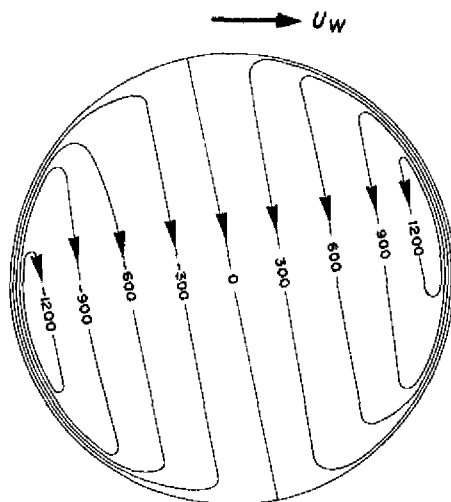
b) HYDR. FLOW PARABOLIC H



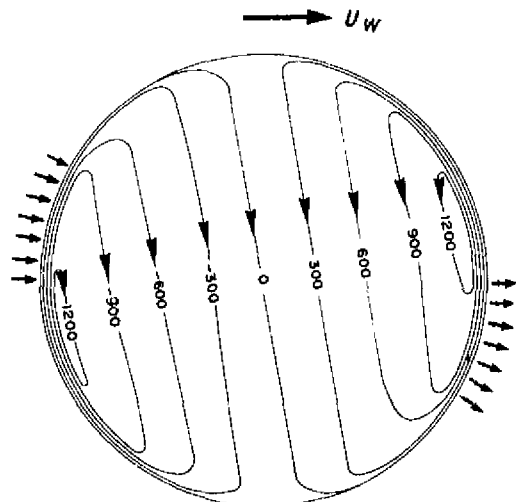
c) HYDR. FLOW,  $E_{u,xy} \times 10$



d) HYDR. FLOW,  $E_{u,xy} \times 100$



e) WIND FLOW



f) WIND FLOW + HYDR. FLOW

STREAM FUNCTIONS IN SHALLOW LAKE,  $\varnothing = 200$  km  
 PARABOLIC DEPTH  $h = 0 \rightarrow 70$  m (EXCEPT a)) HOMOGENEOUS DENSITY. UNITS  $10^2$  m<sup>3</sup>/s

JM

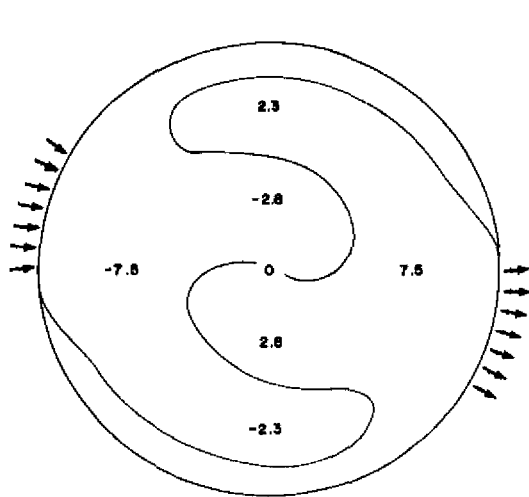
HAMBLIN (1969)

A4

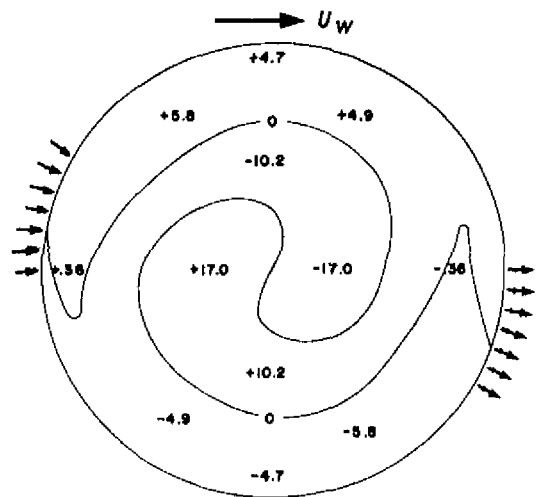
DELFT HYDRAULICS LABORATORY

R898-II-1026

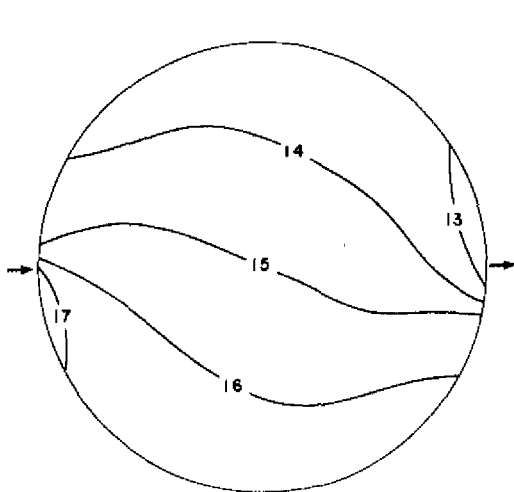
FIG.14



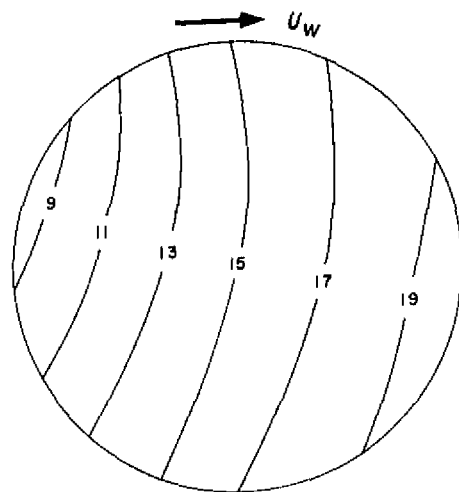
a) HYDR. FLOW



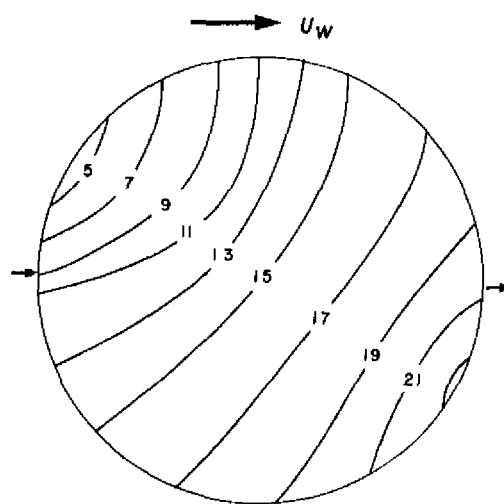
b) HYDR. FLOW + WIND FLOW



c) HYDR. FLOW



d) WIND FLOW



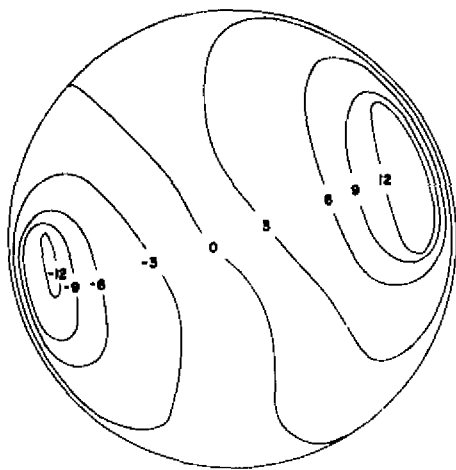
e) WINDFLOW + HYDR. FLOW

a), b) UP-AND DOWNWELLING HOMOGENEOUS SYSTEM  
 c), d), e) DEPTH OF UPPER LAYER (IN m) IN TWO-LAYER MODEL. UNDISTURBED DEPTH 15 m

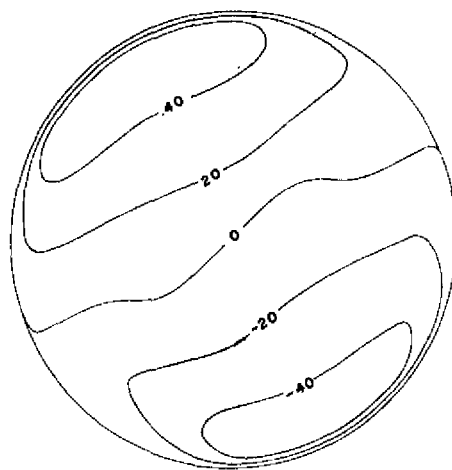
JM

HAMBLIN (1969)

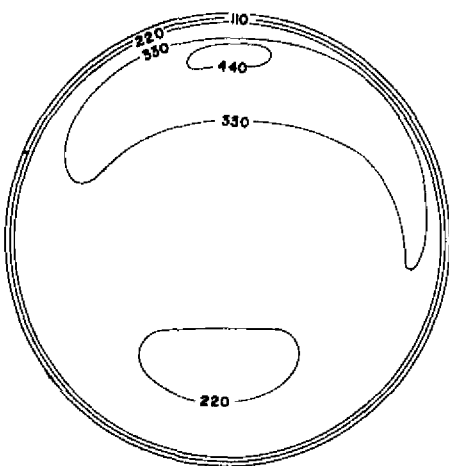
A4



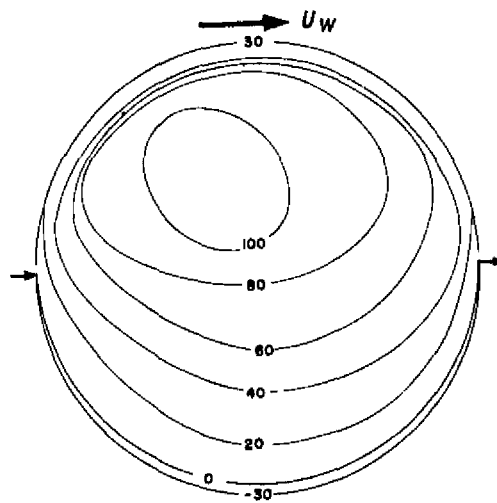
a) HYDR. FLOW IN UPPER LAYER



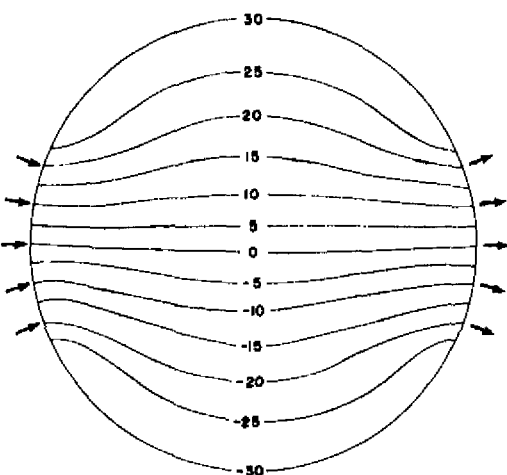
b) WIND FLOW IN UPPER LAYER



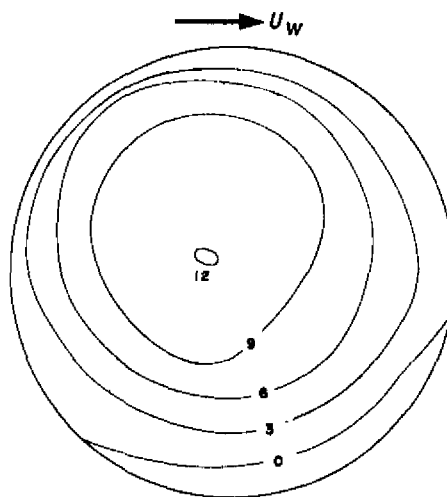
c) WIND FLOW + HYDR. FLOW IN UPPER LAYER



d) WIND FLOW + HYDR. FLOW



e) HYDR. FLOW



f) WIND FLOW

STREAM FUNCTIONS IN TWO-LAYER MODEL  
 a), b), c) LOWER LAYER CIRCULATION  
 d), e), f) UPPER LAYER CIRCULATION

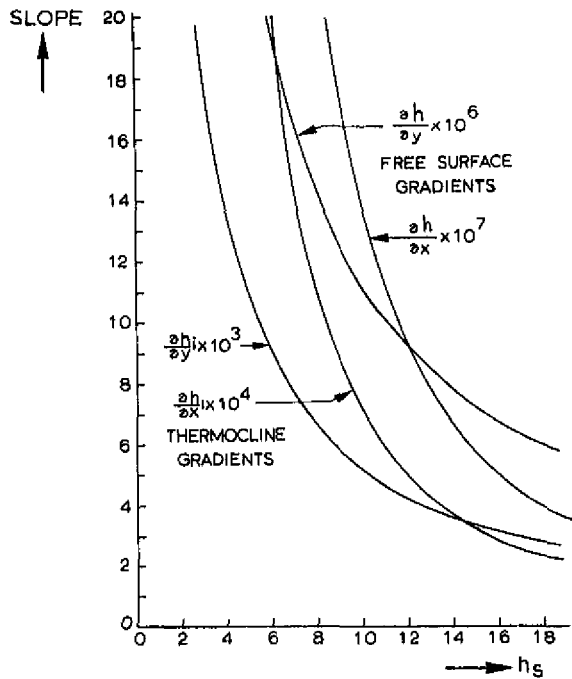
JM

HAMBLIN (1969)

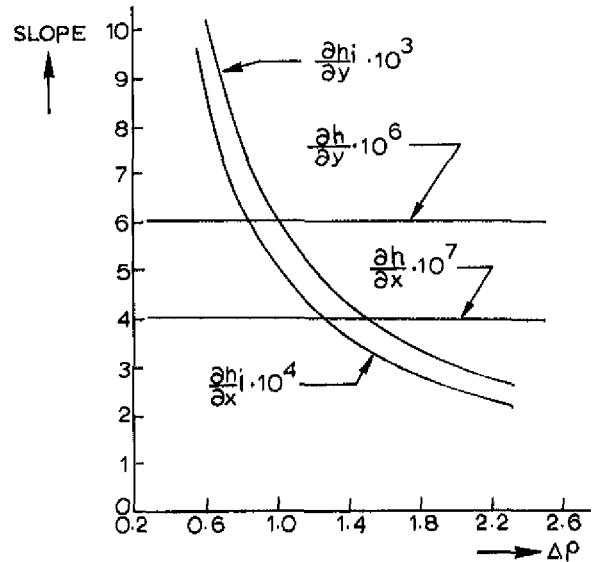
A4

DELFT HYDRAULICS LABORATORY

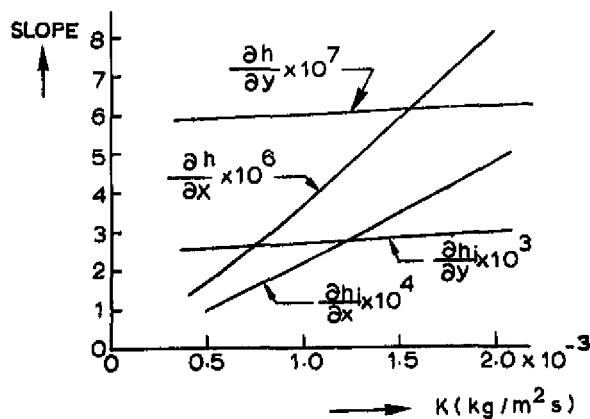
R 898-II-1028 FIG.16



a)



b)



c)

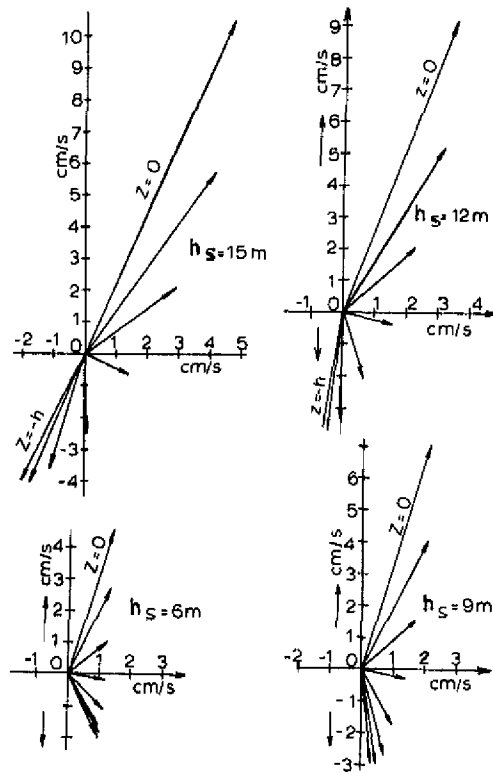
FREE SURFACE  $(\frac{\partial h}{\partial x}, \frac{\partial h}{\partial y})$  AND THERMOCLINE  $(\frac{\partial h_i}{\partial x}, \frac{\partial h_i}{\partial y})$  INCLINATION VERSUS  
 a)  $h_s$     b)  $\Delta\rho$     c)  $k = f(v_1, v_2)$

JM

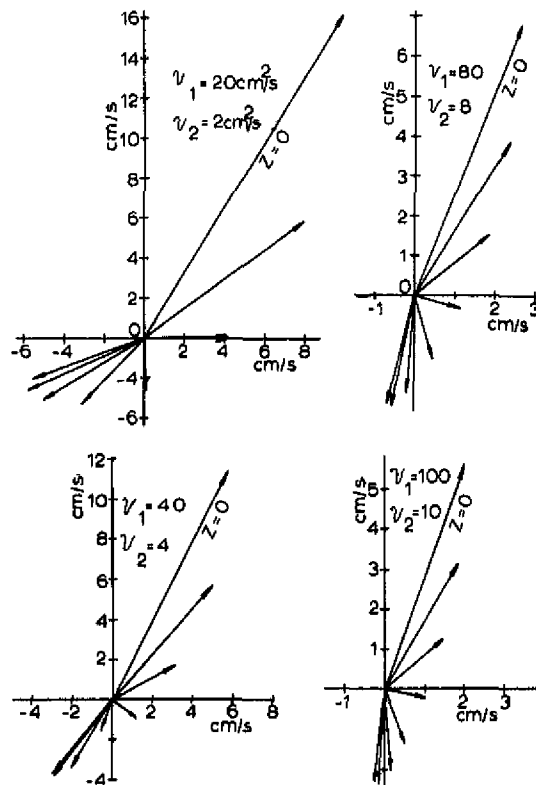
LIGGETT AND  
 LEE (1971)

A4

a)



b)



FLOW VELOCITY VECTORS ON SEVERAL DEPTHS IN THE EPIILMNIION VERSUS

a)  $h_s$       b)  $v_1, v_2$

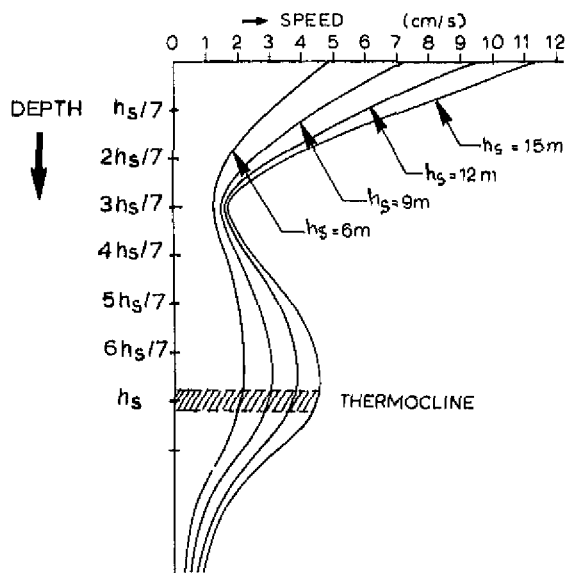
JM

LIGGETT AND  
LEE (1971)

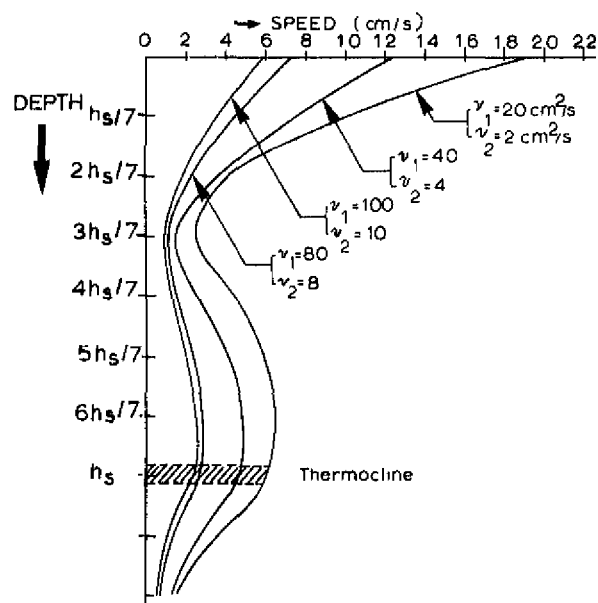
A4

DELFT HYDRAULICS LABORATORY

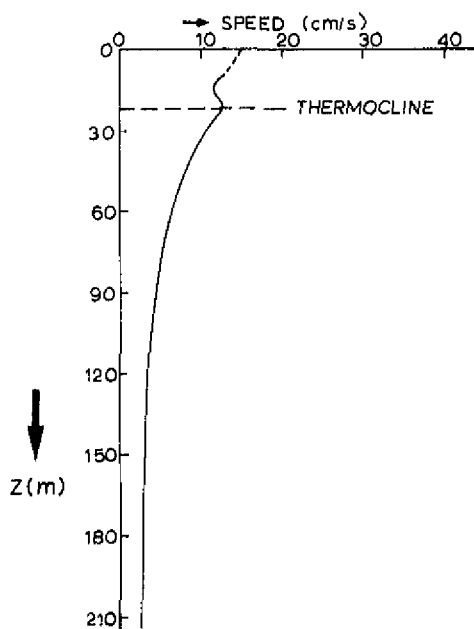
R898-II-1030 FIG.18



a)



b)



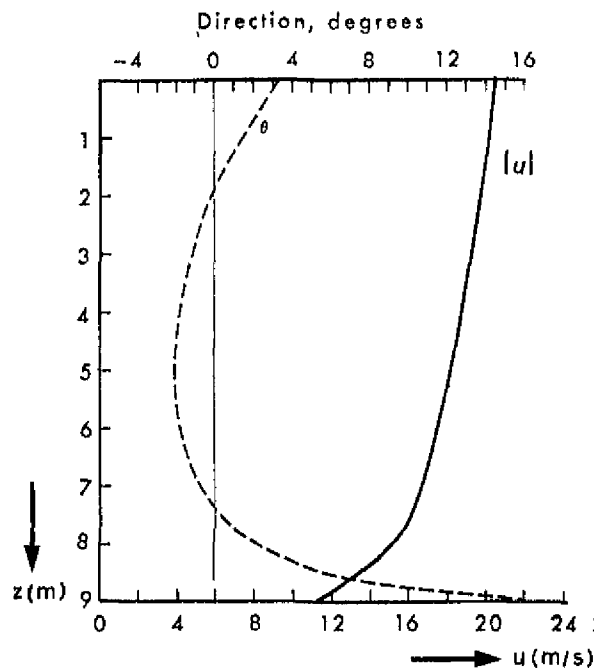
c)

FLOW VELOCITY IN EPILIMNION AND THERMOCLINE  
 REGION VERSUS a)  $h_s$  b)  $\nu_1, \nu_2$   
 c) MEASUREMENTS OF VERBER (1965)

JM

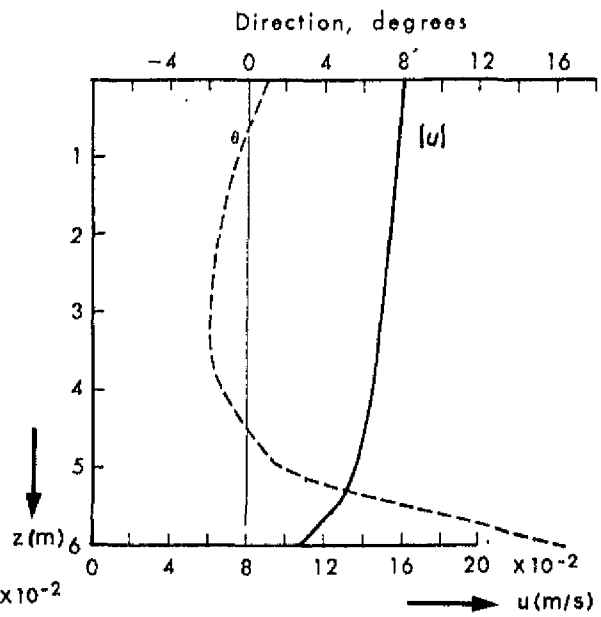
LIGGETT AND  
 LEE (1971)

A4



(a)

$U_w = 5 \text{ m/s}$   
 $E_{u,z} = 0.009 \text{ m}^2/\text{s}$



(b)

$U_w = 4 \text{ m/s}$   
 $E_{u,z} = 0.007 \text{ m}^2/\text{s}$

CALCULATED WIND-INDUCED  $\vec{u}$ -PROFILES NEAR  
 THE COAST. ON-SHORE WIND, ANGLE  $60^\circ$

JM

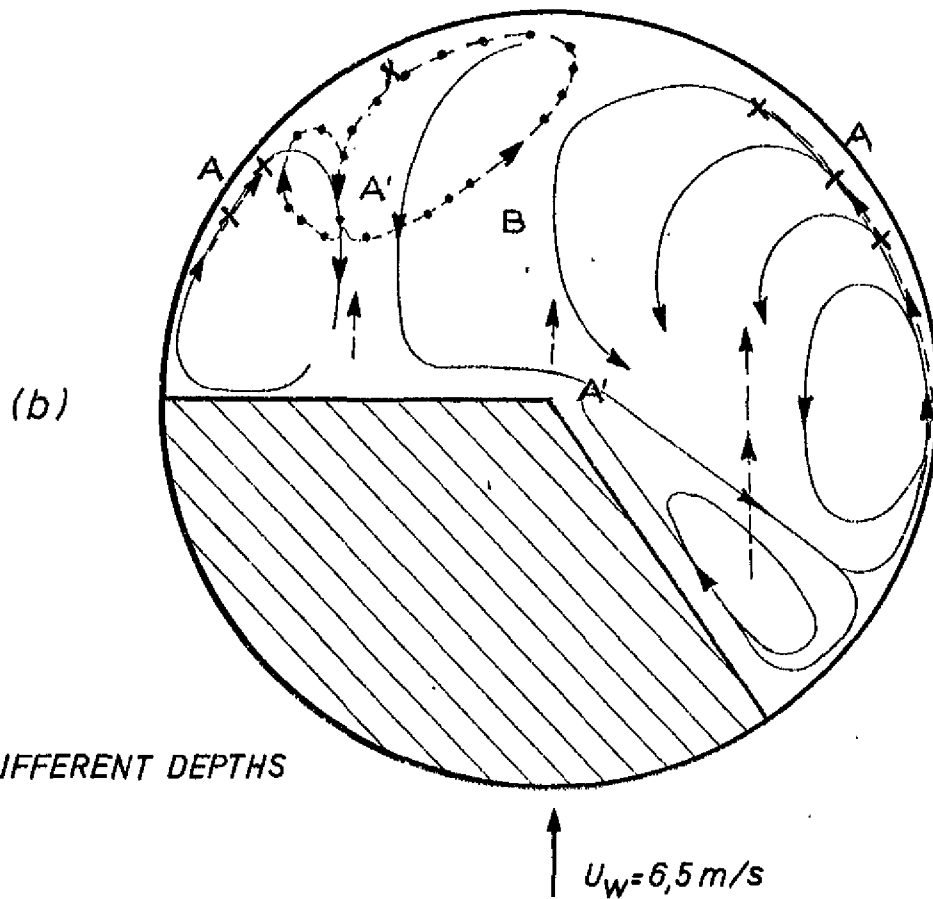
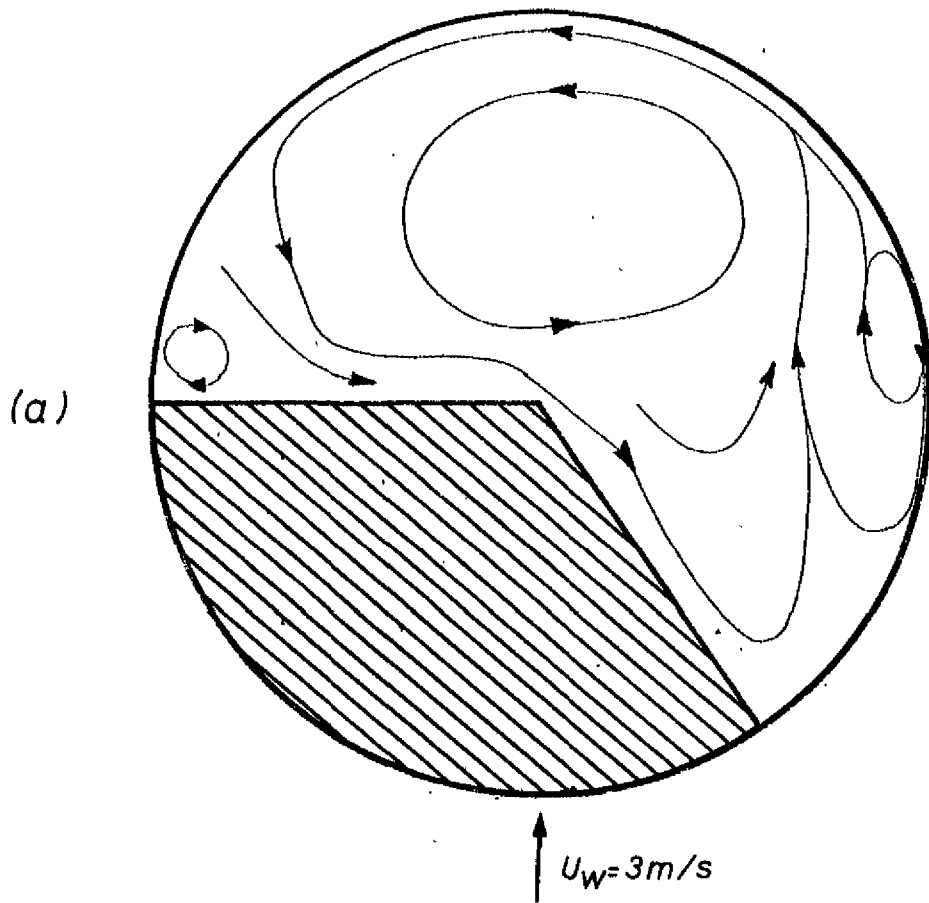
MURRAY (1975)

A4

DELFT HYDRAULICS LABORATORY

R898-II-1016

FIG.20



A, B DIFFERENT DEPTHS

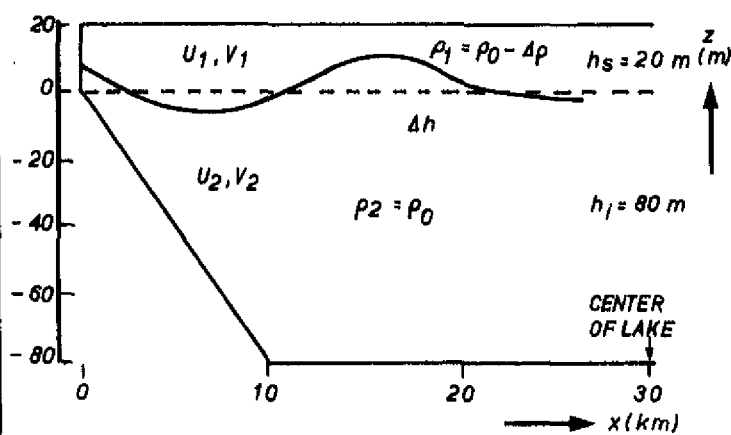
WIND-DRIVEN CIRCULATIONS IN CYLINDRICAL BASIN

BEMBARON(1975) A4

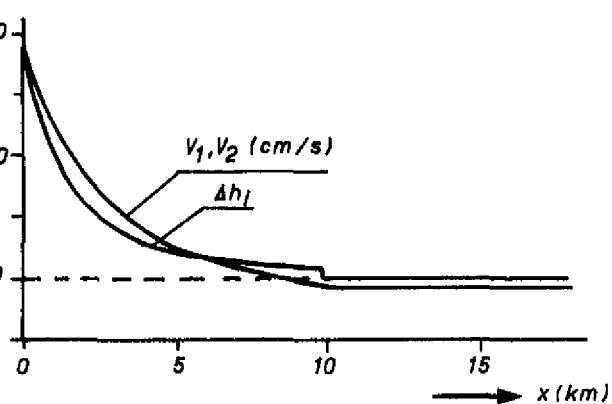
DELFT HYDRAULICS LABORATORY

R.898-II-1017 FIG. 21

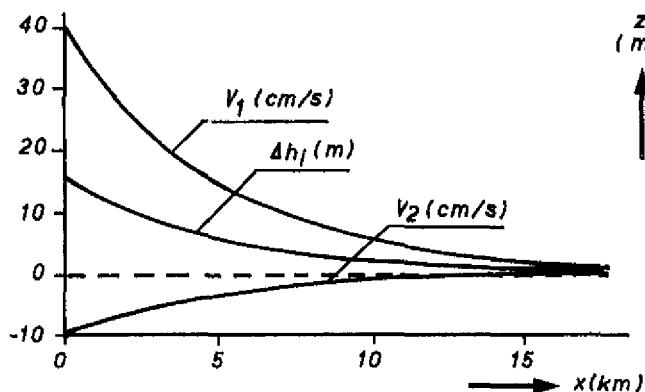
WK



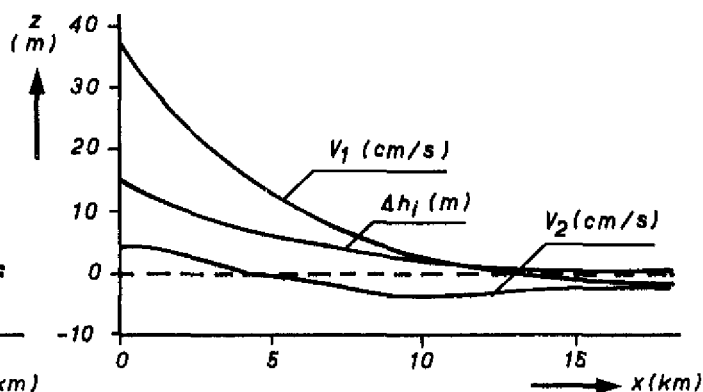
a) CROSS SECTION : DEFINITION SKETCH



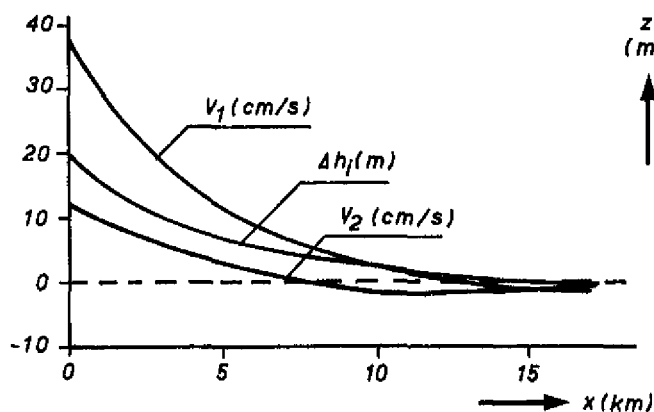
b)  $\Delta P = 0$



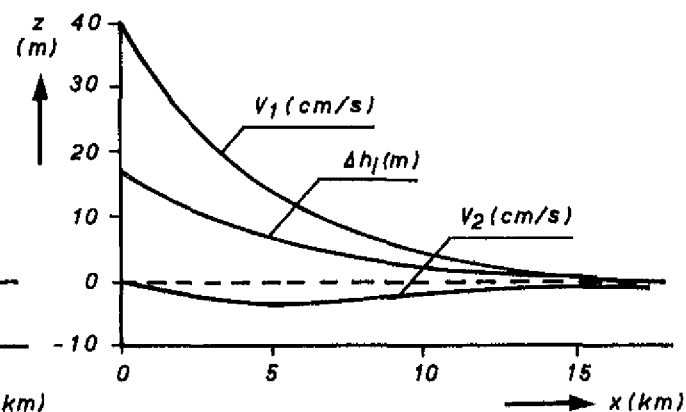
c) HOMOGENEOUS  $h$  ( FLAT BOTTOM BASIN )



d) CASE ACCORDING TO (a)



e)  $\Delta P$  HALVED



f) BOTTOM SLOPE DOUBLED

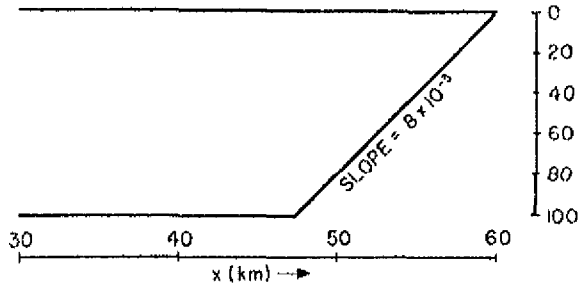
VERTICALLY AVERAGED LONGSHORE CURRENT IN UPPER ( $v_1$ ) AND LOWER ( $v_2$ ) LAYER, AND THERMOCLINE DISPLACEMENT  $\Delta h_i$  AFTER  $10^5$  s

WIND-INDUCED CIRCULATIONS ( NON-STATIONARY )  
IN TWO-LAYER BASIN

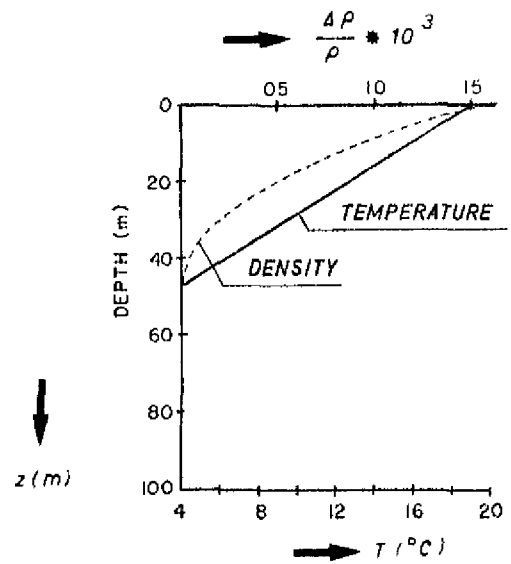
JM  
BENNETT (1974) A4

DELFT HYDRAULICS LABORATORY

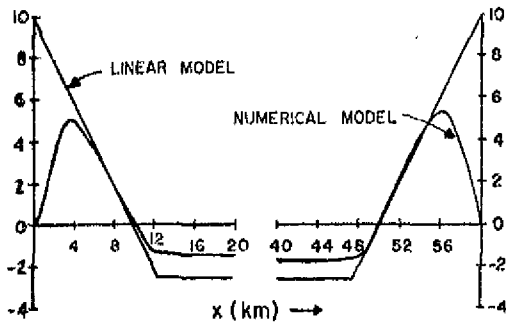
R 898-II-1018 FIG.22



a) CROSS SECTION

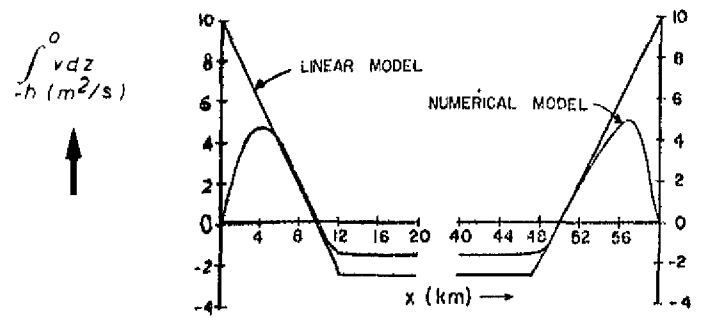


b) TEMPERATURE STRATIFICATION

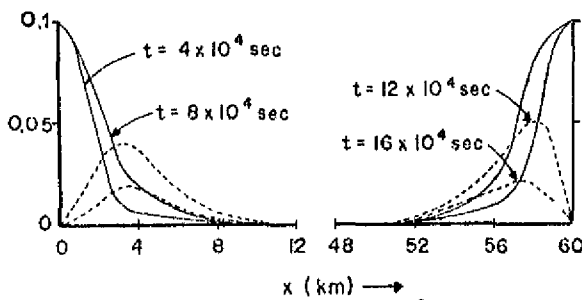


LONGSHORE TRANSPORT AT  $t = 10^5 s$

c) HOMOGENEOUS BASIN

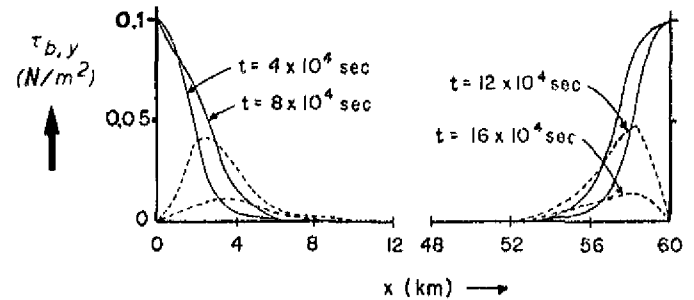


d) STRATIFIED BASIN



LONGSHORE COMPONENT OF BOTTOM STRESS  $\tau_{b,y}$   
 $\tau_0 = 0.1 N/m^2$  ON TIME INTERVAL  $t : 0 \rightarrow 10^5 s$   
 $\tau_0 = 0$  FOR  $t > 10^5 s$

e) HOMOGENEOUS BASIN



f) STRATIFIED BASIN

WIND-INDUCED CIRCULATIONS (NON-STATIONARY)  
 IN HOMOGENEOUS AND STRATIFIED BASIN

BENNETT (1974)

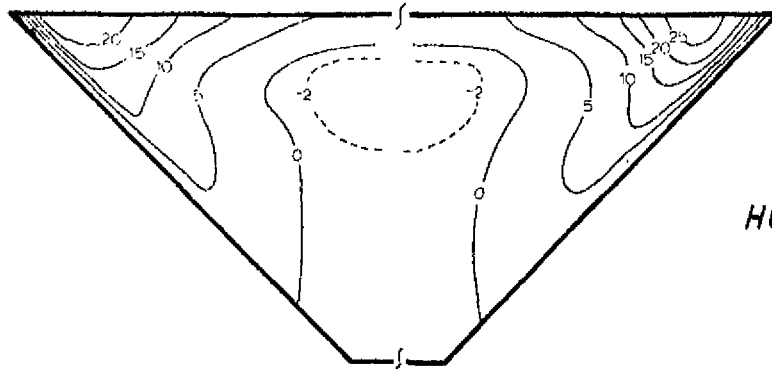
JM

A4

DELFT HYDRAULICS LABORATORY

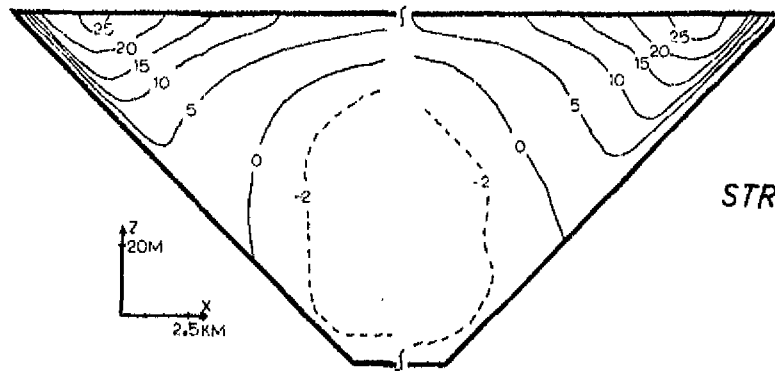
R898-II-1019

FIG. 23

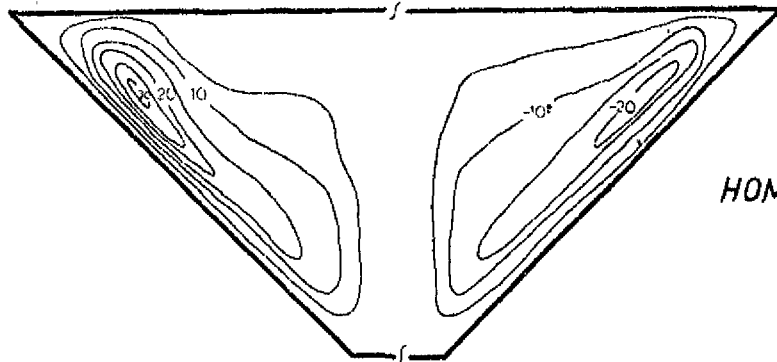


HOMOGENEOUS

a)

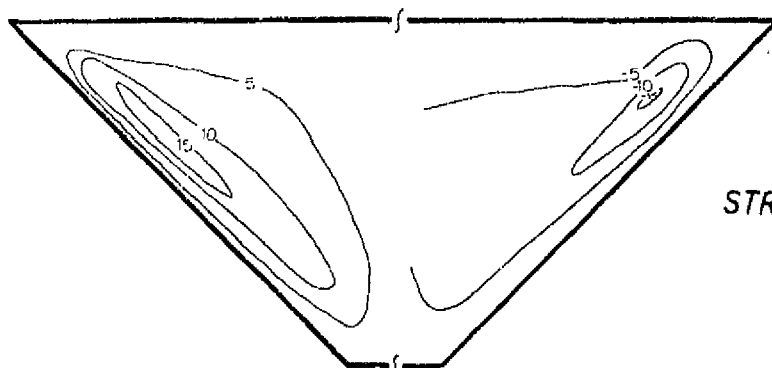


STRATIFIED



HOMOGENEOUS

b)



STRATIFIED

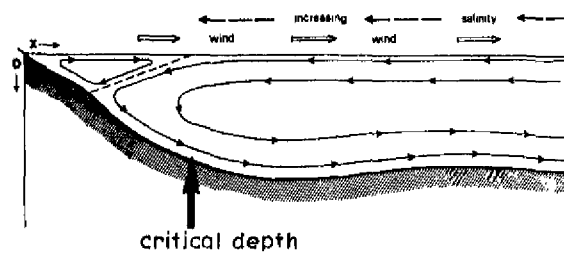
a) LONGSHORE CURRENT ( $v$  IN cm/s) at  $t = 10^5$  s

b) VERTICAL CURRENT ( $w$  IN cm/s) at  $t = 10^5$  s

JM

BENNETT (1974)

A4



COMBINED EFFECT OF WIND-INDUCED CIRCULATION  
AND COUNTERACTING SALINITY-DRIVEN CIRCULATION  
IN AN ESTUARY

BRONGERSMA AND  
GROEN (1969)

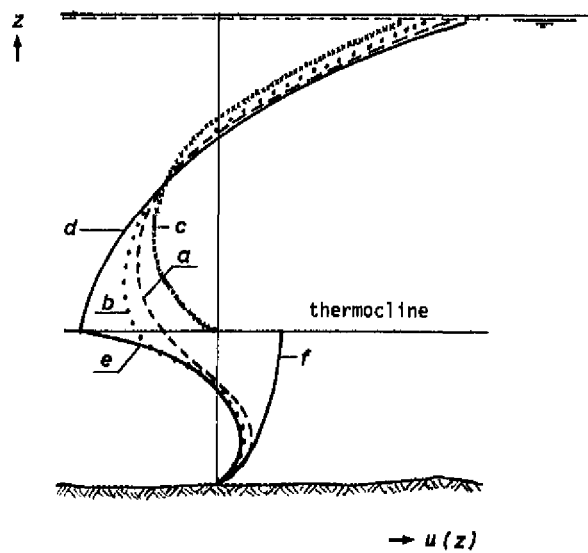
JM

A4

DELFT HYDRAULICS LABORATORY

R898-II- 1021

FIG.25



2D WIND DRIVEN CIRCULATIONS AT SEVERAL VALUES  
OF  $\epsilon_{U,S}$ ,  $\epsilon_{U,I}$  AND  $\tau_i$  (SEE TEXT)

BENGTSSON (1973b)

JM

A4

DELFT HYDRAULICS LABORATORY

R 898-II - 1022

FIG. 26

p.o. box 177

delft

the netherlands